

SYNTHESIS AND ANALYSIS OF SPATIAL,  
TWO-LOOP, SIX-LINK MECHANISMS

By

DILIP KOHLI

Bachelor of Technology  
Indian Institute of Technology  
Kanpur, India  
1969

Master of Technology  
Indian Institute of Technology  
Kanpur, India  
1971

Submitted to the Faculty of the Graduate College  
of the Oklahoma State University  
in partial fulfillment of the requirements  
for the Degree of  
DOCTOR OF PHILOSOPHY  
December, 1973

Thesis  
1713D  
K 795  
Cap. 2

APR 10 1974

SYNTHESIS AND ANALYSIS OF SPATIAL,  
TWO-LOOP, SIX-LINK MECHANISMS

Thesis Approved:

*Armenian H. San.*

Thesis Adviser

*M. M. Maroun*

*Larry D. Zelle*

*Donald W. Erace*

*N. N. Duxon*

Dean of the Graduate College

877235

## ACKNOWLEDGMENTS

My sincere gratitude is expressed to all who have helped in any way to make this study possible. In particular, I am grateful to Dr. A. H. Soni, chairman of my advisory committee, for providing me many opportunities to grow in the mechanism science area, for suggesting to me this problem, and for encouragement he provided to carry it through. I am also grateful to my other committee members, Dr. D. Grace, for encouragement, helpful suggestions and guidance, Dr. L. Zirkle and Dr. M. Mamoun for counsel and encouragement.

A large and active group of "mechanism researchers" has been an asset during the course of this work. I am obliged to "The Mechanisms Man," Professor L. E. Torfason, for friendship, for lively discussions about this work, and for going through the rough draft in detail. To other mechanisms men, Mr. Jack Lee, Mr. John Vadasz, Mr. Rick Coutant, Mr. Michael McKee, Mr. Brad Grant, Mr. Louis Loeff, and Mr. Siddhanty, I offer my gratitude.

I am thankful to Mrs. Barbara Moore for her patience and expert typing.

## TABLE OF CONTENTS

Chapter	Page
I. INTRODUCTION. . . . .	1
1.1. Synthesis of Space Mechanisms. . . . .	1
1.2. Analysis of Space Mechanisms . . . . .	4
1.3. Present Study. . . . .	5
II. SUCCESSIVE SCREW DISPLACEMENT METHOD OF CLOSED-FORM DISPLACEMENT ANALYSIS . . . . .	8
2.1. Successive Screw Displacements . . . . .	9
2.2. Pair Geometry and Constraint Equations . . . . .	17
2.2.1. Spheric Pair (Figure 3) . . . . .	17
2.2.2. Revolute Pair (Figure 4). . . . .	19
2.2.3. Cylinder Pair (Figure 5). . . . .	20
2.2.4. Prismatic Pair (Figure 6) . . . . .	20
2.2.5. Helical Pair (Figure 7) . . . . .	22
2.3. Ternary Link in Space. . . . .	24
2.4. Loop Closure Equations . . . . .	24
III. APPLICATION TO MECHANISM ANALYSIS . . . . .	33
3.1. Analysis of RCSR-CSR Mechanism . . . . .	33
3.2. Analysis of RSCR-CCC Mechanism . . . . .	49
3.3. Kinematic Analysis of RSCR-PSC Mechanism . . . . .	57
3.4. Kinematic Analysis of HCCC-RSC Mechanism . . . . .	64
3.5. Kinematic Analysis of RCCGG-GC Mechanism . . . . .	77
IV. DEVELOPMENT OF TOOLS FOR SYNTHESIS OF SPATIAL, TWO-LOOP MECHANISMS. . . . .	88
4.1. Location of Lines in the Rigid Body in Motion. . . . .	88
4.2. Chain of Rigid Bodies and Pair Constraints . . . . .	92
4.3. Synthesis of Dyads . . . . .	93
4.4. Synthesis of Triads. . . . .	101
4.4.1. C-C-R Triad . . . . .	103
4.4.2. C-C-S Triad . . . . .	107
4.4.3. C-S-C Triad . . . . .	107
4.4.4. C-S-S Triad . . . . .	109
4.4.5. Constraints Due to Space Ternary Links . . . . .	111

Chapter	Page
V. SYNTHESIS OF TWO-LOOP, SPATIAL, SIX-LINK MECHANISMS . . . . .	114
5.1. Synthesis of Watt's RSSR-RSR Mechanism . . . . .	114
5.2. Extension of Screw Triangle Geometry to Synthesis of Spatial, Two-Loop, Six-Link Mechanisms. . . . .	120
5.2.1. Stephenson-3 Fixed Pivot Type Mechanism . . . . .	122
5.2.2. Synthesis of Watt's Six-Link, Two- Loop, Spatial Mechanisms. . . . .	129
VI. CONCLUSIONS . . . . .	150
BIBLIOGRAPHY . . . . .	153

## LIST OF TABLES

Table	Page
I. Analysis of RSCR-CSR Mechanism . . . . .	50
II. Analysis of RSCR-CCC Mechanism . . . . .	58
III. Example Analysis of RSCR-PSC Mechanism . . . . .	65
IV. Example Analysis of HCCC-RSC Mechanism . . . . .	78
V. Kinematic Analysis of RCCC-RSC Mechanism . . . . .	85
VI. Velocity Analysis of RCCC-RSC Mechanism. . . . .	86
VII. Acceleration Analysis of RCCC-CSR Mechanism. . . . .	87
VIII. Synthesis of RCCC-CCC Stephenson Mechanism for Variety of Motion Programs. * . . . .	126
IX. Example Synthesis of Stephenson's Six-Link Mechanisms for Multiple Function Generation. . . . .	130
X. Synthesis of Watt's Mechanism for Variety of Motion Programs. . . . .	133
XI. Example Synthesis of Watt's RCCC-CCC Mechanism for Coordinated Motions of Input-Link and Rigid Body . . . . .	138
XII. Constraints on the Screws of Watt's-3 Fixed Pivot Type Mechanism. . . . .	141
XIII. Constraints on the Screws of Stephenson-2 Fixed Pivot Type-1 Mechanism . . . . .	142
XIV. Constraints on the Screws of Stephenson-2 Fixed Pivot Type-2 Mechanism . . . . .	143

LIST OF FIGURES

Figure	Page
1. A Rigid Body Connected to the Ground Via a Cylinder Pair. . . .	10
2. A Rigid Body Connected to the Ground Via Two Cylinder Pairs . .	13
3. Two Rigid Bodies Connected Via a Spherical Pair . . . . .	18
4. Two Rigid Bodies Connected Via a Revolute Pair. . . . .	18
5. Two Rigid Bodies Connected Via a Cylinder Pair. . . . .	21
6. Two Rigid Bodies Connected Via a Prismatic Pair . . . . .	21
7. Two Rigid Bodies Connected Via a Helical Pair . . . . .	23
8. A Ternary Link in Space . . . . .	25
9. An RCCG Mechanism . . . . .	27
10. Unfolded Positions of the Chains Obtained From RCCG Mechanism . . . . .	28
11. Six-Link, Spatial RSCR-GSR Mechanism. . . . .	34
12. Unfolded Position of First-Loop of RSCR-GSR Mechanism . . . . .	37
13. Unfolded Position of Second-Loop of RSCR-GSR Mechanism. . . . .	38
14. Six-Link, Spatial RCSR-CCC Mechanism. . . . .	51
15. Unfolded Position of Second Loop of RCSR-GSR Mechanism. . . . .	53
16. Six-Link, Spatial RCSR-PSC Mechanism. . . . .	59
17. Unfolded Position of Second Loop of RSCR-PSC Mechanism. . . . .	61
18. Six-Link, Spatial HCCC-RSC Mechanism. . . . .	66
19. Unfolded Position of First Loop of HCCC-RSC Mechanism . . . . .	69
20. Unfolded Position of Second Loop of HCCC-RSC Mechanism. . . . .	70
21. A RCCCC-CC Spatial, Six-Link Mechanism. . . . .	79



Figure	Page
22. Unfolded Position of First Loop of Spatial RCGCG-CC Mechanism . . . . .	81
23. Unfolded Position of Second Loop of Spatial RCGCG-CC Mechanism . . . . .	82
24. A Rigid Body Connected to Ground Via C-C Dyad . . . . .	94
25. A Rigid Body Connected to the Ground Via a Triad. . . . .	102
26. A Rigid Body Connected to the Ground Via a C-C-R Triad. . . . .	104
27. A Rigid Body Connected to the Ground Via a C-C-S Triad. . . . .	108
28. A Rigid Body Connected to the Ground Via a C-S-C Triad. . . . .	108
29. A Rigid Body Connected to the Ground Via a C-S-S Triad. . . . .	110
30. Screw Constraints on a Ternary Link in Space. . . . .	112
31. A Watt's Type Six-Link RSSR-RSR Mechanism for Spatial Rigid Body Guidance . . . . .	115
32. Stephenson-3 Fixed Type Mechanism . . . . .	123
33. Screw Triangle Circuit Formed by Constraints of the Stephenson-3 Fixed Type Mechanism . . . . .	127
34. Watt's-2 Fixed Pivot Type Mechanism . . . . .	131
35. Screw Triangle Circuit Formed by Constraints of the Watt's-2 Fixed Type Mechanism. . . . .	134
36. Watt's-3 Fixed Pivot Type Mechanism . . . . .	144
37. Screw Triangle Circuit for Watt's-3 Fixed Pivot Mechanism . . . . .	145
38. Stephenson-2 Fixed Pivot Type-1 Mechanism . . . . .	146
39. Screw Triangle Circuit for Stephenson-2 Fixed Pivot Type-1 Mechanism . . . . .	147
40. Stephenson-2 Fixed Pivot Type-2 Mechanism . . . . .	148
41. Screw Triangle Circuit for Stephenson-2 Fixed Type-2 Mechanism . . . . .	149

## CHAPTER I

### INTRODUCTION

Recently Soni and Harrisberger [1] surveyed the art of mechanisms science and indicated the existence of nearly 12,000 publications of scholarly level. A detailed examination of these publications [2, 3] shows that there is a considerable interest in kinematic synthesis and analysis of spatial mechanisms.

The central problem in synthesis is to determine the dimensions of linkages required to perform specified jobs. Such specifications may include guiding a rigid body, coordinating motions of input and output links, generating a curve in space, etc. The central problem in kinematic analysis of spatial mechanisms is to calculate the relative motion of the moving links provided the kinematic parameters of a linkage are known.

#### 1.1. Synthesis of Space Mechanisms

The subject of synthesis of single loop mechanisms has been of great interest to research kinematicians in the U.S. in the past two decades. A systematic approach to synthesize an RSSR mechanism, where driving and driven members move on mutually perpendicular axes was formulated by Novodvorskii [4]. Stepanoff [5] solved the generalized case of non-perpendicular planes of driving and driven members. A complete solution to this problem was given by N. I. Levitskii and K. K. Shakvazian [6], who applied the least square technique for finite position synthesis up

to eight precision positions. Denavit and Hartenberg [7] derived loop closure equations of RSSR and RCCC mechanisms and showed that equations are linear up to a limited number of precision positions.

In general, synthesis problems involved coordinating motions of input and output links of relatively few mechanisms like RSSR and RCCC. It was, however, Wilson [8] who changed this trend. Using the analogy of planar kinematic synthesis problems, Wilson introduced the rigid body guidance problem in spatial synthesis and also showed that function-generation problems can be converted to a rigid body guidance problem by taking inversion about the input or output link. Wilson's contribution also includes derivation of relationships to calculate center point and spheric point curves.

In 1965 Harrisberger [9], in his historic paper on the survey of three-dimensional mechanisms, enumerated a large number of three-dimensional mechanisms, for which synthesis procedures were as yet unexploited. Harrisberger's contribution led Roth [10, 11, 12] and Chen [13, 14] to investigate the loci of special lines and points associated with spatial motion and to propose a general theory for computing the number and locus of points in a rigid body in finite or infinitesimal motion which have their several positions satisfying the constraints of binary or combined link chains. Because of the nonlinearity of the constraints, the methods [10-14], though quite suitable for spatial, four-bar mechanisms, were unsuitable for mechanisms with a large number of links. In these references, the problem solved was that of rigid body guidance. Problems such as generating a curve in space, generating surfaces, etc., still remained untouched.

Soni and Harrisberger [15] and Soni and Huang [16] introduced

transmission characteristics as optimality criterion for designing space mechanisms. Using the analogy of planar kinematic synthesis, Soni and Huang [17] extended the point position reduction to design spatial, four-bar mechanisms. Rao, Sandor, Kohli, and Soni [18] developed a general closed-form synthesis procedure to synthesize function generators for a maximum number of precision positions.

Sandor [19], Sandor and Bishopp [20] introduced methods of dual number quaternions and stretch rotation tensor to find loop closure equations of spatial mechanisms. The methods proposed were general enough to include generation of space curves, etc., but the complexity of the equations for mechanisms with a large number of links limited their use to four-link mechanism synthesis. Suh [21, 22] employed  $4 \times 4$  matrices for synthesis of space mechanisms where design equations are expressed as constraint equations in order to obtain constrained motion. Suh [23] also investigated the differential displacement synthesis of spatial mechanisms. Kohli and Soni [24] employed matrix methods to synthesize spherical four-link and six-link mechanisms for multiply separated positions of a rigid body in spherical motion. The simplicity of Suh's method is undoubtedly appealing, but large numbers of synthesis equations render such methods unsuitable for synthesis of spatial mechanisms with more than four links.

Recently, Tsai and Roth [25, 26, 27] used screw triangle geometry to synthesize open-loop kinematic chains for completely and incompletely specified positions of a rigid body. The proposed method is quite simple and permits synthesis of mechanisms with helical pairs.

The only contribution in spatial, two-loop, six-link mechanisms is by Kohli and Soni [28] who gave synthesis procedures for mechanisms with

revolute, cylinder and helical pairs.

## 1.2. Analysis of Spatial Mechanisms

Kinematic analysis of space mechanisms was initiated by the significant contribution of Dimentberg [30]. Dimentberg [30, 31] demonstrated the use of dual numbers and screw calculus to obtain closed-form displacement relationships of an RCCC and other four-, five-, six-, and seven-link spatial mechanisms. Denavit [33] derived closed-form displacement relationships for a spatial RCCC mechanism using dual Euler angles. Yang [34] also derived such relationships for RCCC mechanisms using dual quaternions.

Vectors were first used by Chace [35] to derive closed-form displacement relations of RCCC mechanisms. Wallace and Freudenstein [36] also used vectors to obtain closed-form displacement relationships of RRSRR and RRERR mechanisms.

Yang [37] proposed a general formulation using dual numbers to conduct displacement analysis of RCRGR spatial, five-link mechanisms. Soni and Pamidi [38] extended this application of  $(3 \times 3)$  matrices with dual elements to obtain closed-form displacement relations of RCCRR mechanisms. The methods need further modification when a mechanism contains a spherical pair.

Yuan [39] employed screw coordinates to obtain closed-form displacement relations for RRCCR and other spatial mechanisms. The approach does not seem to have any advantage over other methods.

Jenkins and Crossley [40], Sharma and Torfason [41], Dukkipati and Soni [42] used the method of generated surfaces to conduct the analysis of single-loop mechanisms containing a spheric pair. Hartenberg and

Denavit [43] contributed iterative techniques to conduct the displacement analysis of spatial mechanisms using  $(4 \times 4)$  matrices. Uicker [44, 45] explored in further detail the  $(4 \times 4)$  matrix approach of Hartenberg and Denavit. Soni and Harrisberger [46] contributed an iterative approach for performing kinematic analysis using  $(3 \times 3)$  matrices with dual elements. Kohli and Soni [47, 48] used finite screws to conduct displacement analysis of single-loop and two-loop space mechanisms involving revolute, prismatic, cylinder, helical and spheric pairs.

The survey of literature shows that the art of synthesis and analysis of single-loop space mechanisms has attained a sufficient maturity level, and synthesis and analysis of two-loop, six-link mechanisms is virtually unexplored.

A systematic approach was devised by Soni and Huang [49, 50] to perform structural analysis and synthesis of multi-loop kinematic chains with or without general constraints. The generalized approach was used to enumerate all two-loop, spatial, six-link mechanisms with or without general constraints. The result of this structural synthesis shows that there are 14 types, 936 kinds, and 545,277 two-loop, six-link spatial kinematic chains. Dukkupati [51] investigated the existence criteria of two-loop, overconstrained mechanisms and performed displacement analysis of two types of mechanisms. We are unaware of any work on synthesis of spatial mechanisms except that by Kohli and Soni [28].

### 1.3. Present Study

The objectives of the present study are to develop unified synthesis and analysis procedures for spatial, two-loop, six-link mechanisms. The five basic configurations, Stephenson-1, Stephenson-2, Stephenson-3,

Watt's-1 and Watt's-2 mechanisms are examined for finitely, infinitesimally or multiply-separated position synthesis problems using screw triangle geometry and successive screw displacements. The maximum number of positions for which a six-link mechanism may be synthesized for different types of problems depends upon the type of pairs used and their arrangements within the mechanism. Synthesis problems included in the present study are

1. Rigid Body Guidance
2. Function Generation
3. Guidance for Incompletely Specified Specification of Rigid Body

Kinematic analysis of spatial six-link Watt's and Stephenson type mechanisms is conducted using successive screw displacements. Kinematic analysis of a mechanism involves the following problems:

1. Derivation of closed-form displacement relationships
2. Derivation of closed-form velocity and acceleration relations

Specifically, the present study

1. develops a generalized approach to synthesize two-loop mechanisms with kinematic pairs such as revolute pairs, prism pairs, helical pairs, spherical pairs, and cylinder pairs.
2. incorporates completely and incompletely specified positions of the rigid body for finitely, infinitesimally, or multiply-separated problems of synthesis.
3. develops a generalized approach to obtain closed-form relationships to calculate position, velocity, and acceleration in space mechanisms for various values of input displacements.

Chapter II presents the development of generalized tools for analysis of space mechanisms. Chapter III presents examples of 5 six-link space mechanisms. Chapter IV develops general procedures for synthesis of six-link mechanisms for a variety of motion programs. Chapter V presents examples of synthesis of six-link mechanisms using the generalized procedures. Finally, Chapter VI presents findings and conclusions of the present study.



## CHAPTER II

### SUCCESSIVE SCREW DISPLACEMENT METHOD OF CLOSED-FORM DISPLACEMENT ANALYSIS

Kinematic analysis is the inverse problem to kinematic synthesis. In kinematic analysis we are given a mechanism, and we are required to compute the position of the components of the mechanism for various positions of the input link. To obtain all the possible configurations which a mechanism takes, closed-form displacement relationships must be developed. Such relationships permit one to compute the positions of various links and the rotations and translations of various pairs for consecutive positions of the input link. In performing kinematic analysis, we also compute the infinitesimal motion of mechanism links in terms of the infinitesimal motion of the input link. This leads us to velocity and acceleration analysis of mechanisms.

In general, there exist many positions of the mechanism for one position of the input link. The number of configurations a mechanism takes depends upon the combination and types of pairs in the mechanism. In general, this is reflected in a polynomial relating the output-input displacements. But many times, due to the mathematical complexity of the elimination processes, this polynomial contains extraneous solutions which do not correspond to any physical assembly of the mechanism, and consequently these roots must be neglected for obtaining the correct number of loop closures.

In what follows, a closed-form method for displacement, velocity and acceleration analysis of space mechanisms is developed.

### 2.1. Successive Screw Displacements

When two positions of a rigid body are given, there are an infinite number of ways the body may be transferred from one position to another. One of the simplest ways to accomplish this is through screw motion (Chasel's theorem). Chasel's theorem states that a rigid body can be moved from any one specified position to any other by a movement consisting of a rotation around a straight line accompanied by a translation parallel to the straight line. This is called screw motion and is unique in its representation. A displacement denotes the difference in two positions of a rigid body. Therefore, displacements specified in screw motion form are unique.

Displacements at pairs may be regarded as screw displacements. At a cylinder pair (C), the displacement is a screw of variable pitch; at a helical pair (H), a constant pitch; at a revolute pair (R), an infinite pitch; at a spherical pair (S), displacement is a pure rotation about a fixed point (i.e., the screw axis passes through the spherical point, and there is no translation).

We shall consider here a cylinder pair since it is the most general screw, and all other screws associated with revolute, prism, helical and spheric pairs may be derived from it. We shall consider the location of lines or points and their derivatives when the body to which the line or point is associated undergoes a series of successive screw displacements about the joints.

Figure 1 shows a rigid body  $\Sigma$  attached to a cylindrical pair B in a

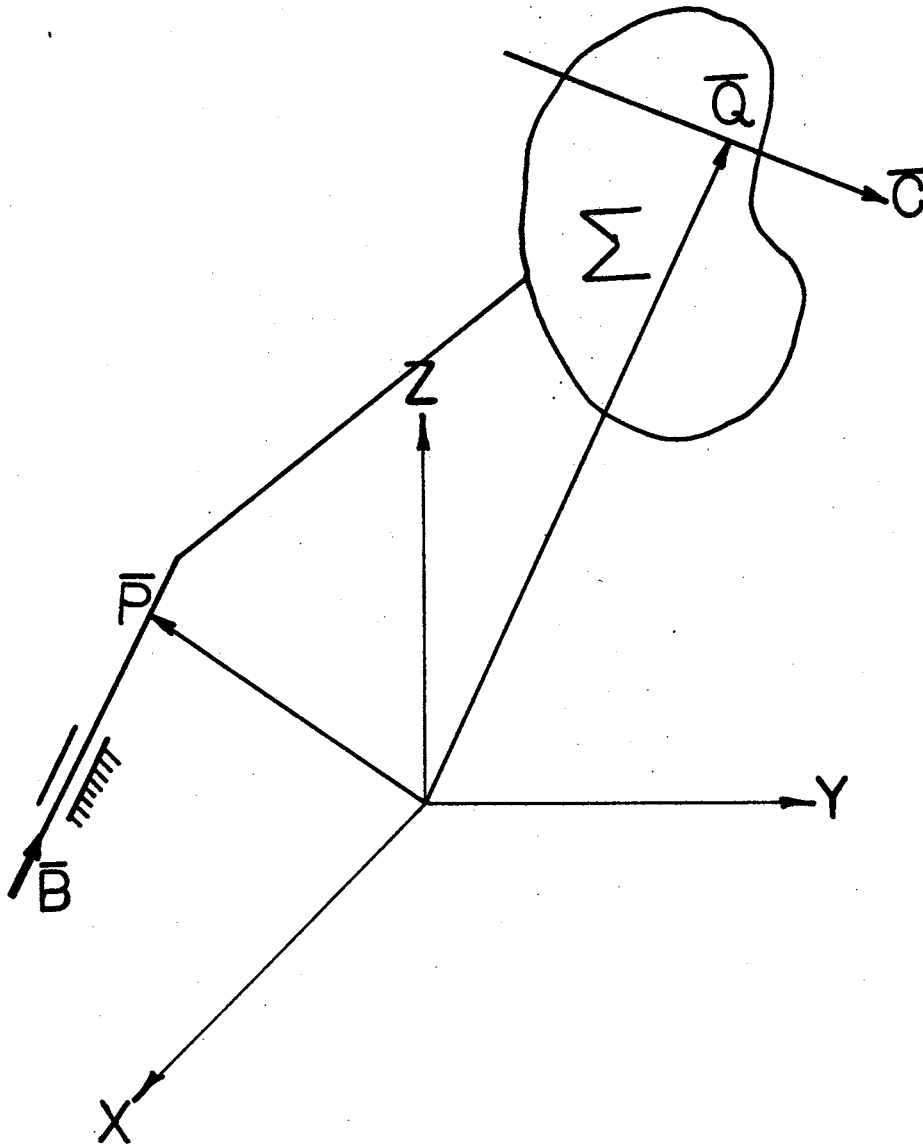


Figure 1. A Rigid Body Connected to the Ground Via a Cylinder Pair

rectangular coordinate system OXYZ. This joint can take screw displacements, i.e., rotations about and translations along the axis of the joint.

The following vectors are defined:

$\bar{B}$  is a unit vector defining the direction of the axis of the joint.

$\bar{P}$  is a vector from the origin to a point P on the axis.

$\bar{C}$  is a unit vector defining the direction of a line in  $\Sigma$ .

$\bar{Q}$  is a vector from the origin to a point Q on the line in  $\Sigma$ .

In what follows, cosine and sine are denoted by letters C and S followed by the angle.

Now if  $\Sigma$  is displaced through screw motion at joint B consisting of a rotation about  $\bar{B}$  by  $\theta_B$  and translations  $S_B$  along axis  $\bar{B}$ ; then  $\Sigma$  occupies the position  $\Sigma_j$ . The direction of line ( $\bar{C}_j$ ) in  $\Sigma_j$  is given by

$$\bar{C}_j = C\theta_B [\bar{C} - (\bar{C} \cdot \bar{B})\bar{B}] + S\theta_B (\bar{B} \times \bar{C}) + (\bar{C} \cdot \bar{B})\bar{B} \quad (2.1)$$

and if the motion is infinitesimal,  $d\bar{C}/dt$ ,  $d^2\bar{C}/dt^2$  are given by

$$\frac{d\bar{C}}{dt} = (\bar{B} \times \bar{C}) \frac{d\theta_B}{dt} \quad (2.2)$$

$$\frac{d^2\bar{C}}{dt^2} = \frac{d^2\theta_B}{dt^2} (\bar{B} \times \bar{C}) + (\bar{B} \times \frac{d\bar{C}}{dt}) \frac{d\theta_B}{dt} \quad (2.3)$$

$d\bar{B}/dt = 0$  since  $\bar{B}$  is fixed to the pair axes.

The displaced position of point Q is given by

$$\begin{aligned}\bar{Q}_j = & C\theta_B [(\bar{Q}-\bar{P}) - \{(\bar{Q}-\bar{P}) \cdot \bar{B}\} \bar{B}] + \bar{P} + \bar{B} S_B \\ & + S\theta_B (\bar{B} \times (\bar{Q}-\bar{P})) \\ & + \{(\bar{Q}-\bar{P}) \cdot \bar{B}\} \bar{B}\end{aligned}\quad (2.4)$$

The velocities and acceleration of Q are given by

$$\frac{d\bar{Q}}{dt} = \bar{B} \times (\bar{Q}-\bar{P}) \frac{d\theta_B}{dt} + \bar{B} \frac{dS_B}{dt} \quad (2.5)$$

$$\begin{aligned}\frac{d^2\bar{Q}}{dt^2} = & \bar{B} \times (\bar{Q}-\bar{P}) \frac{d^2\theta_B}{dt^2} \\ & + \frac{d\theta_B}{dt} \bar{B} \times \left( \frac{d\bar{Q}}{dt} - \frac{d\bar{P}}{dt} \right) + \bar{B} \frac{d^2S_B}{dt^2}\end{aligned}\quad (2.6)$$

where

$$\frac{d\bar{P}}{dt} = \bar{B} \frac{dS_B}{dt}$$

Hence,

$$\begin{aligned}\frac{d^2\bar{Q}}{dt^2} = & \bar{B} \times [\bar{B} \times (\bar{Q}-\bar{P})] \left( \frac{d\theta_B}{dt} \right)^2 + \bar{B} \frac{d^2S_B}{dt^2} \\ & + [\bar{B} \times (\bar{Q}-\bar{P})] \frac{d^2\theta_B}{dt^2}\end{aligned}\quad (2.7)$$

Figure 2 shows a rigid body attached to a binary line where both joints can take screw displacements. Second joint is completely defined by a point  $\bar{P}$  and unit vector  $\bar{B}$ . Note that one element of A is fixed while B is a moving joint. We first give screw displacement at joint B and then

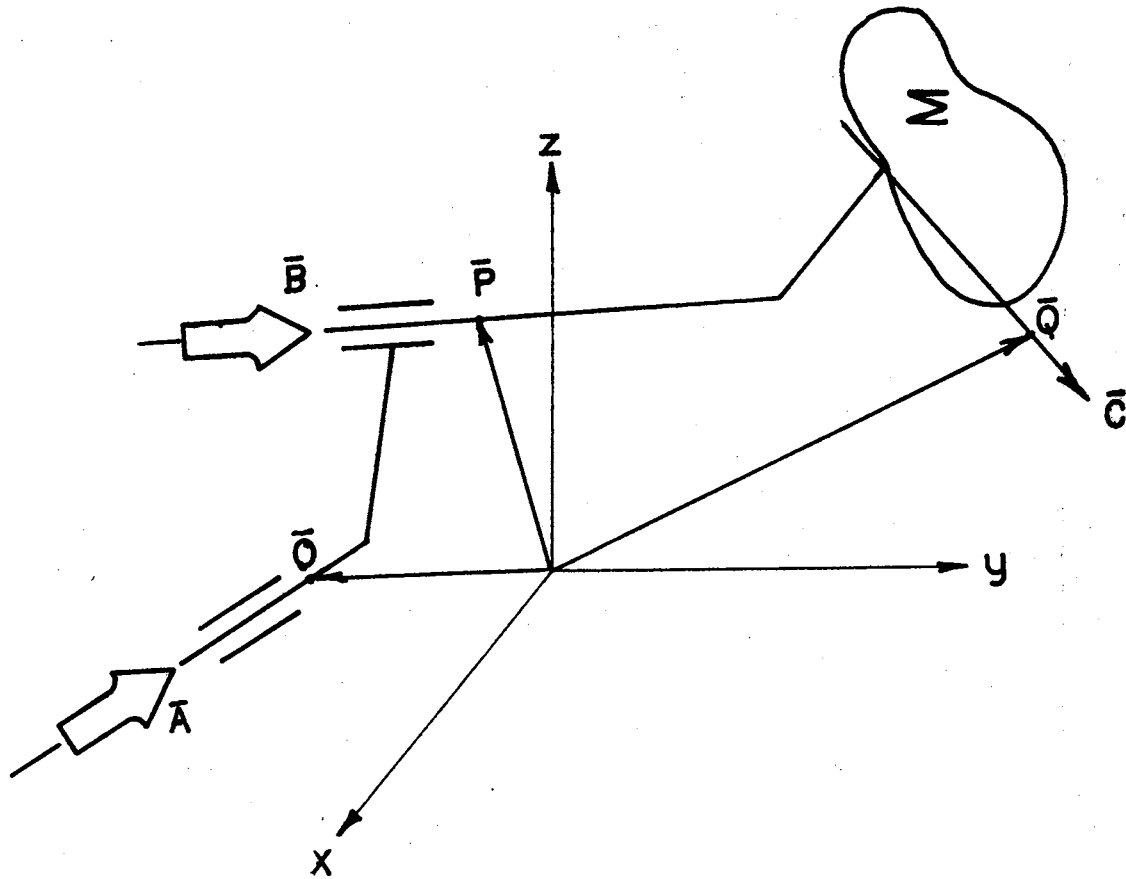


Figure 2. A Rigid Body Connected to the Ground Via Two Cylinder Pairs

at A,  $\Sigma$  occupies  $\Sigma'$  after displacement at B and  $\Sigma_j$  after displacement at A. Let  $\theta_A$  and  $\theta_B$  be rotational motions and  $S_A$  and  $S_B$  be linear displacements at joints A and B, then the first displaced position of  $\bar{C}'$  of line  $\bar{C}$  in  $\Sigma'$  is given by

$$\bar{C}' = C\theta_B[\bar{C} - (\bar{C} \cdot \bar{B})\bar{B}] + S\theta_B(\bar{B} \times \bar{C}) + (\bar{C} \cdot \bar{B})\bar{B} \quad (2.8)$$

$$\begin{aligned} \bar{Q}' &= C\theta_B[(\bar{Q} - \bar{P}) - \{(\bar{Q} - \bar{P}) \cdot \bar{B}\}\bar{B}] + \bar{B}S_B + \bar{P} \\ &+ S\theta_B[\bar{B} \times (\bar{Q} - \bar{P})] + \{(\bar{Q} - \bar{P}) \cdot \bar{B}\}\bar{B} \end{aligned} \quad (2.9)$$

and final displaced position  $\bar{C}_j$  in  $\Sigma_j$  is given by

$$\bar{C}_j = C\theta_A[\bar{C}' - (\bar{C}' \cdot \bar{A})\bar{A}] + S\theta_A(\bar{A} \times \bar{C}') + (\bar{C}' \cdot \bar{A})\bar{A} \quad (2.10)$$

$$\begin{aligned} \bar{Q}_j &= C\theta_A[(\bar{Q}' - \bar{O}) - \{(\bar{Q}' - \bar{O}) \cdot \bar{A}\}\bar{A}] \\ &+ S\theta_A[\bar{A} \times (\bar{Q}' - \bar{O})] + \bar{A}S_A \\ &+ \{(\bar{Q}' - \bar{O}) \cdot \bar{A}\}\bar{A} + \bar{O} \end{aligned} \quad (2.11)$$

Rearranging Equation (2.10), we get

$$\begin{aligned} \bar{C}_j &= C\theta_B[C\theta_A\bar{L}_1 + S\theta_A\bar{L}_2 + \bar{L}_3] \\ &+ S\theta_B[C\theta_A\bar{M}_1 + S\theta_A\bar{M}_2 + \bar{M}_3] \\ &+ C\theta_A\bar{K}_1 + S\theta_A\bar{K}_2 + \bar{K}_3 \end{aligned} \quad (2.12)$$

where

$$\begin{aligned}
\bar{L}_1 &= \bar{J}_1 - (\bar{J}_1 \cdot \bar{A}) \bar{A} \\
\bar{L}_2 &= (\bar{A} \times \bar{J}_1) \\
\bar{L}_3 &= (\bar{J}_1 \cdot \bar{A}) \bar{A} \\
\bar{M}_1 &= \bar{J}_2 - (\bar{J}_2 \cdot \bar{A}) \bar{A} \\
\bar{M}_2 &= (\bar{A} \times \bar{J}_2) \\
\bar{M}_3 &= (\bar{J}_2 \cdot \bar{A}) \bar{A} \\
\bar{J}_1 &= \bar{C} - (\bar{C} \cdot \bar{B}) \bar{B} \\
\bar{J}_2 &= (\bar{B} \times \bar{C}) \\
\bar{J}_3 &= (\bar{C} \cdot \bar{B}) \bar{B} \\
\bar{K}_1 &= \bar{J}_3 - (\bar{J}_3 \cdot \bar{A}) \bar{A} \\
\bar{K}_2 &= (\bar{A} \times \bar{J}_3) \\
\bar{K}_3 &= (\bar{J}_3 \cdot \bar{A}) \bar{A}
\end{aligned}$$

Derivatives of  $\bar{C}$  are written as

$$\begin{aligned}
\frac{d\bar{C}}{dt} &= \bar{L}_2 \frac{d\theta_A}{dt} + \frac{d\theta_B}{dt} (\bar{M}_1 \times \bar{M}_3) + \bar{K}_2 \\
&= \left[ \bar{A} \frac{d\theta_A}{dt} + \bar{B} \frac{d\theta_B}{dt} \right] \times \bar{C} \quad (2.13)
\end{aligned}$$

$$\begin{aligned}
\frac{d^2\bar{C}}{dt^2} &= \left[ \bar{A} \frac{d^2\theta_A}{dt^2} + \frac{d\bar{B}}{dt} \frac{d\theta_B}{dt} + \bar{B} \frac{d^2\theta_B}{dt^2} \right] \times \bar{C} \\
&\quad + \left[ \bar{A} \frac{d\theta_A}{dt} + \bar{B} \frac{d\theta_B}{dt} \right] \times \frac{d\bar{C}}{dt} \quad (2.14)
\end{aligned}$$



where

$$\frac{d\bar{B}}{dt} = (\bar{A} \times \bar{B}) \frac{d\theta_A}{dt}$$

Similarly

$$\begin{aligned} \frac{d\bar{Q}}{dt} &= [(\bar{Q}' - \bar{O}) - \{(\bar{Q}' - \bar{O}) \cdot \bar{A}\} \bar{A}]' \\ &\quad + \frac{d\theta_A}{dt} [\bar{A} \times (\bar{Q}' - \bar{O})] + \bar{A} \frac{dS_A}{dt} \\ &\quad + [\{(\bar{Q}' - \bar{O}) \cdot \bar{A}\} \bar{A}]' + \frac{d\bar{O}}{dt} \end{aligned} \quad (2.15)$$

$$\begin{aligned} \frac{d\bar{Q}}{dt} &= [\bar{B} \times (\bar{Q} - \bar{P})] \frac{d\theta_B}{dt} + \bar{B} \frac{dS_B}{dt} \\ &\quad + \frac{d\theta_A}{dt} [\bar{A} \times (\bar{Q} - \bar{O})] + \bar{A} \frac{dS_A}{dt} \end{aligned} \quad (2.16)$$

$$\begin{aligned} \frac{d^2\bar{Q}}{dt^2} &= [\bar{B} \times (\frac{d\bar{Q}}{dt} - \frac{d\bar{P}}{dt}) + \frac{d\bar{B}}{dt} \times (\bar{Q} - \bar{P})] \frac{d\theta_B}{dt} \\ &\quad + [\bar{B} \times (\bar{Q} - \bar{P})] \frac{d^2\theta_B}{dt^2} + \bar{B} \frac{d^2S_B}{dt^2} \\ &\quad + \frac{d\bar{B}}{dt} \frac{dS_B}{dt} + \frac{d^2\theta_A}{dt^2} [\bar{A} \times (\bar{Q} - \bar{O})] \\ &\quad + \frac{d\theta_A}{dt} [\bar{A} \times (\frac{d\bar{Q}}{dt} - \frac{d\bar{O}}{dt})] + \bar{A} \frac{d^2S_A}{dt^2} \end{aligned} \quad (2.17)$$

where

$$\frac{d\bar{o}}{dt} = \bar{A} \frac{dS_A}{dt}$$

$d\bar{P}/dt$ ,  $d\bar{B}/dt$  as shown in Equations (2.5) and (2.2) are obtained by permuting  $\bar{P}$  with  $\bar{Q}$  and  $\bar{B}$  with  $\bar{C}$ .

We conclude then that displaced positions of lines or points and their derivatives may be obtained by providing successive screw displacements. For finitely separated positions, we use finite screws from Equations (2.10) and (2.11); while for infinitesimally separated positions we use infinitesimal screws described by infinitesimal screw displacements at joints by Equations (2.13) through (2.17).

## 2.2. Pair Geometry and Constraint Equations

Let two chains of rigid bodies be connected to two elements of a pair. The displaced positions of pairs are usually obtained independently from two sides. The geometry of the pair places certain constraints on the motion of two chains connected to the two elements. In this section we describe the constraints placed by pair geometry on the motion of these two chains. Note that these constraints can be generalized to constraints on two screw chains. Screw 1 and Screw 2 referred to herein will describe equivalent screw displacements of two screw chains.

### 2.2.1. Spheric Pair (Figure 3)

If screws  $\hat{S}_1$  and  $\hat{S}_2$  (where the hat denotes the screw) are connected by a spheric pair, then the constraint that the spherical pair places on the screw displacements  $\hat{S}_1$  and  $\hat{S}_2$  (shown in Figure 3) may be expressed as follows.

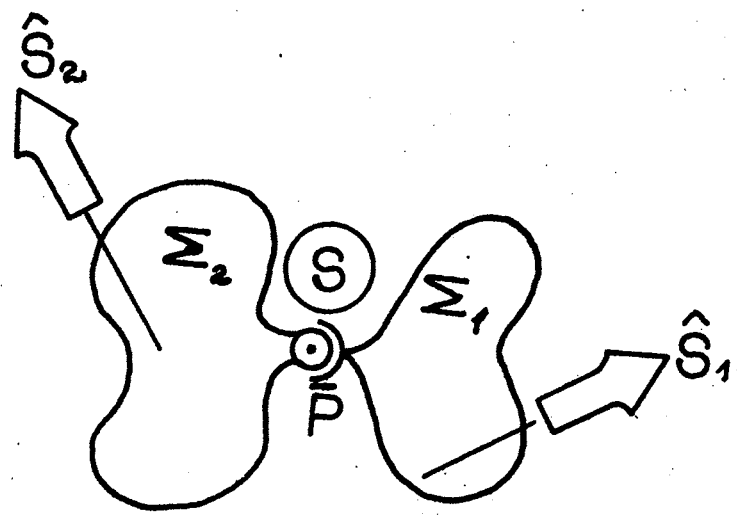


Figure 3. Two Rigid Bodies Connected Via a Spherical Pair

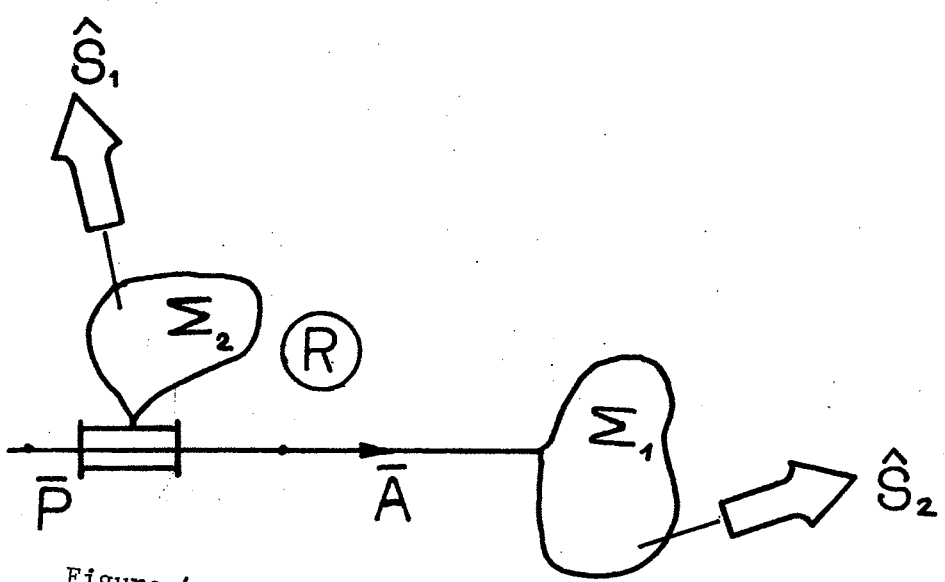


Figure 4. Two Rigid Bodies Connected Via a Revolute Pair

1. After the displacement is carried out, the displaced position of the spherical point (denoted by P) considered on Screw 1 and Screw 2 must be the same.

$$\bar{P}_j(\hat{S}_1) = \bar{P}_j(\hat{S}_2) \quad (2.18)$$

2. For infinitesimal motions the derivatives of the point P, computed from screw motions of  $\hat{S}_1$  and  $\hat{S}_2$ , are equal.

$$\bar{P}'(\hat{S}_1) = \bar{P}'(\hat{S}_2) \quad (2.19)$$

In general, for  $n^{\text{th}}$  order infinitesimal motion

$$\bar{P}^n(\hat{S}_1) = \bar{P}^n(\hat{S}_2) \quad (2.20)$$

### 2.2.2. Revolute Pair (Figure 4)

Figure 4 shows two screws  $\hat{S}_1$  and  $\hat{S}_2$  connected via a revolute joint.

A revolute pair puts the following constraints on the screw displacements  $\hat{S}_1$  and  $\hat{S}_2$ :

1. The displaced position of revolute axis  $\bar{A}$  when considered on screw  $\hat{S}_1$  must be the same as that when considered on screw  $\hat{S}_2$ .

$$\bar{A}_j(\hat{S}_1) = \bar{A}_j(\hat{S}_2) \quad (2.21)$$

2. The displaced position of a point on the revolute axis (P) when considered on screw  $\hat{S}_1$  must be the same as that when considered on screw  $\hat{S}_2$ .

$$\bar{P}_j(\hat{S}_1) = \bar{P}_j(\hat{S}_2) \quad (2.22)$$

3. For infinitesimal displacements, derivatives of axes and point

from Screw 1 and Screw 2 are equated.

$$\bar{A}^n(\hat{S}_1) = \bar{A}^n(\hat{S}_2) \quad (2.23)$$

and

$$\bar{P}^n(\hat{S}_1) = \bar{P}^n(\hat{S}_2) \quad (2.24)$$

### 2.2.3. Cylinder Pair (Figure 5)

For finite displacements, the conditions are

$$\bar{A}_j(\hat{S}_1) = \bar{A}_j(\hat{S}_2) \quad (2.25)$$

$$\bar{P}_j(\hat{S}_1) = \bar{P}_j(\hat{S}_2) + \bar{A}_j t \quad (2.26)$$

where  $t$  is the translation at the cylinder pair.

For infinitesimally separated positions the conditions are

$$\bar{A}^n(\hat{S}_1) = \bar{A}^n(\hat{S}_2) \quad (2.27)$$

$$P^n(\hat{S}_1) = \bar{P}^n(\hat{S}_2) + \frac{d^n}{d\tau^n}(\bar{A}t) \quad (2.28)$$

### 2.2.4. Prismatic Pair (Figure 6)

A prism pair does not allow any relative rotational motion between two lines. Hence, the condition that a prism pair puts on Screws 1 and 2 is that screws  $\hat{S}_1$  and  $\hat{S}_2$  are parallel.

Let  $\bar{B}$ , a unit vector, intersect at a constant angle the pair axes  $\bar{A}$ .

Then the condition for bodies to have common prismatic pair is

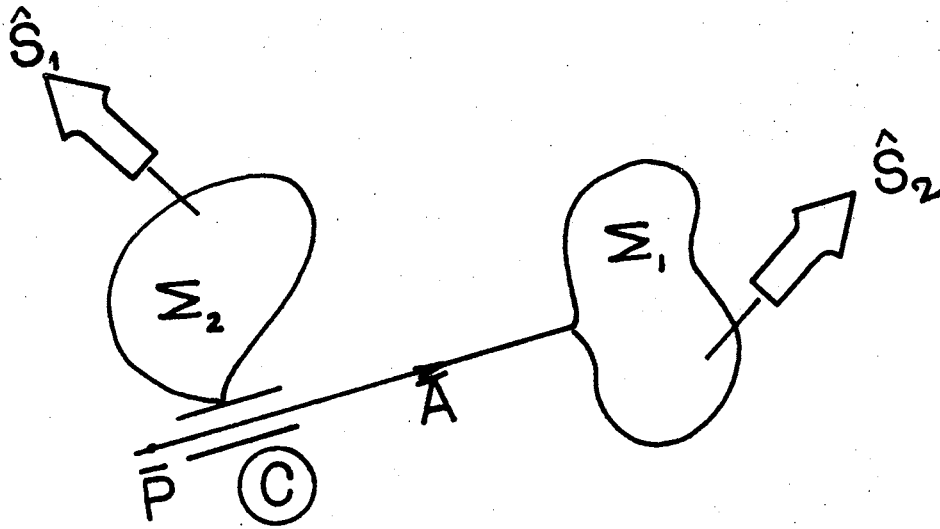


Figure 5. Two Rigid Bodies Connected Via a Cylinder Pair

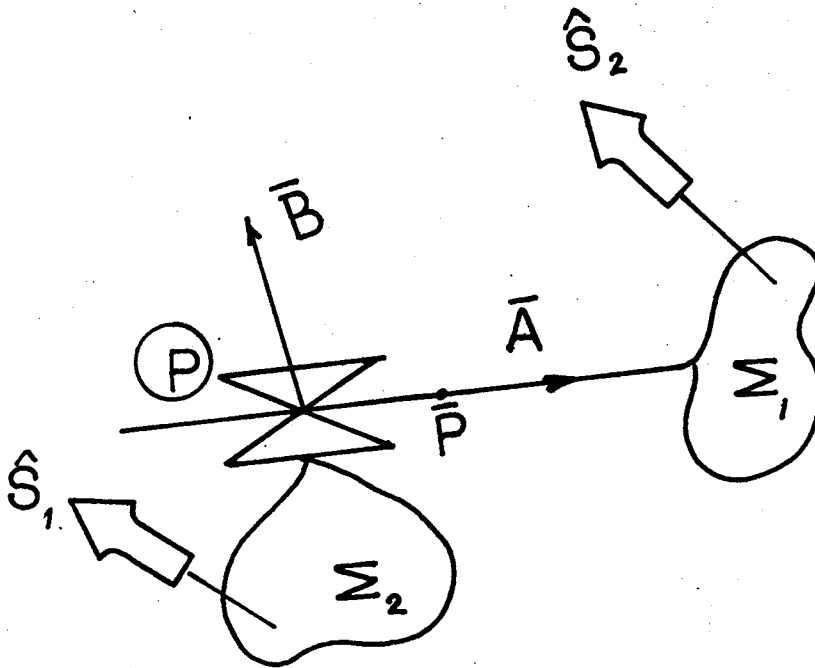


Figure 6. Two Rigid Bodies Connected Via a Prismatic Pair

$$\bar{A}_j(\hat{S}_1) = \bar{A}_j(\hat{S}_2) \quad (2.29)$$

$$\bar{B}_j(\hat{S}_1) = \bar{B}_j(\hat{S}_2) \quad (2.30)$$

$$\bar{P}_j(\hat{S}_1) = \bar{P}_j(\hat{S}_2) + \bar{A}_j t \quad (2.31)$$

For infinitesimal motion

$$\bar{A}^n(\hat{S}_1) = \bar{A}^n(\hat{S}_2) \quad (2.32)$$

$$\bar{B}^n(\hat{S}_1) = \bar{B}^n(\hat{S}_2) \quad (2.33)$$

$$\bar{P}_j^n(\hat{S}_1) = \bar{P}_j^n(\hat{S}_2) + (\bar{A} t)^n \quad (2.34)$$

where  $t$  is the translation at prismatic pair.

#### 2.2.5. Helical Pair (Figure 7)

The constraint on the motion of screws  $\hat{S}_1$  and  $\hat{S}_2$  is expressed by

$$\bar{A}_j(\hat{S}_1) = \bar{A}_j(\hat{S}_2) \quad (2.35)$$

$$\bar{P}_j(\hat{S}_1) = \bar{P}_j(\hat{S}_2) + \bar{A}_j t \quad (2.36)$$

$$t = \rho (\theta_2 - \theta_1) \quad (2.37)$$

where  $t$  is the translation at the helical pair

$\theta_2$  and  $\theta_1$  are rotations of Screws 2 and 1

$\theta_2 - \theta_1$  is the rotation at the helical pair

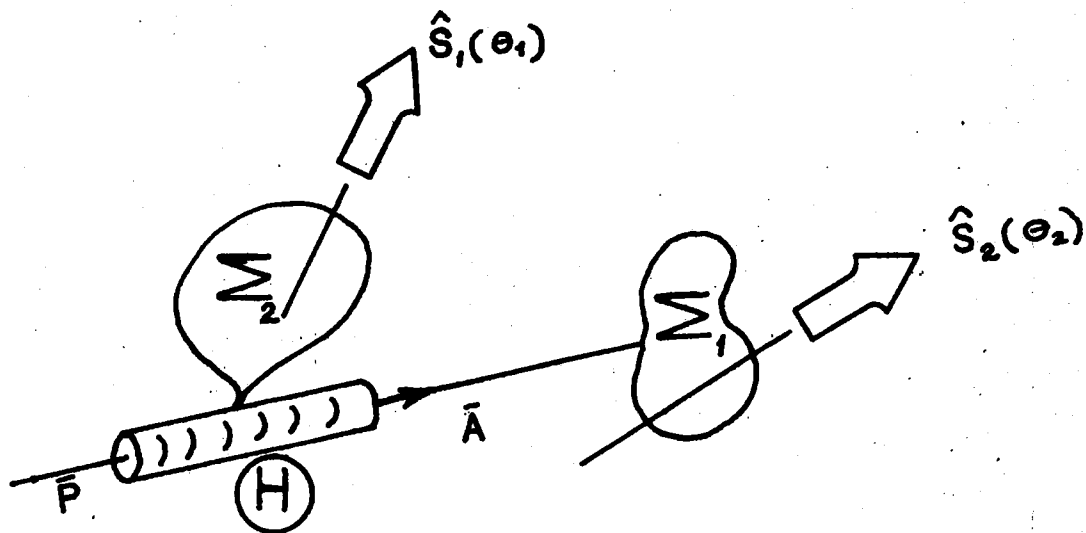


Figure 7. Two Rigid Bodies Connected Via a Helical Pair



$\rho$  is the pitch of the helical pair.

### 2.3. Ternary Link in Space

A ternary link is a rigid body containing three elements of pairs. The pair axes are defined by their screw axes which are, in general, non-parallel, nonintersecting lines in space. The direction of links and kinks are so chosen that the ternary link forms a closed loop. The ternary link has 12 parameters (3 link lengths, 3 kink lengths, 3 twist angles and 3 included angles, but only 6 of these are independent parameters).

Two link lengths, 2 twist angles, an included angle and included kink length are chosen here as independent parameters. Note that loop closure equations may be written traversing two sides of the ternary link. Figure 8 shows a ternary link where one of the joints is connected to link  $a_k$ . Let two sides of ternary link meeting at this joint be  $a_{k-1}$  and  $a_{k+1}$ ,  $\theta_t$  be the included angle between  $a_{k-1}$  and  $a_{k+1}$ ,  $S_{c_1}$  be the kink at this joint. Let the rotation of  $a_{k-1}$  relative to  $a_k$  be  $\theta$  and kink along pair axis be  $S_p$ . then rotation and translation parameters for side  $a_{k+1}$  are  $(180^\circ + \theta + \theta_t)$  and  $(S_{c_1} + S_p)$ .

### 2.4. Loop Closure Equations

The loop closure equations of a mechanism are derived using the following:

1. The mechanism is separated at some convenient pair or pairs such that the mechanism is divided into open loop kinematic chains. The open loop chains are then unfolded such that all perpendiculars to the pair axes lie along a line. This is possible only if the kink links at the

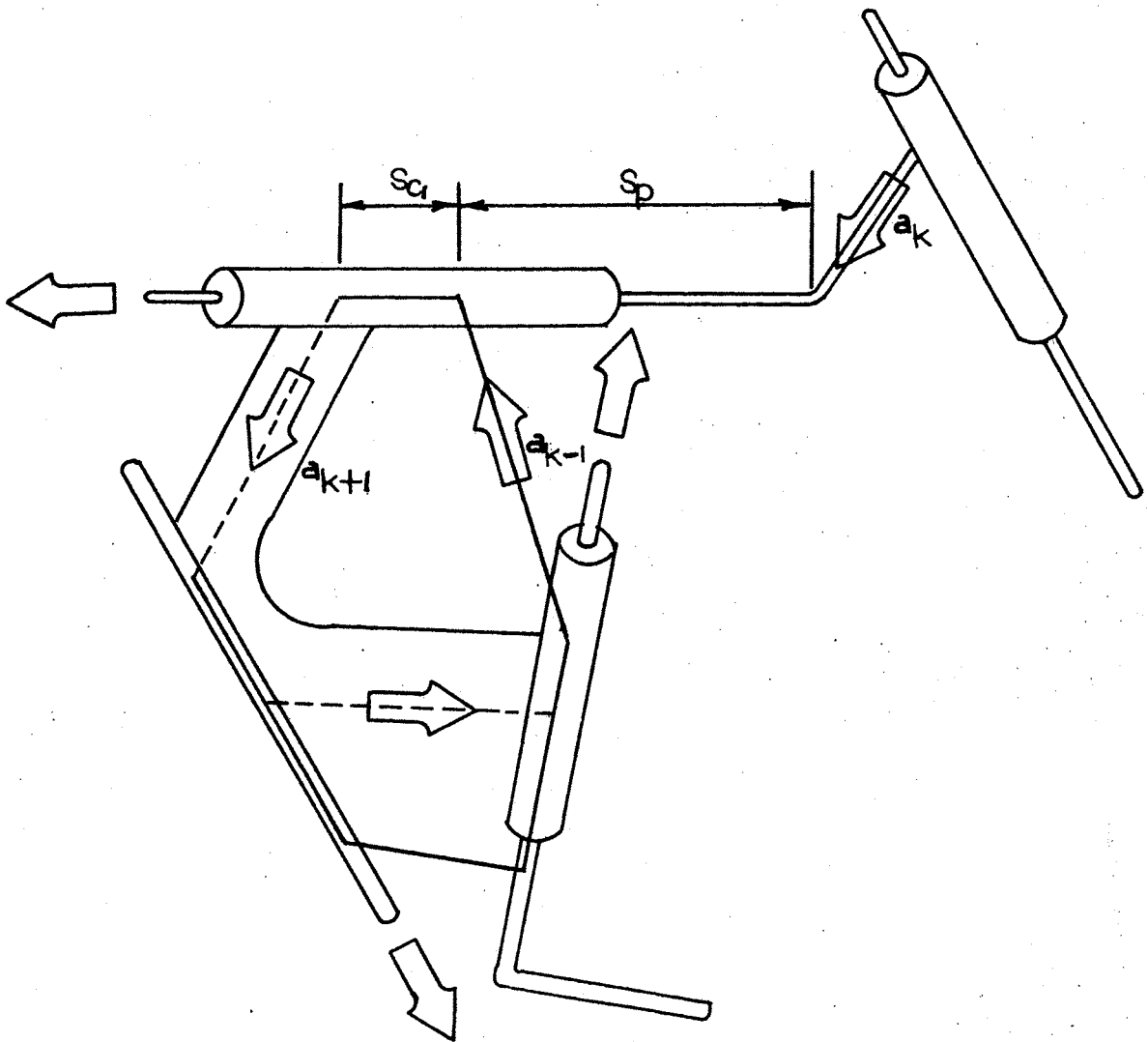


Figure 8. A Ternary Link in Space

pairs are reduced to zero, and the angle between the links is also zero.

Note that the link lengths and offset distances have directional sense of the loop and form a continuous directed polygon in space. Twist angles,  $\alpha_i$ 's, are angles between the adjacent pair axes measured in positive screw sense about directed link lengths, while rotation angles at pairs are angles between the adjacent links measured in positive screw sense about the directed offset distance common to the links. Throughout this work, this convention is followed to bring uniformity.

Figure 9 shows a RCGC mechanism. A is a revolute pair; B, C, and D are three cylinder pairs. Unit vectors parallel to the pair axes at pairs A, B, C and D are denoted by  $\hat{A}$ ,  $\hat{B}$ ,  $\hat{C}$ , and  $\hat{D}$ .  $P'Q$ ,  $Q'R$ ,  $R'T$  and  $T'P$  are perpendiculars between pair axes at A and B, B and C, C and D, and D and A. Note also that these are equal to link lengths  $a_1$ ,  $a_2$ ,  $a_3$  and  $a_4$  respectively. Note from Figure 9 that  $PP'$ ,  $QQ'$ ,  $RR'$  and  $TT'$  denote the kink lengths at the pairs and are denoted by  $S_1$ ,  $S_2$ ,  $S_3$  and  $S_4$ .

The mechanism is separated into two open loop chains by separating two elements of the cylinder pair located at C.  $ABC_1$  and  $DC_2$  become two open loop chains, where  $C_1$  and  $C_2$  are two elements of the pair at C. Now let the offset distances or kink lengths in the chains go to zero, i.e., let Q and Q', P and P' coincide in the chain  $ABC_1$ , and T and T', R and R' coincide in chain  $DC_2$ . Let the rotation angles at the pairs go to zero. In such a position all links are along a straight line as shown in Figure 10. In Figure 10, the mechanism has been unfolded along the Y axis. Let the rotation angles at pairs A, B, C, D be  $\theta_1$ ,  $\theta_2$ ,  $\theta_3$  and  $\theta_4$ , and let the twist angles between the pair axes be  $\alpha_1$ ,  $\alpha_2$ ,  $\alpha_3$ ,  $\alpha_4$ . Then in the unfolded positions of chain  $S_1 = S_2 = S_3 = S_4 = \theta_1 = \theta_2 = \theta_3 = \theta_4 = 0$ , and the vectors pointing in the direction of the pair axes and vectors  $\bar{R}(=\bar{R}')$ ,

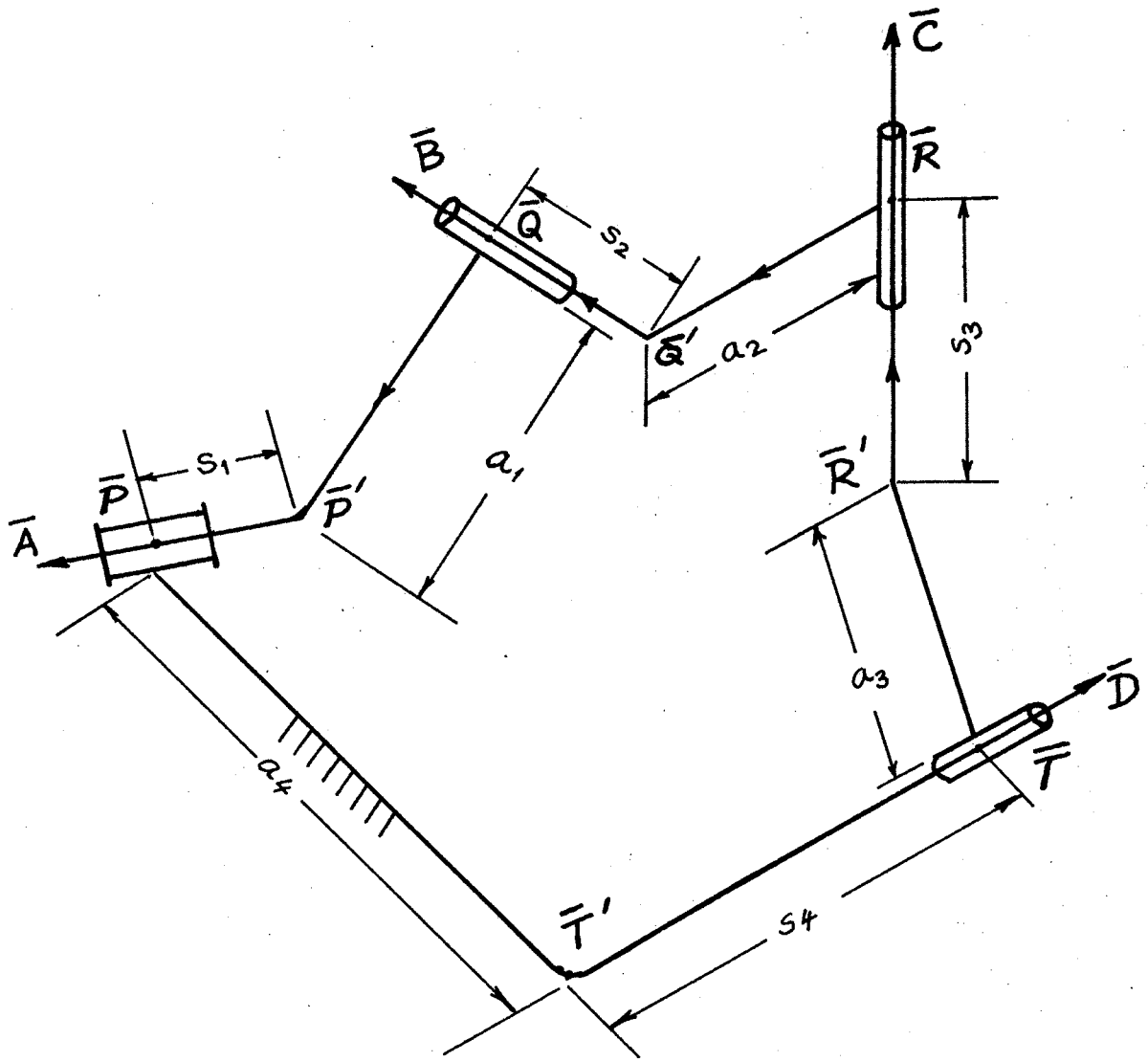


Figure 9. An RCCC Mechanism

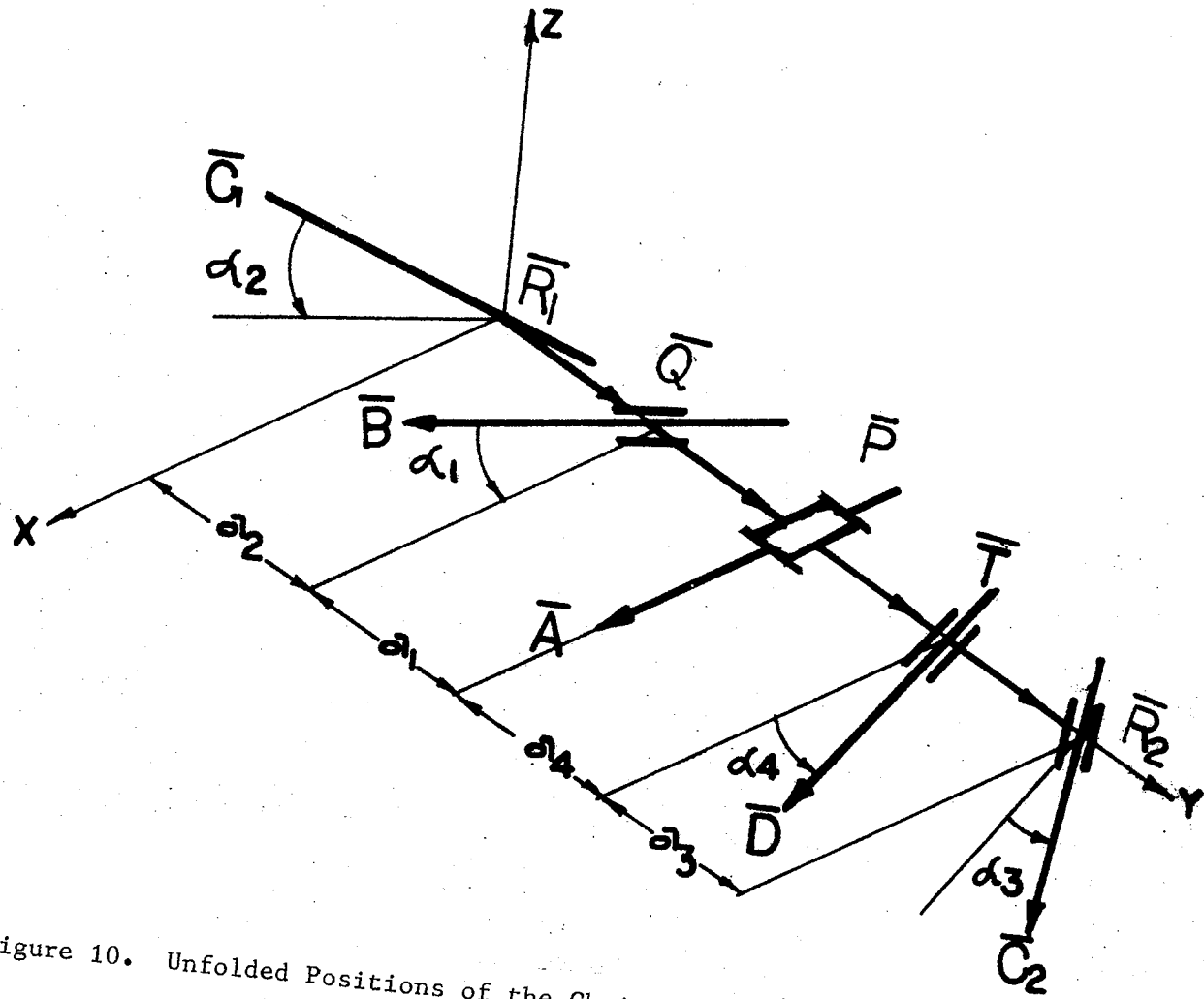


Figure 10. Unfolded Positions of the Chains Obtained From RCGG Mechanism

$\bar{P}(=\bar{P}')$ ,  $\bar{Q}(=\bar{Q}')$  and  $\bar{T}(=\bar{T}')$  are related to the twist angles and the link lengths by the following:

$$\bar{A} = \vec{l}$$

$$\bar{B} = \cos \alpha_1 \vec{l} + \sin \alpha_1 \vec{K}$$

$$\bar{C}_1 = \cos(\alpha_1 + \alpha_2) \vec{l} + \sin(\alpha_1 + \alpha_2) \vec{K}$$

$$\bar{D} = \cos(\alpha_4) \vec{l} - \sin(\alpha_4) \vec{K}$$

$$\bar{C}_2 = \cos(\alpha_3 + \alpha_4) \vec{l} - \sin(\alpha_3 + \alpha_4) \vec{K}$$

$$\bar{R}_1 = 0 \vec{l} + 0 \vec{j} + 0 \vec{K}$$

$$\bar{Q} = a_2 \vec{j}$$

$$\bar{P} = (a_1 + a_2) \vec{j}$$

$$\bar{T} = (a_1 + a_2 + a_4) \vec{j}$$

$$\bar{R}_2 = (a_1 + a_2 + a_3 + a_4) \vec{j}$$

2. The mechanism is next re-assembled by applying appropriate but often unknown pair motions. These pair motions, in general, may be considered as screw motions at the pairs. Since mechanism link lengths and offset distances have a directed sense, we note that  $\theta$ 's are measured in the opposite sense to the screw displacements for pairs left of the fixed link, while screw displacements at pairs are in the positive sense for the pairs to the right of the fixed link. This maintains a proper notation throughout. The pair motions at the input pair are known while

pair motion at other pairs are required to be computed to conduct displacement analysis.

For example, for the chain shown in Figure 10, the final position of  $\bar{C}_1$  and  $\bar{R}_1$  is obtained by screwing  $\bar{C}_1$  and  $\bar{R}_1$  about screw  $\hat{B}$  (screw axis direction -  $\bar{B}$ , screw axis passing through  $\bar{Q}$ , rotation  $\Theta_2$  and translation  $S_2$ ) and then about  $\hat{A}$  (screw axis direction -  $\bar{A}$ , screw axis passing through  $\bar{P}$ , rotation angle  $\Theta_1$  and constant slide  $S_1$ ). Note that screw axis direction has been reversed because  $\Theta$ 's are measured in the opposite sense to the screw displacements. The final position of the C pair may also be located by screwing  $\bar{C}_2$  and  $\bar{R}_2$  about  $\hat{D}$  (screw axis direction  $\bar{D}$ , screw axis passing through  $\bar{T}$ , rotation  $\Theta_4$  and translation  $S_4$ ).

3. The final position of the pair thus obtained from the successive screw displacements in the kinematic chain is constrained by the pair constraints.

For example, using the constraint condition from Equations (2.25) and (2.26) for the final positions of  $\bar{C}_1$ ,  $\bar{C}_2$ ,  $\bar{R}_1$ ,  $\bar{R}_2$ , we obtain

$$(\bar{C}_1) \text{ final position from chain } ABC_1 = (\bar{C}_2) \text{ final position from chain } DC_2 \quad (2.38)$$

$$(\bar{R}_1) \text{ final position from chain } ABC_1 = (\bar{R}_2) \text{ final position from chain } DC_2 + (\bar{C}_2)_{\text{final}} S_3 \quad (2.39)$$

4. The equations obtained in Step 3 are loop closure equations. All unwanted variables are eliminated to obtain one equation in one unknown which is usually in polynomial form.

5. The equations obtained in Step 4 are rearranged so that other parameters may be computed in closed form. Note that since the mecha-

nism loop has directional sense, the screws in the left side of the fixed link are negative screw displacements, while those on the right side of the fixed link are positive screw displacements.

6. Once all the variables of screws at pairs have been computed for a value of input screw, the displaced position of any link of the mechanism may be computed by locating the displaced position of the pairs and links.

7. For velocity and acceleration analysis, the velocity and accelerations of the pairs are obtained from two sides in the  $j^{\text{th}}$  position. The infinitesimal pair constraints are then used to obtain velocity and acceleration analysis equations. In general, these equations are linear in unknown rotation velocities, translational or sliding velocities, rotational acceleration and translational accelerations.

Four operators  $\Delta_1, \Delta_2, \Delta_3,$  and  $\Delta_4$  are defined. These will help make analysis equations more compact.  $\Delta_1$  gives the final position of a unit vector  $\bar{C}$  when it is rotated about axis  $\bar{B}$  by angle  $\theta_B$

$$(\bar{C})_{\text{final}} = \Delta_1 (\bar{C}, \bar{B}, \theta_B)$$

where the right hand side is defined in Equation (2.1).

$\Delta_2$  provides the final position of a unit vector  $\bar{C}$  when it is successively rotated about  $\bar{B}$  by  $\theta_B$  and  $\bar{A}$  by  $\theta_A$ .

$$(\bar{C})_{\text{final}} = \Delta_2 (\bar{C}, \bar{B}, \bar{A}, \theta_B, \theta_A)$$

where the right hand side is defined in Equation (2.10).

$\Delta_3$  gives the final position of a vector to a point ( $\bar{Q}$ ) when it is screwed by screw  $\hat{B}$  (unit vector  $\bar{B}$ , passing through P, rotation  $\theta_B$  and translation  $S_B$ ).



$$(\bar{Q})_{\text{final}} = \Delta_3 (\bar{Q}, \bar{P}, \bar{B}, \theta_B, S_B)$$

where the right hand side is defined in Equation (2.4).

$\Delta_4$  provides the final position of a vector  $(\bar{Q})$  to a point Q when it is successively screwed by screws  $\hat{B}$  (Unit vector  $\bar{B}$ , passing through  $\bar{P}$ , rotation  $\theta_B$ , and translation  $S_B$ ) and  $\hat{A}$  (unit vector  $\bar{A}$ , passing through  $\bar{O}$ , rotations  $\theta_A$  and translation  $S_A$ ).

$$(Q)_{\text{final}} = \Delta_4 (\bar{Q}, \bar{P}, \bar{O}, \bar{B}, \bar{A}, \theta_B, \theta_A, S_B, S_A)$$

where the right hand side is defined in Equation (2.11).

In the next chapter examples of five spatial, two-loop mechanisms using the method described here are presented.

## CHAPTER III

### APPLICATION TO MECHANISM ANALYSIS

In this chapter, the general method developed in Chapter II is used to conduct displacement, velocity and acceleration analysis of five types of two-loop, six-link mechanisms.

#### 3.1. Analysis of RCSR-CSR Mechanism

Figure 11 shows a Stephenson-3, fixed pivot RCSR-CSR space mechanism. A, D and G are three revolute pairs. One element of each of these pairs is fixed to the ground. Moving pairs B and E are cylindrical pairs. Spherical pairs are located at points C and F. The directional sense of the loop is shown in Figure 11. Unit vectors parallel to the pair axes at pairs A, B, D, E and G are denoted by  $\bar{A}$ ,  $\bar{B}$ ,  $\bar{D}$ ,  $\bar{E}$  and  $\bar{G}$  respectively.

The mechanism shown in Figure 11 has two independent directed loops ABCD and ABEFG. In loop ABCD,  $a_1$  is the link length between the pair axes at A and B;  $a_2$  is the perpendicular distance from the spherical point Q on the pair axes at B;  $a_3$  is the perpendicular distance from the spherical point Q on the pair axes at D;  $a_4$  is the link length between the pair axes A and D.  $S_1$  is the offset distance at the revolute pair at A and is constant;  $S_2$  is the offset distance at the cylinder pair located at B;  $S_4$  is the offset distance at the revolute pair at D and is constant. Note that the directions of link lengths  $a_1$ ,  $a_2$ ,  $a_3$ ,  $a_4$  and offset distances  $S_1$ ,  $S_2$  and  $S_4$  are so chosen that a continuous, directed, space polygon is

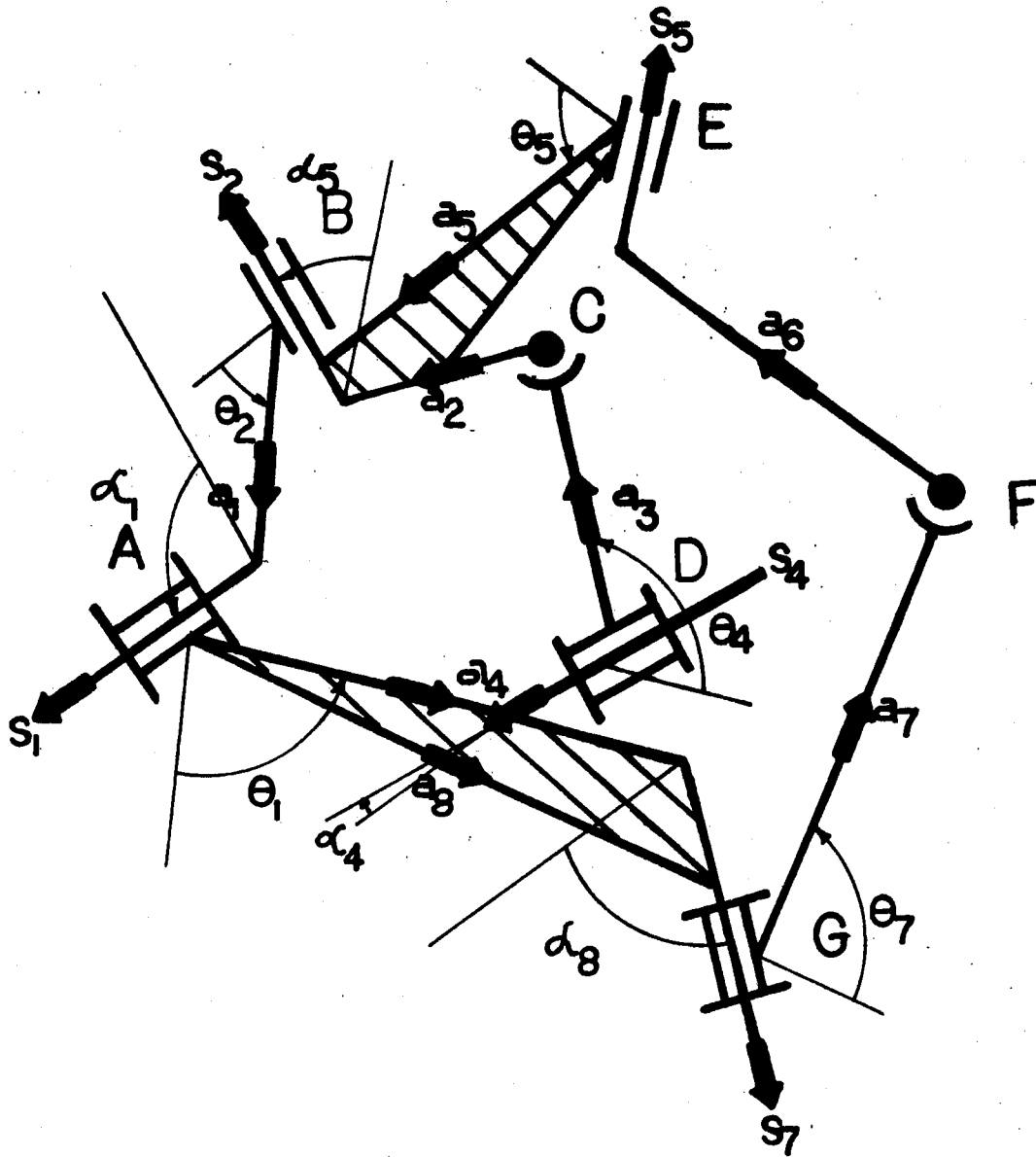


Figure 11. Six-Link Spatial RSCR-CSR Mechanism

formed. Twist angles are measured between adjacent pair axes in right hand screw sense about directed link lengths. In loop ABCD,  $\alpha_1$  is the twist angle between the pair axes at B and A;  $\alpha_4$  between the pair axes at A and D. Rotation  $\theta_1$  is the angle between links  $a_1$  and  $a_4$  measured in positive screw about the directed offset distance  $S_1$ . Similarly,  $\theta_2$  is the angle between links  $a_1$  and  $a_2$ , measured in positive sense about the directed offset  $S_2$ ;  $\theta_4$  is the angle between  $a_3$  and  $a_4$ , measured about offset  $S_4$ . In loop ABEFG,  $a_5$  is the link length between the pair axes at B and E;  $a_6$  is the perpendicular distance from the spheric point U to the axis at E;  $a_7$  is the perpendicular distance from the spheric point U on the axis at pair G;  $a_8$  is the link length between the pair axes at A and G.  $S_5$  and  $S_7$  are the offset distances at pairs at E and G.  $\alpha_5$  and  $\alpha_8$  are the twist angles between the pair axes at B and E, and the axes at A and G.  $\theta_5$  and  $\theta_8$  denote the rotation angles between links  $a_5$  and  $a_6$  and  $a_7$  and  $a_8$  measured in positive sense about offset distances  $S_5$  and  $S_8$ . Due to ternary links ADG and BCE, the rotation angles and offset distance at the revolute pair at A and the cylinder pair at B in loop ABEFG are different from those of ABCD. For loop ABEFG, the rotations at pair A and B are  $\theta_1 + \theta_{c_1}$  and  $\theta_2 + \theta_{c_2}$  respectively and the offset distances are  $S_1 + S_{c_1}$  and  $S_2 + S_{c_2}$ . Note  $\theta_{c_1}$ ,  $S_{c_1}$ ,  $\theta_{c_2}$  and  $S_{c_2}$  are ternary link parameters and

$$\theta_{c_1} = \theta_{t_1} + 180^\circ$$

$$\theta_{c_2} = \theta_{t_2} + 180^\circ$$

where  $\theta_{t_1}$  and  $\theta_{t_2}$  are the included angles of the ternary link with  $a_5$  and  $a_8$  reversed. Similarly,  $S_{c_1}$  and  $S_{c_2}$  are kinks of the ternary link at

A and B pairs.

The mechanism is separated into four open loop chains by dividing it at two spherical pairs located at C and F. The open loop chains are unfolded along a straight line such that all the links are collinear pointing in one direction. At this position, the rotation angles between the links and also kinks at the pairs are zero.

Unfolded chains are shown in Figures 12 and 13. Following vectors are defined from Figures 12 and 13.

Vectors parallel to the pair axes are:

$$\bar{A} = \vec{i} \quad (3.1)$$

$$\bar{B} = \cos \alpha_1 \vec{i} + \sin \alpha_1 \vec{k} \quad (3.2)$$

$$\bar{E} = \cos(\alpha_1 + \alpha_5) \vec{i} + \sin(\alpha_1 + \alpha_5) \vec{k} \quad (3.3)$$

$$\bar{D} = \cos(\alpha_4) \vec{i} - \sin(\alpha_4) \vec{k} \quad (3.4)$$

$$\bar{G} = \cos \alpha_8 \vec{i} - \sin \alpha_8 \vec{k} \quad (3.5)$$

Vectors locating the pair axes in space are:

$$\bar{u}_1 = 0 \quad (3.6)$$

$$\bar{T} = a_6 \vec{j} \quad (3.7)$$

$$\bar{P} = (a_5 + a_6) \vec{j} \quad (3.8)$$

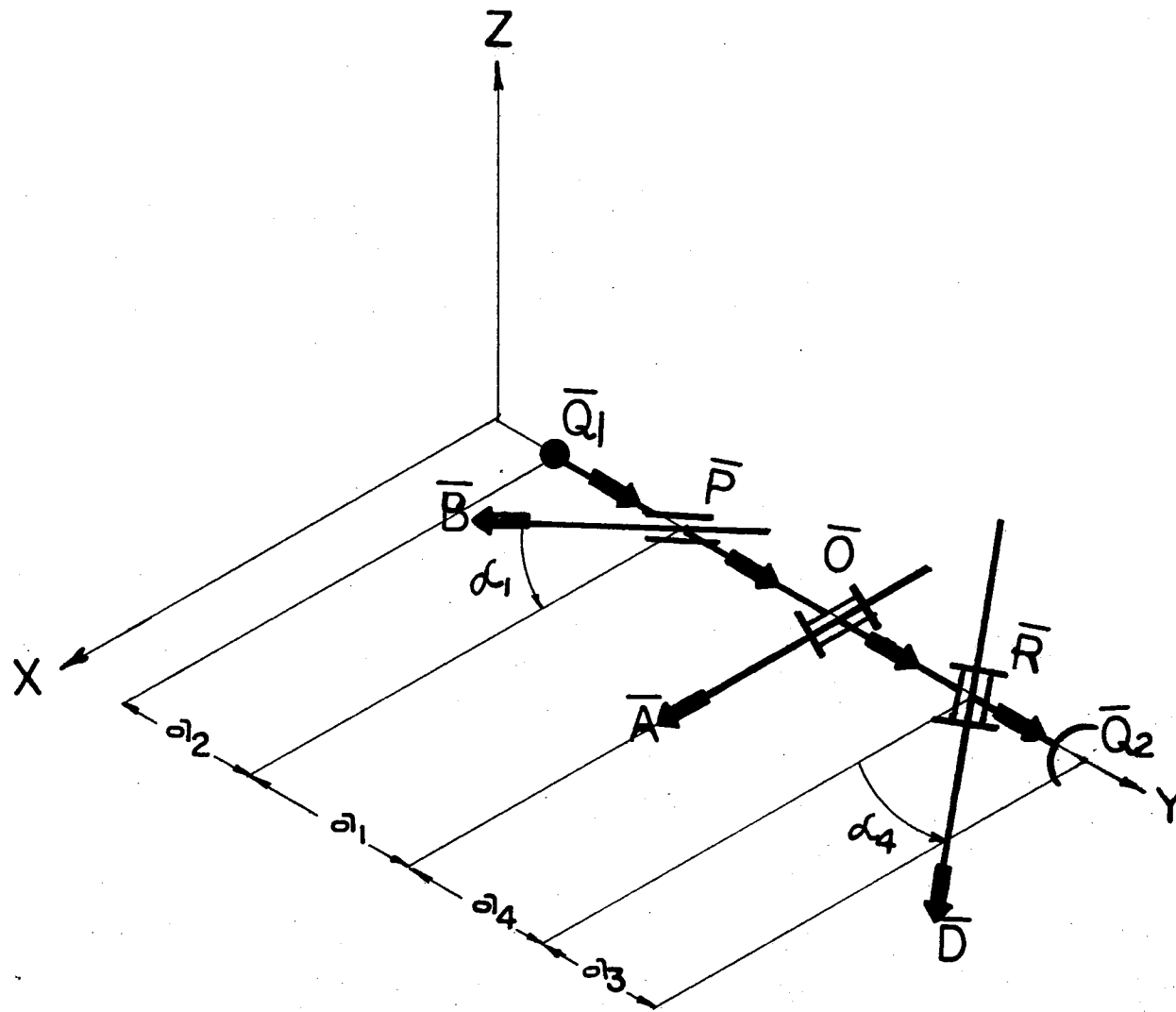


Figure 12. Unfolded Position of First-Loop of RSGR-CSR Mechanism

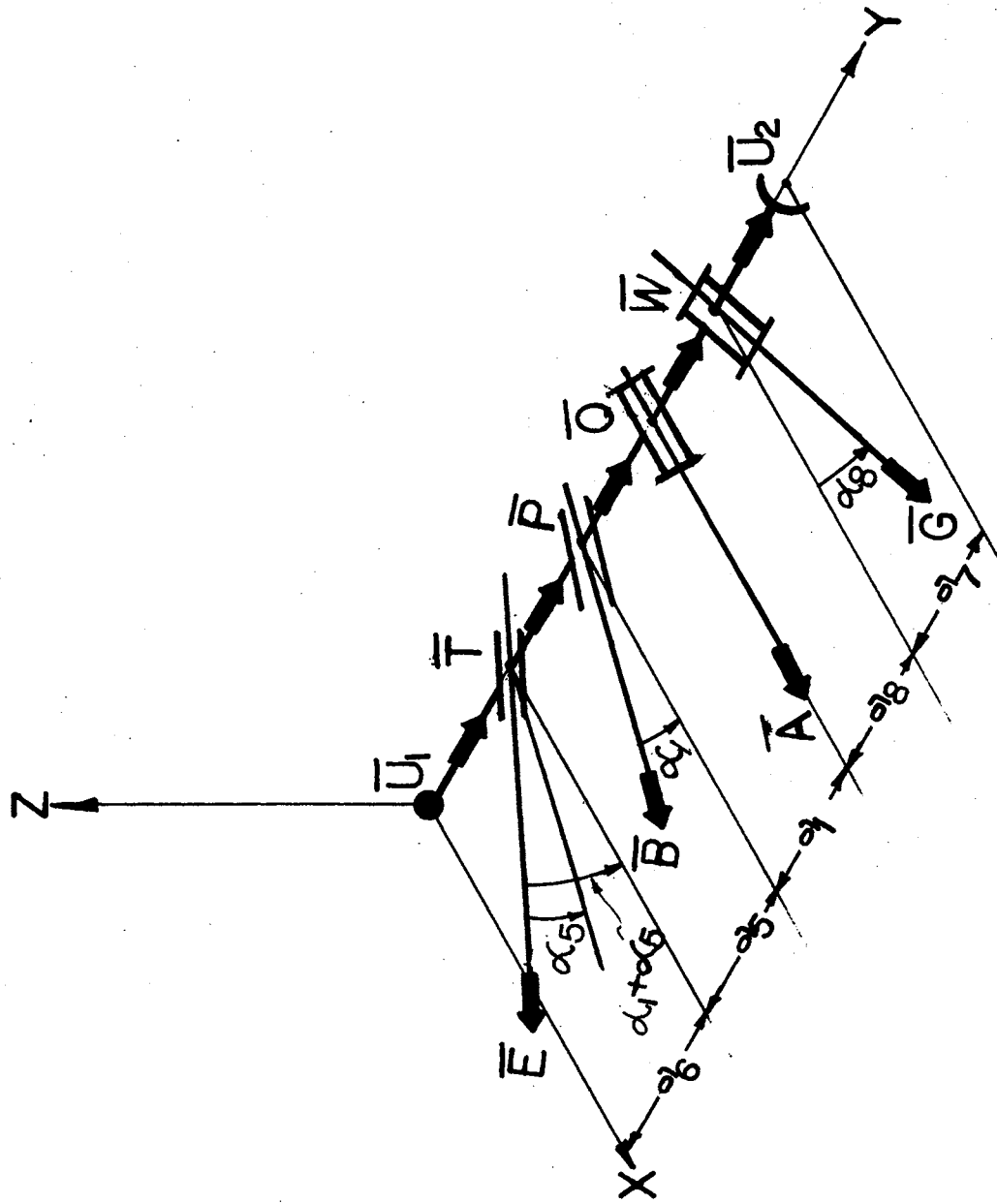


Figure 13. Unfolded Position of Second-Loop of RSCR-GSR Mechanism

$$\bar{O} = (a_1 + a_5 + a_6) \vec{j} \quad (3.9)$$

$$\bar{Q}_1 = (a_5 + a_6 - a_2) \vec{j} \quad (3.10)$$

$$\bar{W} = (a_1 + a_5 + a_6 + a_8) \vec{j} \quad (3.11)$$

$$\bar{u}_2 = (a_1 + a_5 + a_6 + a_7 + a_8) \vec{j} \quad (3.12)$$

$$\bar{R} = (a_1 + a_4 + a_5 + a_6) \vec{j} \quad (3.13)$$

$$\bar{Q}_2 = (a_1 + a_5 + a_6 + a_4 + a_3) \quad (3.14)$$

We first analyze the loop ABCD. The final position of  $Q_1$  may be obtained by screwing it about  $\hat{B}$  and then about  $\hat{A}$ . These screws are negative screws. Screw  $\hat{B}$  consists of rotations  $\theta_2$  and translation  $S_2$ ; screw  $\hat{A}$  consists of rotation  $\theta_1$  and translation  $S_1$ . The final position of spheric pair Q may also be obtained by screwing  $\bar{Q}_2$  about  $\hat{D}$ . This screw consists of rotation  $\theta_4$  and translation  $S_4$ . The final position of Q obtained from two sides is then equated. Let subscript j denote this displaced position.

$$\begin{aligned} \bar{Q}_{1j} = & c\theta_1 [(\bar{Q}'_1 - \bar{O}) - \{(\bar{Q}'_1 - \bar{O}) \cdot \bar{A}\} \bar{A}] \\ & - s\theta_1 [\bar{A} \times (\bar{Q}'_1 - \bar{O})] + \bar{O} \\ & + \{(\bar{Q}'_1 - \bar{O}) \cdot \bar{A}\} \bar{A} - \bar{A} S_1 \end{aligned} \quad (3.15)$$

where

$$\begin{aligned} \bar{Q}'_1 = & c\theta_2 [(\bar{Q}_1 - \bar{P}) - \{(\bar{Q}_1 - \bar{P}) \cdot \bar{B}\} \bar{B}] - \bar{B} S_2 \\ & + \bar{P} - s\theta_2 [\bar{B} \times (\bar{Q}_1 - \bar{P})] + \{(\bar{Q}_1 - \bar{P}) \cdot \bar{B}\} \bar{B} \end{aligned} \quad (3.16)$$



and also,

$$\begin{aligned}\bar{Q}_{2j} &= C\theta_4 [(\bar{Q}_2 - \bar{R}) - \{(\bar{Q}_2 - \bar{R}) \cdot \bar{D}\} \bar{D}] \\ &\quad + S\theta_4 [\bar{D} \times (\bar{Q}_2 - \bar{R})] + \bar{R} + \bar{D} S_4 \\ &\quad + \{(\bar{Q}_2 - \bar{R}) \cdot \bar{D}\} \bar{D}\end{aligned}\quad (3.17)$$

Now equating the final position of spheric pair  $Q_1$  obtained from two chains, that is,

$$\bar{Q}_{1j} = \bar{Q}_{2j} \quad (3.18)$$

we get

$$C\theta_2 \bar{N}_1 + S\theta_2 \bar{N}_2 + \bar{N}_3 - \bar{B}_j S_2 = C\theta_4 \bar{J}_1 + S\theta_4 \bar{J}_2 + \bar{J}_3 \quad (3.19)$$

where

$$\begin{aligned}\bar{N}_1 &= C\theta_1 [\bar{I}_1 - (\bar{I}_1 \cdot \bar{A}) \bar{A}] - S\theta_1 (\bar{A} \times \bar{I}_1) + (\bar{I}_1 \cdot \bar{A}) \bar{A} \\ \bar{N}_2 &= C\theta_1 [\bar{I}_2 - (\bar{I}_2 \cdot \bar{A}) \bar{A}] - S\theta_1 (\bar{A} \times \bar{I}_2) + (\bar{I}_2 \cdot \bar{A}) \bar{A} \\ \bar{N}_3 &= C\theta_1 [\bar{I}_3 - (\bar{I}_3 \cdot \bar{A}) \bar{A}] - S\theta_1 (\bar{A} \times \bar{I}_3) + \\ &\quad + \bar{O} - \bar{A} S_1 + (\bar{I}_3 \cdot \bar{A}) \bar{A} \\ \bar{I}_1 &= (\bar{Q}_1 - \bar{P}) - \{(\bar{Q}_1 - \bar{P}) \cdot \bar{B}\} \bar{B} \\ \bar{I}_2 &= -\bar{B} \times (\bar{Q}_1 - \bar{P}) \\ \bar{I}_3 &= \{(\bar{Q}_1 - \bar{P}) \cdot \bar{B}\} \bar{B} + \bar{P} - \bar{O} \\ \bar{B}_j &= C\theta_1 [\bar{B} - (\bar{B} \cdot \bar{A}) \bar{A}] - S\theta_1 (\bar{A} \times \bar{B}) + (\bar{B} \cdot \bar{A}) \bar{A}\end{aligned}$$

$$\bar{J}_1 = (\bar{Q}_2 - \bar{R}) - \{(\bar{Q}_2 - \bar{R}) \cdot \bar{D}\} \bar{D}$$

$$\bar{J}_2 = \bar{D} \times (\bar{Q}_2 - \bar{R})$$

$$\bar{J}_3 = \{(\bar{Q}_2 - \bar{R}) \cdot \bar{D}\} \bar{D} + \bar{R} + \bar{D} S_4$$

Dotting Equation (3.19) with  $(\bar{N}_1 \times \bar{B}_j)$  and  $(\bar{N}_2 \times \bar{B}_j)$  we get two equations expressing  $C\theta_2$  and  $S\theta_2$  as follows.

$$C\theta_2 = \frac{(\bar{N}_2 \times \bar{B}_j) \cdot (\bar{J}_1 C\theta_4 + \bar{J}_2 S\theta_4 + (\bar{J}_3 - \bar{N}_3))}{(\bar{N}_2 \times \bar{B}_j) \cdot \bar{N}_1} \quad (3.20)$$

$$S\theta_2 = \frac{(\bar{N}_1 \times \bar{B}_j) \cdot (\bar{J}_1 C\theta_4 + \bar{J}_2 S\theta_4 + (\bar{J}_3 - \bar{N}_3))}{(\bar{N}_1 \times \bar{B}_j) \cdot \bar{N}_2} \quad (3.21)$$

Squaring Equations (3.20) and (3.21) and using the identity  $C^2\theta_2 + S^2\theta_2 = 1$ , we get

$$\sum_{n=0}^4 P_n \tan^{n/2} \theta_4 = 0 \quad (3.22a)$$

where

$$P_4 = A_1^2 + B_1^2 - 2A_1A_3 - 2B_1B_3 + 1 + A_3^2 + B_3^2$$

$$P_3 = -4A_1A_2 - 4B_1B_2 + 4A_2A_3 + 4B_2B_3$$

$$P_2 = 4(A_2^2 + B_2^2) + 2(A_3^2 + B_3^2) - 2(A_1^2 + B_1^2) - 2$$

$$P_1 = 4(A_1 A_2 + B_1 B_2) + 4(A_2 A_3 + B_2 B_3)$$

$$P_0 = A_1^2 + B_1^2 + 2(A_1 A_3 + B_1 B_3) + A_3^2 + B_3^2 - 1$$

$$A_1 = (\bar{N}_2 \times \bar{B}_j) \cdot \bar{J}_1 / (\bar{N}_2 \times \bar{B}_j) \cdot \bar{N}_1 \quad (3.22b)$$

$$A_2 = (\bar{N}_2 \times \bar{B}_j) \cdot \bar{J}_2 / (\bar{N}_2 \times \bar{B}_j) \cdot \bar{N}_1$$

$$A_3 = (\bar{N}_2 \times \bar{B}_j) \cdot \bar{J}_3 / (\bar{N}_2 \times \bar{B}_j) \cdot \bar{N}_1$$

$$B_1 = (\bar{N}_1 \times \bar{B}_j) \cdot \bar{J}_1 / (\bar{N}_1 \times \bar{B}_j) \cdot \bar{N}_2$$

$$B_2 = (\bar{N}_1 \times \bar{B}_j) \cdot \bar{J}_2 / (\bar{N}_1 \times \bar{B}_j) \cdot \bar{N}_2$$

$$B_3 = (\bar{N}_1 \times \bar{B}_j) \cdot \bar{J}_3 / (\bar{N}_1 \times \bar{B}_j) \cdot \bar{N}_2$$

From Equation (3.22) we may obtain at most four real roots of  $\theta_4$ ; for each real root of  $\theta_4$ ,  $\theta_2$  may be obtained using Equations (3.20) and (3.21).  $S_2$  may then be expressed using Equation (3.19) as

$$S_2 = C\theta_4 (\bar{J}_1 \cdot \bar{B}_j) + S\theta_4 (\bar{J}_2 \cdot \bar{B}_j) + (\bar{J}_3 \cdot \bar{B}_j) - (\bar{N}_3 \cdot \bar{B}_j) - C\theta_2 (\bar{N}_1 \cdot \bar{B}_j) - S\theta_2 (\bar{N}_2 \cdot \bar{B}_j) \quad (3.23)$$

The position of the spherical pair is computed using Equation (3.15) or Equation (3.17).

Note that  $\bar{U}_1$ ,  $\bar{T}$ ,  $\bar{E}_j$  and  $\bar{G}_j$  are functions of known quantities and are described below.

$$\begin{aligned}\bar{u}_1' &= C\theta_1 [(\bar{u}_1'' - \bar{o}) - \{(\bar{u}_1'' - \bar{o}) \cdot \bar{A}\} \bar{A}] \\ &\quad - S\theta_1 [\bar{A} \times (\bar{u}_1'' - \bar{o})] + \bar{o} - \bar{A} S_1 \\ &\quad + \{(\bar{u}_1'' - \bar{o}) \cdot \bar{A}\} \bar{A}\end{aligned}$$

$$\begin{aligned}\bar{u}_1'' &= C(\theta_2 + \theta_{c_2}) [(\bar{u}_1 - \bar{p}) - \{(\bar{u}_1 - \bar{p}) \cdot \bar{B}\} \bar{B}] \\ &\quad - S(\theta_2 + \theta_{c_2}) [\bar{B} \times (\bar{u}_1 - \bar{p})] + \bar{p} - \bar{B}(S_2 + S_{c_2}) \\ &\quad + \{(\bar{u}_1 - \bar{p}) \cdot \bar{B}\} \bar{B}\end{aligned}$$

$$\begin{aligned}\bar{T}' &= C\theta_1 [(\bar{T}'' - \bar{o}) - \{(\bar{T}'' - \bar{o}) \cdot \bar{A}\} \bar{A}] - \bar{A} S_1 \\ &\quad - S\theta_1 [\bar{A} \times (\bar{T}'' - \bar{o})] + \{(\bar{T}'' - \bar{o}) \cdot \bar{A}\} \bar{A} + \bar{o}\end{aligned}$$

$$\begin{aligned}\bar{T}'' &= C(\theta_2 + \theta_{c_2}) [(\bar{T} - \bar{p}) - \{(\bar{T} - \bar{p}) \cdot \bar{B}\} \bar{B}] \\ &\quad - S(\theta_2 + \theta_{c_2}) [\bar{B} \times (\bar{T} - \bar{p})] + \bar{p} \\ &\quad + \{(\bar{T} - \bar{p}) \cdot \bar{B}\} \bar{B} - \bar{B}(S_2 + S_{c_2})\end{aligned}$$

$$\begin{aligned}\bar{E}_j &= C\theta_1 [\bar{E}' - (\bar{E}' \cdot \bar{A}) \bar{A}] - S\theta_1 (\bar{A} \times \bar{E}') \\ &\quad + (\bar{E}' \cdot \bar{A}) \bar{A}\end{aligned}$$

$$\begin{aligned}\bar{E}' &= C(\theta_2 + \theta_{c_2}) [\bar{E} - (\bar{E} \cdot \bar{B}) \bar{B}] + (\bar{E} \cdot \bar{B}) \bar{B} \\ &\quad - S(\theta_2 + \theta_{c_2}) [\bar{B} \times \bar{E}]\end{aligned}$$

This completes the displacement analysis of loop ABCD. Next the loop ABEFG is analyzed. The final position of  $\bar{U}$  is obtained by screwing  $\bar{U}_1$  successively by screw  $\hat{E}$  (parallel to  $\bar{E}$ , passing through  $\bar{T}$ , rotation  $\theta_5$ , translation  $S_5$ ), screw  $\hat{B}$  (parallel to  $\bar{B}$ , passing through  $\bar{P}$ , rotation  $\theta_2 + \theta_{c_2}$ , translation  $S_2 + S_{c_2}$ ), screw  $\hat{A}$  (parallel to  $\bar{A}$ , passing through  $\bar{O}$ , rotation  $\theta_1$ , translation  $S_1$ ). The final position of  $\bar{U}$  may also be obtained by screwing  $\bar{U}_2$  successively by screw  $\hat{G}$  (parallel to  $\bar{G}$ , passing through  $\bar{W}$ , rotation  $\theta_7$ , translation  $S_7$ ) and screw  $\hat{A}$  (parallel to  $\bar{A}$ , rotation  $\theta_{c_1}$ , translation  $S_{c_1}$ ). Note that screws for the left hand side of the fixed link are negative screws. Equating the two final positions of the second spheric pair, that is,

$$\bar{U}_{1j} = \bar{U}_{2j}$$

we obtain

$$\begin{aligned} & \cos[(\bar{u}'_1 - \bar{T}') - \{(\bar{u}'_1 - \bar{T}') \cdot \bar{E}_j\} \bar{E}_j] \\ & - \sin[\bar{E}_j \times (\bar{u}'_1 - \bar{T}')] + \{(\bar{u}'_1 - \bar{T}') \cdot \bar{E}_j\} \bar{E}_j \\ & + \bar{T}' - \bar{E}_j S_5 \\ & = \cos[(\bar{u}'_2 - \bar{W}') - \{(\bar{u}'_2 - \bar{W}') \cdot \bar{G}_j\} \bar{G}_j] \\ & + \sin[\bar{G}_j \times (\bar{u}'_2 - \bar{W}')] \\ & + \bar{W}' + \bar{G}_j S_7 + \{(\bar{u}'_2 - \bar{W}') \cdot \bar{G}_j\} \bar{G}_j \end{aligned}$$

$$\begin{aligned}\bar{u}'_2 = & C\theta c_1 [(\bar{u}_2 - \bar{o}) - \{(\bar{u}_2 - \bar{o}) \cdot \bar{A}\} \bar{A}] \\ & + S\theta c_1 [\bar{A} \times (\bar{u}_2 - \bar{o})] + \bar{A} s c_1 \\ & + \{(\bar{u}_2 - \bar{o}) \cdot \bar{A}\} \bar{A}\end{aligned}$$

Equation (3.24) may be written as

$$\begin{aligned}\bar{I}'_1 C\theta_5 + \bar{I}'_2 S\theta_5 + \bar{I}'_3 - \bar{E}_j S_5 \\ = \bar{J}'_1 C\theta_7 + \bar{J}'_2 S\theta_7 + \bar{J}'_3\end{aligned}\quad (3.25)$$

where definitions of vectors  $\bar{I}'_1$ ,  $\bar{I}'_2$ ,  $\bar{I}'_3$ ,  $\bar{J}'_1$ ,  $\bar{J}'_2$ , and  $\bar{J}'_3$  follow from Equation (3.24) and these are functions of known quantities.

Eliminating  $S\theta_5$  and  $C\theta_5$  from Equation (3.25) by dotting Equation (3.25) by  $\bar{I}'_1 \times \bar{E}_j$  and  $\bar{I}'_2 \times \bar{E}_j$ , we get

$$C\theta_5 = \frac{(\bar{I}'_2 \times \bar{E}_j) \cdot (\bar{J}'_1 C\theta_7 + \bar{J}'_2 S\theta_7 + \bar{J}'_3 - \bar{I}'_3)}{(\bar{I}'_2 \times \bar{E}_j) \cdot \bar{I}'_1}\quad (3.26)$$

and similarly

$$S\theta_5 = \frac{(\bar{I}'_1 \times \bar{E}_j) \cdot (\bar{J}'_1 C\theta_7 + \bar{J}'_2 S\theta_7 + \bar{J}'_3 - \bar{I}'_3)}{(\bar{I}'_1 \times \bar{E}_j) \cdot \bar{I}'_2}\quad (3.27)$$

or

$$C\theta_5 = C_1 C\theta_7 + C_2 S\theta_7 + C_3$$

$$S\theta_5 = D_1 C\theta_7 + D_2 S\theta_7 + D_3$$

where definitions of  $C_1$ ,  $C_2$ ,  $C_3$ ,  $D_1$ ,  $D_2$ , and  $D_3$  follow from Equations

(3.26) and (3.27). Squaring Equations (3.26) and (3.27) and using the identity  $C^2\theta_5 + S^2\theta_5 = 1$ , we obtain

$$\sum_{i=0}^4 Z_i \tan^{i/2} \theta_7 \quad (3.28)$$

where  $Z_i$ 's are known functions of  $C_1, C_2, C_3, D_1, D_2$ , and  $D_3$ .  $Z_i$  may be obtained from Equation (3.22a) by replacing  $P_i$  by  $Z_i$ , A's by C's and B's by D's.

There are at most four values of  $\theta_7$  from Equation (3.28) and for each value of  $\theta_7$ ,  $\theta_5$  may be computed using Equations (3.26) and (3.27).  $S_5$  is expressed as

$$S_5 = [\bar{I}_1' C\theta_5 + \bar{I}_2' S\theta_5 + \bar{I}_3'] \cdot \bar{E}_j - [\bar{J}_1' C\theta_7 + \bar{J}_2' S\theta_7 + \bar{J}_3'] \cdot \bar{E}_j \quad (3.29)$$

This completes the displacement analysis of RSCR-CSR mechanism.

Loop ABCD has four loop closures and for each closure of loop 1, there are four closures for loop 2. Hence, for each position of the input link, there are sixteen positions of other links.

The position of any point or line, on any link can be computed by screwing it in the unfolded position about the screws intercepted between that link and the fixed link. Note that after performing the displacement analysis, screws at all the pairs are known. To perform velocity and acceleration analysis, positions of all the links and pairs are computed using known successive screw displacements. Let this position be denoted by subscript  $j$ . Consider the loop  $AB_j Q_j D$ . The velocity

of  $\bar{Q}_j$  may be found by providing infinitesimal screw displacement to Q about  $\hat{B}_j$  and  $\hat{A}_j$ . The velocity of  $\bar{Q}_j$  may also be found by screwing  $\bar{Q}_j$  by infinitesimal screw about  $\hat{D}$ . Equating the velocities obtained from these two methods,

$$\begin{aligned} -\dot{\bar{Q}}_j &= \bar{A} \times (\bar{Q}_j - \bar{O}_j) \omega_1 + \bar{B}_j \times (\bar{Q}_j - \bar{P}_j) \omega_2 \\ &\quad + \bar{B}_j \dot{S}_2 \\ &= -\bar{D} \times (\bar{Q}_j - \bar{R}) \omega_4 \end{aligned} \quad (3.30)$$

Let  $\omega_1$  be the input velocity which is known. Vector Equation (3.30) contains three unknowns  $\omega_2$ ,  $\omega_4$  and  $S_2$ . These may be computed from three linear equations obtained from vector Equation (3.30).

Other velocities in loop ABCD are,

$$\dot{\bar{B}}_j = -(\bar{A} \times \bar{B}_j) \omega_1$$

$$\dot{\bar{P}}_j = -\bar{A} \times (\bar{P}_j - \bar{O}) \omega_1 - \bar{B}_j \dot{S}_2$$

Acceleration analysis of loop 1 is performed by differentiating Equation (3.30) to get,

$$\begin{aligned} \ddot{\bar{Q}}_j &= \bar{A} \times (\dot{\bar{Q}}_j) \omega_1 + \dot{\bar{B}}_j \times (\bar{Q}_j - \bar{P}_j) \omega_2 \\ &\quad + \bar{B}_j \times (\dot{\bar{Q}}_j - \dot{\bar{P}}_j) \omega_2 + \bar{B}_j \ddot{S}_2 + \dot{\bar{B}}_j \dot{S}_2 \\ &\quad + \bar{B}_j \times (\bar{Q}_j - \bar{P}_j) \dot{\omega}_2 \\ &= -\bar{D} \times (\bar{Q}_j - \bar{R}) \dot{\omega}_4 \\ &\quad - \bar{D} \times \dot{\bar{Q}}_j \omega_4 \end{aligned} \quad (3.31)$$

where  $\dot{\omega}_2$  and  $\dot{\omega}_4$  are angular accelerations at pairs B and D,  $\ddot{S}_2$  is trans-



lational acceleration at pair B. These appear as unknowns in vector Equation (3.31) and may be computed from the three linear equations obtained from Equation (3.31).

The procedure for performing velocity and acceleration analysis of the second loop is similar. The velocity of the second spheric pair denoted by  $\bar{U}_j$  is found by providing infinitesimal motions of chains  $AB_jE_jU_j$  and  $ADW_jU_j$ . These two velocities are equated to obtain

$$\begin{aligned}
 -\dot{\bar{u}}_j &= \bar{A} \times (\bar{u}_j - \bar{o}) \omega_1 + \omega_2 \bar{B}_j \times (\bar{u}_j - \bar{p}_j) \\
 &\quad + \bar{E}_j \times (\bar{u}_j - \bar{T}_j) \omega_5 \\
 &\quad + \bar{B}_j \dot{S}_2 + \bar{E}_j \dot{S}_5 \\
 &= -\bar{G}_j \times (\bar{u}_j - \bar{w}_j) \omega_7 \quad (3.32)
 \end{aligned}$$

$\omega_5$ ,  $S_5$  and  $\omega_7$  are computed using the three linear equations obtained from vector Equation (3.32).

Differentiating Equation (3.32) to perform acceleration analysis,

$$\begin{aligned}
 -\ddot{\bar{u}}_j &= \bar{A} \times (\dot{\bar{u}}_j) \omega_1 + \dot{\omega}_2 \bar{B}_j \times (\bar{u}_j - \bar{p}_j) \omega_2 \\
 &\quad + \bar{B}_j \times (\dot{\bar{u}}_j - \dot{\bar{p}}_j) \omega_2 + \dot{\bar{E}}_j \dot{S}_5 + \bar{E}_j \ddot{S}_5 \\
 &\quad + \dot{\bar{E}}_j \times (\bar{u}_j - \bar{T}_j) \omega_5 + \bar{E}_j \times (\dot{\bar{u}}_j - \dot{\bar{T}}_j) \omega_5 \\
 &\quad + \bar{E}_j \times (\dot{\bar{u}}_j - \dot{\bar{T}}_j) \omega_5 + \dot{\bar{B}}_j \dot{S}_2 + \bar{B}_j \ddot{S}_2 \\
 &\quad + \bar{B}_j \times (\dot{\bar{u}}_j - \dot{\bar{p}}_j) \omega_2 \\
 &= -\bar{G}_j \times \dot{\bar{u}}_j \omega_7 - \dot{\omega}_7 \bar{G}_j \times (\bar{u}_j - \bar{w}_j) \quad (3.33)
 \end{aligned}$$

where

$$\begin{aligned}\dot{\bar{E}}_j &= -(\bar{A}\omega_1 + \bar{B}_j\omega_2) \times \bar{E}_j \\ -\bar{T}_j &= \bar{A} \times (\bar{T}_j - \bar{O}) \omega_1 + \bar{B}_j \times (\bar{T}_j - P_j) \omega_2 \\ &\quad + \bar{B}_j \dot{S}_2 + \bar{E}_j \dot{S}_5\end{aligned}$$

$\dot{\omega}_5$ ,  $\ddot{S}_5$  and  $\dot{\omega}_7$  are computed using the three linear equations obtained from Vector Equation (3.33).

Now the velocity and acceleration of any point or line on any coupler link can be computed since instantaneous screws at all the pairs are known. Table I presents a numerical example of displacement analysis of a RSCR-CSR mechanism.

### 3.2. Analysis of RSCR-CCG Mechanism

Figure 14 shows a Stephenson-3 fixed pivot type RSCR-CCG mechanism. This mechanism is obtained by replacing in Figure 11 the spherical pair at F by a cylinder pair and the revolute pair at G by a cylinder pair. The nomenclature of Figure 11 is retained here. Additional parameters necessary to specify the mechanism are  $\alpha_6$ , the twist angle between the axes at pairs E and F, measured in positive sense about link  $a_6$ ;  $\alpha_7$ , the twist angle between the axes at pairs F and G, measured in positive sense about length  $a_7$ ;  $S_6$  and  $S_7$  variable offset distances at the cylinder pairs at F and G, measured in positive sense to close the directed loop.

Since the loop ABCD of Figure 14 and Figure 11 are the same, the analysis of the two is the same. Note that the analysis of loop ABCD is performed independent of loop ABEFG. Loop ABEFG is analyzed by separating the two elements of the cylinder pair located at F, thus dividing the

TABLE I

## ANALYSIS OF RSCR-CSR MECHANISM

Parameters of the mechanism are:

$$\alpha_1 = 30^\circ, \alpha_2 = 40^\circ, \alpha_4 = 15^\circ, \alpha_5 = 20^\circ, \alpha_6 = 50^\circ, \theta_2 = 18^\circ, s_2 = 0.1$$

$$s_1 = 0.1, s_4 = 0, s_8 = 0.01, a_1 = 1.0, a_2 = 1.5, a_3 = 1.3, a_4 = 0.8$$

$$a_5 = 1.2, a_6 = 0.8, a_7 = 0.65, a_8 = 0.95, \theta_{c1} = -10^\circ, s_{c1} = -0.4$$

One of the 16 solutions is shown below:

$\theta_1$	$\theta_2$	$\theta_4$	$\theta_5$	$\theta_7$	$s_2$	$s_5$
120	68.711	21.631	5.642	51.23	-0.962	0.241
130	53.952	20.010	15.546	43.87	-0.881	0.202
140	41.801	16.552	17.984	35.98	-0.753	0.163
150	30.893	12.302	18.102	27.76	-0.602	0.131
160	20.731	7.563	18.098	19.19	-0.441	0.103
170	11.192	2.364	19.477	9.91	-0.264	0.071
180	-0.725	-0.685	28.376	0.21	-0.095	0.024
190	-8.852	-7.056	41.414	-13.64	0.096	0.021
220	-38.831	-21.555	-55.821	-4.70	0.572	0.204
230	-50.278	-25.494	-47.088	-13.83	0.711	0.206
240	-63.196	-28.432	-36.917	-21.51	0.802	0.215
250	-81.196	-28.030	-12.856	-28.39	0.811	0.241

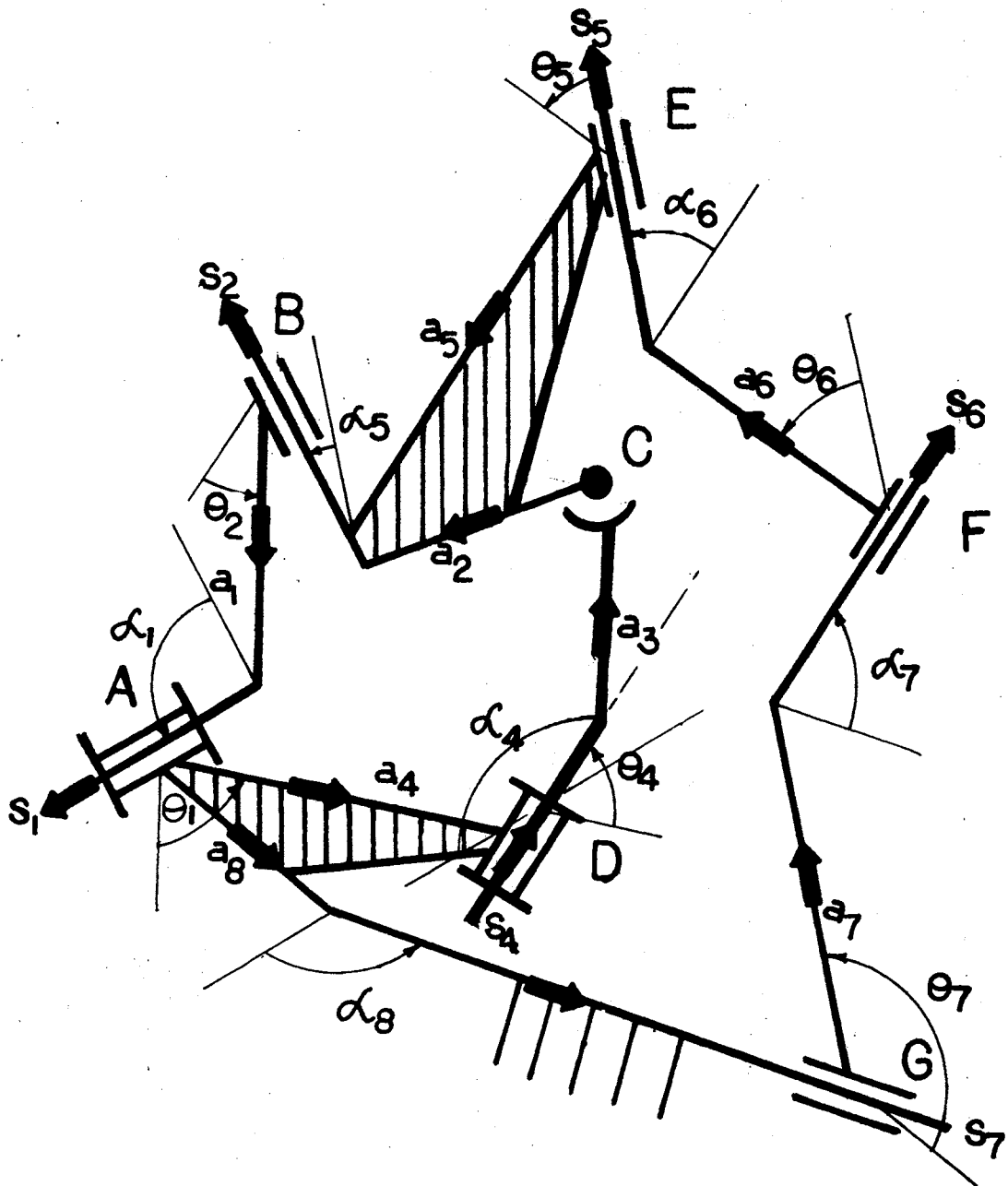


Figure 14. Six-Link, Spatial RCSR-CCC Mechanism

mechanism into two open loop chains  $ABEF_1$  and  $AGF_2$ . The two chains are then unfolded along a straight line as described in Chapter II. The unfolded position of kinematic chains is shown in Figure 15.

The following vectors for Figure 15, in addition to those defined by Equations (3.1) - (3.14), are defined.

$$\bar{F}_1 = \cos(\alpha_1 + \alpha_5 + \alpha_6) \bar{i} + \sin(\alpha_1 + \alpha_5 + \alpha_6) \bar{k}$$

$$\bar{F}_2 = \cos(\alpha_7 + \alpha_8) \bar{i} - \sin(\alpha_7 + \alpha_8) \bar{k}$$

The final position of the axis at F via successive screw displacements of chain  $ABEF_1$  and also via chain  $AGF_2$  is located. Since F is a cylinder pair, we use the pair constraint Equations (2.25) and (2.26) of Chapter II.

The final position of the direction of axes  $\bar{F}_1$  and  $\bar{F}_2$  obtained from two chains are

$$\begin{aligned} (\bar{F}_1)_{\text{final}} = & \cos\theta_5 [\bar{F}_1' - (\bar{F}_1' \cdot \bar{E}') \bar{E}'] + (\bar{F}_1' \cdot \bar{E}') \bar{E}' \\ & - \sin\theta_5 (\bar{E}' \times \bar{F}_1') \end{aligned} \quad (3.35)$$

$$\begin{aligned} (\bar{F}_2)_{\text{final}} = & \cos\theta_7 [\bar{F}_2' - (\bar{F}_2' \cdot \bar{G}') \bar{G}'] + (\bar{F}_2' \cdot \bar{G}') \bar{G}' \\ & + \sin\theta_7 (\bar{G}' \times \bar{F}_2') \end{aligned} \quad (3.36)$$

where

$$\bar{F}_1' = \Delta_2(\bar{F}_1, -\bar{B}, -\bar{A}, \theta_2 + \theta_{c_2}, \theta_1)$$

$$\bar{E}' = \Delta_2(\bar{E}, -\bar{B}, -\bar{A}, \theta_2 + \theta_{c_2}, \theta_1)$$

$$\bar{F}_2' = \Delta_1(\bar{F}_2, \bar{A}, \theta_{c_1})$$

$$\bar{G}' = \Delta_1(\bar{G}, \bar{A}, \theta_{c_1})$$

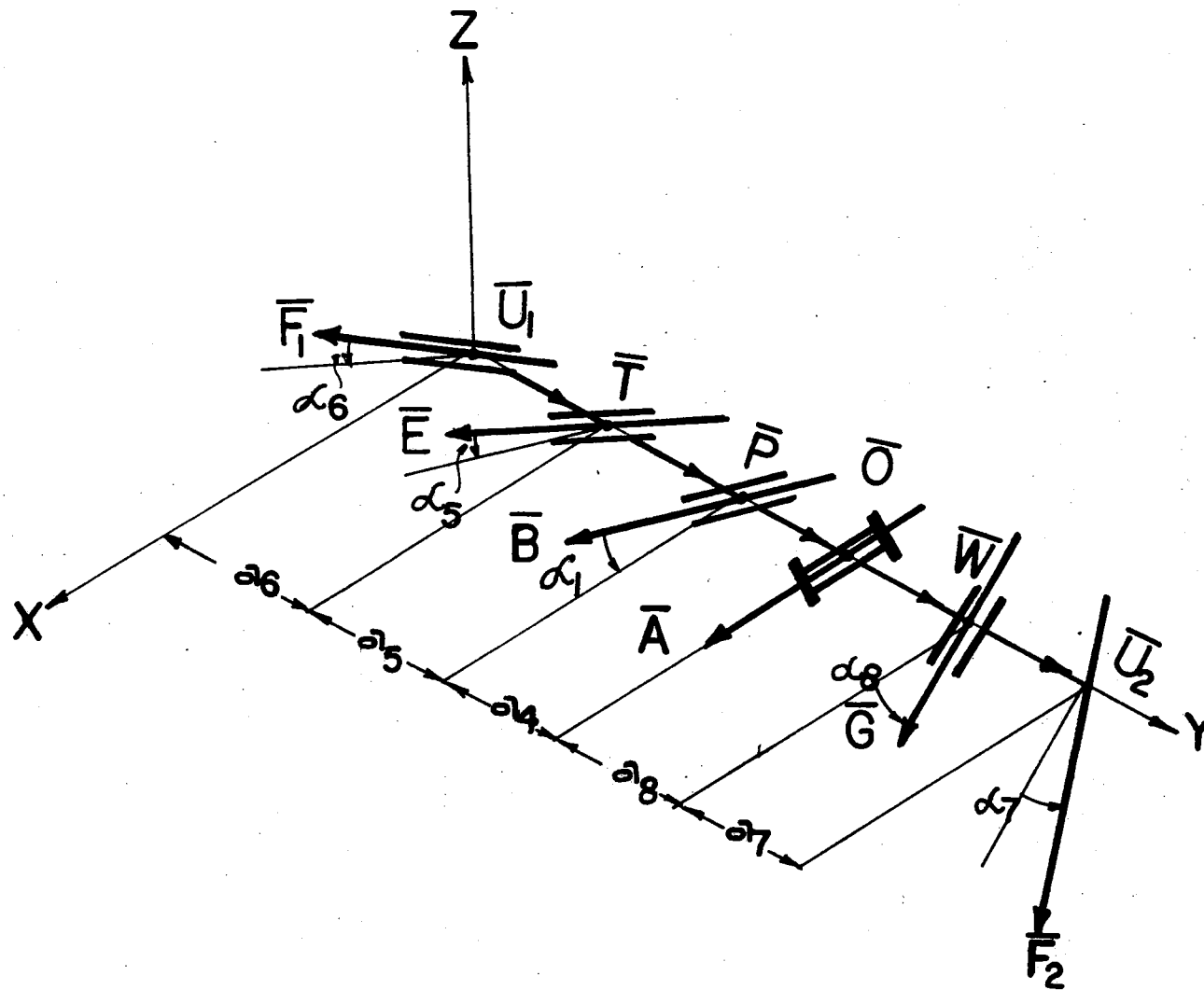


Figure 15. Unfolded Position of Second Loop of RSCR-GCC Mechanism

Note that  $\bar{F}'_1$ ,  $\bar{E}'$ ,  $\bar{F}'_2$  and  $\bar{G}'$  are functions of known screws. Equating the two final positions we get

$$\begin{aligned}\bar{I}_1 \cos \theta_5 + \bar{I}_2 \sin \theta_5 + \bar{I}_3 \\ = \bar{J}_1 \cos \theta_7 + \bar{J}_2 \sin \theta_7 + \bar{J}_3\end{aligned}\quad (3.37)$$

where definitions of  $\bar{I}_1$ ,  $\bar{I}_2$ ,  $\bar{I}_3$ ,  $\bar{J}_1$ ,  $\bar{J}_2$  and  $\bar{J}_3$  follow from Equations (3.35) and (3.36) and are functions of known quantities.

Vector Equation (3.37) provides three equations, but only two of them are independent. Eliminating  $\theta_5$  from Equation (3.37), we obtain

$$X_1 \tan^2 \frac{1}{2} \theta_7 + Y_1 \tan \frac{1}{2} \theta_7 + Z_1 = 0 \quad (3.38)$$

where

$$X_1 = (\bar{I}_1 \times \bar{I}_2) \cdot (\bar{J}_1 - \bar{J}_3 + \bar{I}_3)$$

$$Y_1 = 2 (\bar{I}_1 \times \bar{I}_2) \cdot \bar{J}_2$$

$$Z_1 = (\bar{I}_1 \times \bar{I}_2) \cdot (\bar{J}_1 + \bar{J}_3 - \bar{I}_3)$$

Equation (3.38) provides a maximum of two solutions of  $\theta_7$ . For each value of  $\theta_7$  obtained from Equation (3.38),  $\theta_5$  is calculated from Equation (3.35). Since the rotations of screws at joints  $\bar{E}$  and  $\bar{G}$  are now known, the final position of  $\bar{F}$  and  $\bar{G}$  may be computed. Let this be the  $j^{\text{th}}$  position.  $\theta_6$  is calculated using

$$\cos \theta_6 = \frac{(\bar{E}_j \times \bar{F}_j) \cdot (\bar{F}_j \times \bar{G}_j)}{|\bar{E}_j \times \bar{F}_j| |\bar{F}_j \times \bar{G}_j|}$$

$$\sin \theta_6 = \frac{|(\bar{E}_j \times \bar{F}_j) \times (\bar{F}_j \times \bar{G}_j)|}{|\bar{E}_j \times \bar{F}_j| |\bar{F}_j \times \bar{G}_j|}$$

To calculate the variable kinks at joints E, F and G, the final position of point  $U_2$  is located by providing successive screw displace-

ments to chains  $ABEU_1$  and  $AGU_2$ . Using the pair constraint Equation (2.25)

$$(\bar{U}_2)_{\text{final from chain } AGU_2} + \bar{F}_j S_6 = (\bar{U}_1)_{\text{final from } ABEU_1} \quad (3.40)$$

or

$$\bar{E}_j S_5 + \bar{F}_j S_6 + \bar{G}_j S_7 = \bar{L}V \quad (3.41)$$

where

$$\begin{aligned} \bar{L}V = & \Delta_4 (\bar{u}'_1, \bar{P}, \bar{O}, \bar{B}, \bar{A}, \theta_2 + \theta_{C_2}, \theta_1, S_2 + S_{C_2}, S_1) \\ & - \Delta_4 (\bar{u}_2, \bar{W}, \bar{O}, \bar{G}, \bar{A}, \theta_7, \theta_{C_1}, \bar{O}, S_{C_1}) \end{aligned}$$

and

$$\bar{u}'_1 = \Delta_3 (\bar{u}_1, \bar{T}, \bar{E}, \theta_5, 0)$$

$S_5$ ,  $S_6$  and  $S_7$  are computed using linear equations obtained from vector Equation (3.41).

There are two solutions of loop ABEFG for each solution of loop ABCD. Hence, there are a maximum of eight solutions for each value of the input link. Since the screws at the joints are now known, the displaced position of the mechanism may be found. Let this position be denoted by the subscript  $j$ . Velocity and acceleration analysis of loop ABEFG is performed here. Equating the velocity of  $\bar{F}_j$  obtained from two sides, we obtain

$$\begin{aligned} -\dot{\bar{F}}_j &= [\bar{A}\omega_1 + \bar{B}_j\omega_2 + \bar{E}_j\omega_5] \times \bar{F}_j \\ &= -(\bar{G}_j \times \bar{F}_j) \omega_7 \end{aligned} \quad (3.42)$$



from which we find

$$\omega_5 = - \frac{\bar{G}_j \cdot (\bar{A} \times \bar{F}_j) \omega_1 + \bar{G}_j \cdot (\bar{B}_j \times \bar{F}_j) \omega_2}{\bar{G}_j \cdot (\bar{E}_j \times \bar{F}_j)} \quad (3.43)$$

$$\omega_7 = - \frac{(\bar{A} \times \bar{F}_j) \cdot \bar{E}_j \omega_1 + (\bar{B}_j \times \bar{F}_j) \cdot \bar{E}_j \omega_2}{\bar{E}_j \cdot (\bar{G}_j \times \bar{F}_j)} \quad (3.44)$$

A similar expression may be derived for computing  $\omega_6$  by equating the velocity of  $\bar{E}$  from two sides. To obtain the sliding velocities at pairs E, F and G, the pair constraint Equation (2.28) is used on vector  $\bar{U}_j$ , thus,

$$\begin{aligned} -\dot{\bar{u}}_j &= \bar{A} \times (\bar{u}_j - \bar{o}) \omega_1 + \bar{B}_j \times (\bar{u}_j - \bar{P}_j) \omega_2 \\ &\quad + \bar{E}_j \times (\bar{u}_j - \bar{T}_j) \omega_5 + \bar{B}_j \dot{S}_2 + \bar{E}_j \dot{S}_5 \\ &= -\bar{G}_j \times (\bar{u}_j - \bar{W}_j) \omega_7 - \bar{G}_j \dot{S}_7 - \bar{F}_j \dot{S}_6 \end{aligned} \quad (3.45)$$

Equation (3.45) provides three linear equations to be solved in unknowns  $\dot{S}_5$ ,  $\dot{S}_6$  and  $\dot{S}_7$ .

Expressions for computing angular acceleration at joints E and G are obtained by differentiating Equation (3.42).

$$\begin{aligned} &[\bar{A} \omega_1 + \dot{\bar{B}}_j \omega_2 + \bar{B}_j \dot{\omega}_2 + \dot{\bar{E}}_j \omega_5 + \bar{E}_j \dot{\omega}_5] \times \bar{F}_j \\ &\quad + [\bar{A} \omega_1 + \bar{B}_j \omega_2 + \bar{E}_j \omega_5] \times \dot{\bar{F}}_j \\ &= -(\bar{G}_j \times \bar{F}_j) \dot{\omega}_7 - (\bar{G}_j \times \dot{\bar{F}}_j) \omega_7 \end{aligned} \quad (3.46)$$

Angular accelerations  $\dot{\omega}_5$  and  $\dot{\omega}_7$  are computed using two independent equations from Equation (3.46). Similar analysis at E pair yields the expression for  $\dot{\omega}_6$ .

An expression for calculating sliding velocities at E, F, and G is obtained by differentiating Equation (3.45), thus we find,

$$\begin{aligned}
 & \bar{A} \times \dot{\bar{u}}_j \omega_1 + \bar{B}_j \times (\bar{u}_j - \bar{p}_j) \omega_2 \\
 & + \bar{B}_j \times (\dot{\bar{u}}_j - \dot{\bar{p}}_j) \omega_2 + \bar{B}_j \times (\bar{u}_j - \bar{p}_j) \dot{\omega}_2 \\
 & + \bar{E}_j \times (\bar{u}_j - \bar{t}_j) \omega_5 + \bar{E}_j \times (\dot{\bar{u}}_j - \dot{\bar{t}}_j) \omega_5 \\
 & + \bar{E}_j \times (\bar{u}_j - \bar{t}_j) \dot{\omega}_5 + \bar{B}_j \dot{S}_2 + \bar{B}_j \dot{S}_2 \\
 & + \bar{E}_j \dot{S}_5 + \bar{E}_j \dot{S}_5 \\
 & = -\bar{G}_j \times (\dot{\bar{u}}_j) \omega_7 - \bar{G}_j \times (\bar{u}_j - \bar{w}_j) \dot{\omega}_7 \\
 & - \bar{G}_j \dot{S}_7 - \bar{F}_j \dot{S}_6 - \bar{F}_j \dot{S}_6 \quad (3.47)
 \end{aligned}$$

Translational accelerations  $\ddot{S}_5$ ,  $\ddot{S}_6$  and  $\ddot{S}_7$  are obtained from three linear equations obtained from Equation (3.47). Table II presents displacement analysis of an RSCR-CCC mechanism.

### 3.3. Kinematic Analysis of RCSR-PSC

#### Space Mechanism

Figure 16 shows a Watt's-2 fixed pivot type RCSR-PSC mechanism. Revolute pairs are located at A and D, cylinder pairs at B and E, spherical pairs at C and F, a prismatic pair at G. Note that loop ABCD of Figure 11 is the same as loop ABCD of Figure 16. Additional parameters

TABLE II

## ANALYSIS OF RSCR-GCC MECHANISM

Constant parameters of the mechanism are:

$$\alpha_8 = 0.9, \theta_{c1} = -10^\circ, s_{c1} = -0.22, \theta_{c2} = 15^\circ, s_{c2} = 0.11, \alpha_1 = 10^\circ, \alpha_4 = -30^\circ, \alpha_5 = 40^\circ, \alpha_6 = 45^\circ$$

$$\alpha_7 = 50^\circ, \alpha_8 = 55^\circ, s_1 = 0.1, s_4 = 0, a_1 = 1.0, a_2 = 1.8, a_3 = 2.0, a_4 = 0.8, a_5 = 0.9, a_6 = 1.1, a_7 = 1.2$$

One of the 8 possible solutions is shown below:

$\theta_1$	$\theta_2$	$\theta_4$	$\theta_5$	$\theta_7$	$s_2$	$s_5$	$s_6$	$s_7$
100	77.348	48.376	114.858	-137.935	0.222	1.156	-0.191	-1.689
110	63.938	46.607	128.770	-148.522	0.291	1.542	-0.338	-2.070
120	53.353	42.006	135.910	-153.478	0.295	2.306	-0.492	-2.731
130	43.769	36.219	141.043	-156.588	0.267	3.437	-0.661	-3.701
140	34.681	29.665	145.150	-158.656	0.216	5.130	-0.872	-5.167
150	25.866	22.550	148.337	-159.764	0.148	7.874	-1.193	-7.579
160	17.208	15.015	149.824	-159.206	0.067	12.894	-1.788	-12.056
170	8.650	7.181	145.604	-153.327	-0.022	21.763	-2.933	-19.981
180	-2.853	2.711	159.316	-163.452	0.038	45.983	-5.514	-42.341
190	-8.494	-8.637	92.942	-101.770	-0.207	5.477	-1.982	-3.870
200	-17.029	-16.474	69.295	-79.910	-0.296	0.054	-1.412	1.433
210	-25.636	-24.028	54.602	-67.106	-0.377	-1.373	-1.129	2.926
220	-34.372	-31.180	45.852	-60.132	-0.444	-1.488	-0.966	3.171
230	-43.342	-37.800	41.001	-56.840	-0.494	-1.202	-0.852	3.021
240	-52.745	-43.709	39.183	-56.120	-0.523	-0.823	-0.754	2.752
250	-63.008	-48.563	40.669	-57.759	-0.521	-0.473	-0.653	2.451
260	-75.476	-51.216	48.706	-63.459	-0.466	-0.236	-0.532	2.144

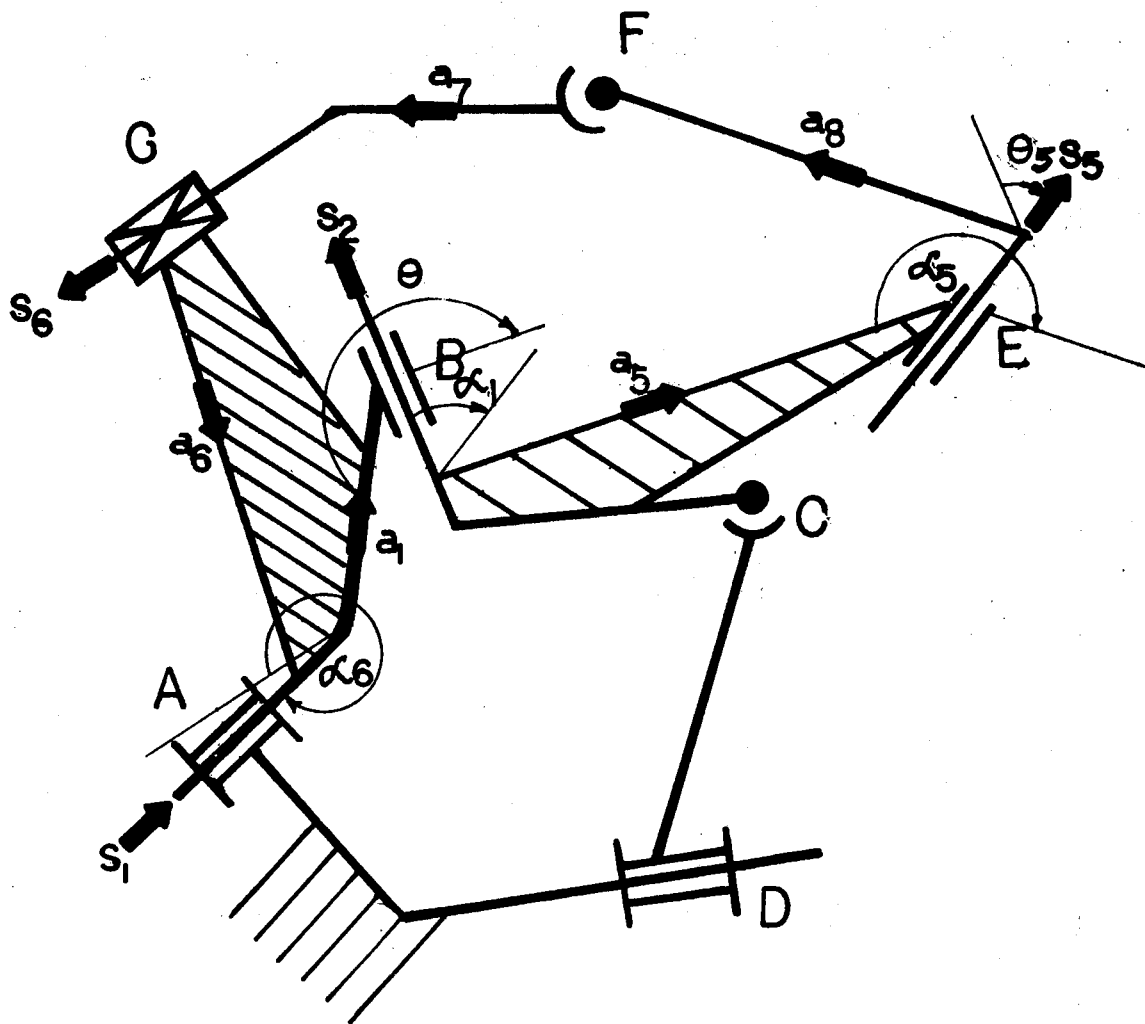


Figure 16. Six-Link Spatial RGSR-PSC Mechanism

to specify the mechanism are,  $a_6$ , link length between pair axes at A and G;  $S_5$ , offset distance at pair E;  $S_6$ , offset distance at pair G. Note that the link lengths and offset distances are so directed that they form a closed directed loop. The twist angle  $\alpha_5$  between the axes at E and B is measured in positive sense about link  $a_5$ , while  $\alpha_6$  between the axes at A and G is measured in positive sense about link  $a_6$ .  $\theta_5$  is the rotation angle between links  $a_5$  and  $a_8$ , measured in positive sense about  $S_5$ . The rotation angle and offset distance between links  $a_1$  and  $a_5$  differ from the rotation angle and offset distance between links  $a_1$  and  $a_2$  by a constant angle  $\theta_{c_2}$  and constant offset  $S_{c_2}$  where  $\theta_{c_2}$  and  $S_{c_2}$  are parameters of ternary links as described in Chapter II. Similarly, the rotation angles and offset distance between links  $a_4$  and  $a_1$  differ by a constant angle  $\theta_{c_1}$  and constant offset  $S_{c_1}$  to the rotation angle and offset between links  $a_6$  and  $a_1$ , where  $\theta_{c_1}$  and  $S_{c_1}$  are the included angle and offset of ternary link ABG at joint A.

Loop ABCD is analyzed as shown in Section 3.1. To conduct the analysis of loop AGFED, the mechanism is divided into two open loop chains by separating two elements of the spherical pair located at F. The unfolded position of the two chains is shown in Figure 17. The following vectors are then defined from Figure 17.

$$\bar{A} = \vec{i}$$

$$\bar{B} = \cos \alpha_1 \vec{i} - \sin \alpha_1 \vec{k}$$

$$\bar{E} = \cos \alpha_1 + \alpha_5 \vec{i} - \sin \alpha_1 + \alpha_5 \vec{k}$$

$$\bar{G} = \cos \alpha_6 \vec{i} + \sin \alpha_6 \vec{k}$$

$$\bar{u}_1 = 0$$

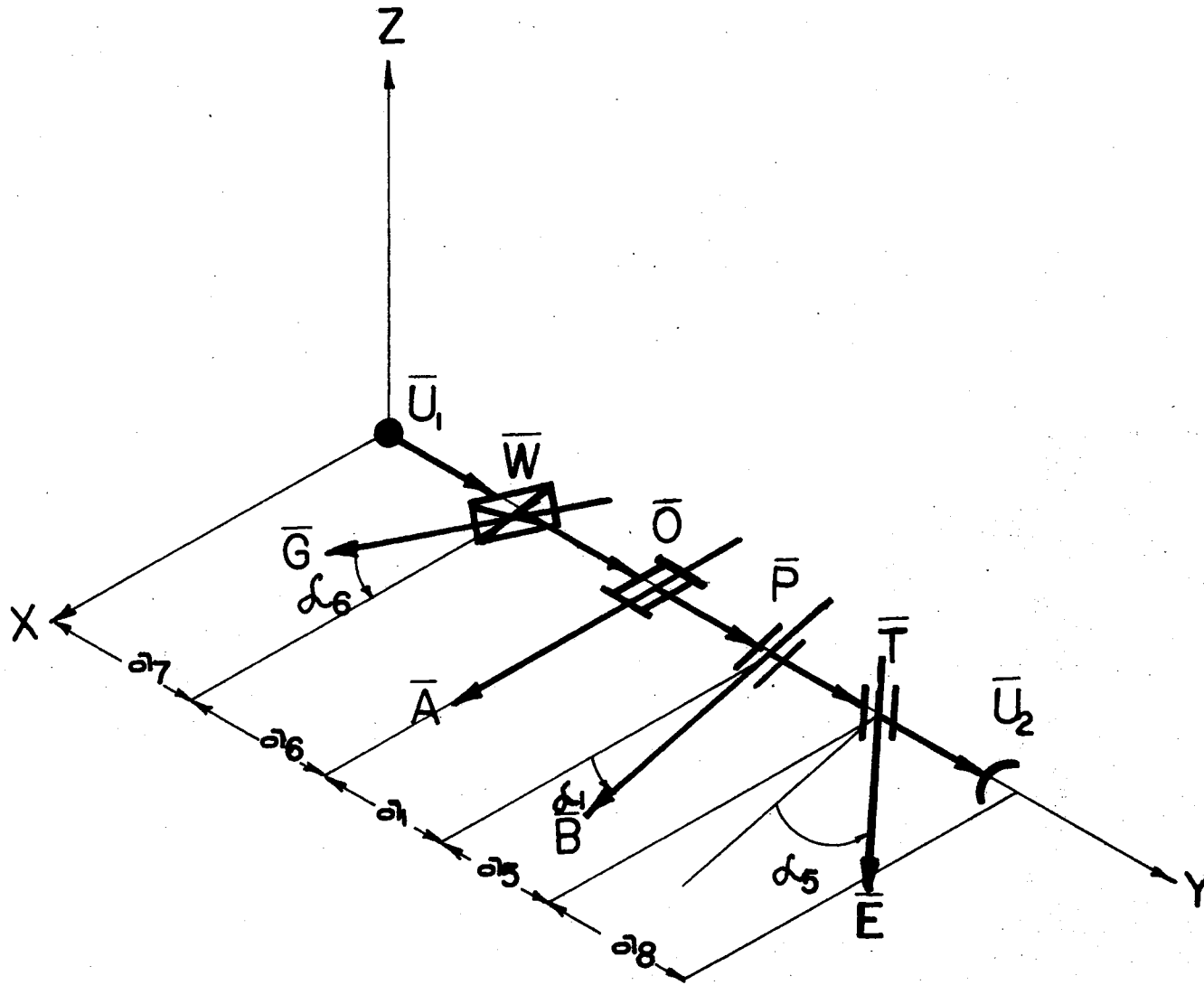


Figure 17. Unfolded Position of Second Loop of RSCR-PSC Mechanism

$$\begin{aligned}
\bar{W} &= a_7 \vec{j} \\
\bar{O} &= (a_6 + a_7) \vec{j} \\
\bar{P} &= (a_1 + a_6 + a_7) \vec{j} \\
\bar{T} &= (a_1 + a_5 + a_6 + a_7) \vec{j} \\
\bar{u}_2 &= (a_1 + a_5 + a_6 + a_7 + a_8) \vec{j} \quad (3.48)
\end{aligned}$$

Spheric pair at U is located using successive screw displacements of chains  $ABEU_2$  and  $AGU_1$ . Equating the two positions of the spheric pair, we obtain

$$\begin{aligned}
&C\theta_5 [(\bar{u}_2' - \bar{T}') - \{(\bar{u}_2' - \bar{T}') \cdot \bar{E}_j\} \bar{E}_j] \\
&+ S\theta_5 [\bar{E}_j \times (\bar{u}_2' - \bar{T}')] + \bar{E}_j S_5 \\
&+ \bar{T}' + \{(\bar{u}_2' - \bar{T}') \cdot \bar{E}_j\} \bar{E}_j \\
&= -\bar{G}_j S_6 + \bar{u}_1' \quad (3.49)
\end{aligned}$$

where

$$\begin{aligned}
\bar{u}_2' &= \Delta_4(\bar{u}_2, \bar{P}, \bar{O}, \bar{B}, \bar{A}, \theta_2 + \theta_{c_2}, \theta_1, S_2 + S_{c_2}, S_1) \\
\bar{T}' &= \Delta_4(\bar{T}, \bar{P}, \bar{O}, \bar{B}, \bar{A}, \theta_2 + \theta_{c_2}, \theta_1, S_2 + S_{c_2}, S_1) \\
\bar{E}_j &= \Delta_2(\bar{E}, \bar{B}, \bar{A}, \theta_2 + \theta_{c_2}, \theta_1) \\
\bar{G}_j &= \Delta_1(\bar{G}, -\bar{A}, \theta_1 + \theta_{c_1}) \\
\bar{u}_1' &= \Delta_3(\bar{u}_1, \bar{O}, -\bar{A}, \theta_1 + \theta_{c_1}, S_{c_1}) \quad (3.50)
\end{aligned}$$

Equation (3.49) may be written as

$$\bar{I}_1' C\theta_5 + \bar{I}_2' S\theta_5 + \bar{I}_3' + \bar{E}_j S_5 = -\bar{G}_j S_6 \quad (3.51)$$

where definitions of  $\bar{I}_1$ ,  $\bar{I}_2$  and  $\bar{I}_3$  follow from Equation (3.49) and are functions of known quantities. Eliminating  $S_5$  and  $S_6$  from Equation (3.51), we get

$$X_1 \tan^2 \frac{1}{2} \theta_5 + Y_1 \tan \frac{1}{2} \theta_5 + Z_1 = 0$$

where

$$\begin{aligned} X_1 &= (\bar{E}_j \times \bar{G}_j) \cdot (\bar{I}_3' - \bar{I}_1') \\ Y_1 &= 2 (\bar{E}_j \times \bar{G}_j) \cdot \bar{I}_2' \\ Z_1 &= (\bar{E}_j \times \bar{G}_j) \cdot (\bar{I}_3' + \bar{I}_1') \end{aligned} \quad (3.52)$$

Equation (3.52) provides at the most two values for  $\theta_5$ . For each value of  $\theta_5$ ,  $S_5$  and  $S_6$  are computed using

$$\begin{aligned} S_5 &= - \frac{(\bar{G}_j \times \vec{c}) \cdot \{ \bar{I}_1' \cos \theta_5 + \bar{I}_2' \sin \theta_5 + \bar{I}_3' \}}{|(\bar{G}_j \times \vec{c}) \cdot \bar{E}_j|} \\ -S_6 &= \frac{(\bar{E}_j \times \vec{f}) \cdot \{ \bar{I}_1' \cos \theta_5 + \bar{I}_2' \sin \theta_5 + \bar{I}_3' \}}{|(\bar{E}_j \times \vec{f}) \cdot \bar{G}_j|} \end{aligned}$$

The velocity analysis of loop AGUED is conducted by equating the velocity of the spheric pair at  $j^{\text{th}}$  position from successive instantaneous screws from two sides.

$$\begin{aligned} \bar{B}_j \times (\bar{u}_j - \bar{p}_j) \omega_2 + \bar{E}_j \times (\bar{u}_j - \bar{t}_j) \omega_5 \\ + \bar{E}_j \dot{S}_5 \\ = - \bar{G}_j \dot{S}_6 \end{aligned} \quad (3.53)$$



$\omega_5$ ,  $\dot{S}_5$  and  $\dot{S}_6$  are computed using three linear equations obtained from vector Equation (3.53). Differentiating Equation (3.53)

$$\begin{aligned} & \dot{\bar{B}}_j \times (\bar{u}_j - \bar{p}_j) \omega_2 + \bar{B}_j \times (\dot{\bar{u}}_j - \dot{\bar{p}}_j) \omega_2 \\ & + \bar{B}_j \times (\bar{u}_j - \bar{p}_j) \dot{\omega}_2 + \dot{\bar{E}}_j \times (\bar{u}_j - \bar{t}_j) \omega_5 \\ & + \bar{E}_j \times (\dot{\bar{u}}_j - \dot{\bar{t}}_j) \omega_5 + \bar{E}_j \times (\bar{u}_j - \bar{t}_j) \dot{\omega}_5 \\ & + \bar{E}_j \ddot{S}_5 + \dot{\bar{E}}_j \dot{S}_5 = - \bar{G}_j \dot{S}_6 - \bar{G}_j \ddot{S}_6 \end{aligned} \quad (3.54)$$

Accelerations  $\ddot{S}_6$ ,  $\dot{\omega}_5$  and  $\ddot{S}_5$  are calculated using Equation (3.54).

This completes the displacement, velocity and acceleration analyses of the mechanism. Finite and infinitesimal screw displacements at joints are thus known and position, velocity and acceleration of any point in the mechanism can be computed. Table III presents an example of analysis of a RSCR-PSC mechanism.

### 3.4. Kinematic Analysis of

#### HCCG-RSC Mechanism

Figure 18 shows a Stephenson type HCCG-RSC mechanism. Input to the mechanism is provided via the helical pair located at A. B, C, D and G are cylinder pairs while E and F are revolute and spherical pairs respectively. The mechanism shown in Figure 18 has two independent directed loops ABCD and AEFGD. In loop ABCD,  $a_1$  is the link length between the pair axes at pairs A and B;  $a_2$  is the link length between the pairs at B and C;  $a_3$  is the link length between the pairs at C and D;  $a_4$  is the link length between the pairs at A and D. The offset distances at pairs A, B, C and D are denoted by  $S_1$ ,  $S_2$ ,  $S_3$  and  $S_4$ . Note that the link

TABLE III

## EXAMPLE ANALYSIS OF RSCR-PSC MECHANISM

The constant parameters of the mechanism are:

$$\theta_{c_2} = 15^\circ, s_{c_2} = 0.1, s_1 = 0.1, s_4 = 0, \alpha_1 = 20^\circ, \alpha_4 = 25^\circ, \alpha_5 = -30^\circ, \\ \alpha_6 = 15^\circ, a_1 = 0.6, a_2 = 0.8, a_3 = 0.8, a_4 = 0.5, a_5 = 0.4, a_6 = 0.8, \\ a_7 = 0.3, a_8 = 0.4$$

One of the 8 solutions is shown below:

$\theta_1$	$\theta_2$	$\theta_4$	$\theta_5$	$s_5$	$s_6$	$s_2$
130	63.629	8.368	117.351	1.287	-0.207	-1.002
140	48.078	8.132	86.306	1.157	-0.298	-0.874
150	35.372	5.889	65.097	0.946	-0.319	-0.701
160	24.065	2.753	48.572	0.705	-0.323	-0.508
170	14.079	-1.336	36.268	0.473	-0.339	-0.307
180	-0.926	-0.869	27.519	0.132	-0.319	-0.089
190	-9.011	-6.495	27.393	-0.019	-0.436	0.114
200	-19.212	-10.304	33.741	-0.182	-0.578	0.318
210	-30.052	-13.698	45.204	-0.335	-0.738	0.514
220	-41.751	-16.612	61.172	-0.489	-0.887	0.695
230	-54.896	-18.710	83.197	-0.656	-0.982	0.847
240	-71.254	-18.716	120.703	-0.876	-0.903	0.938

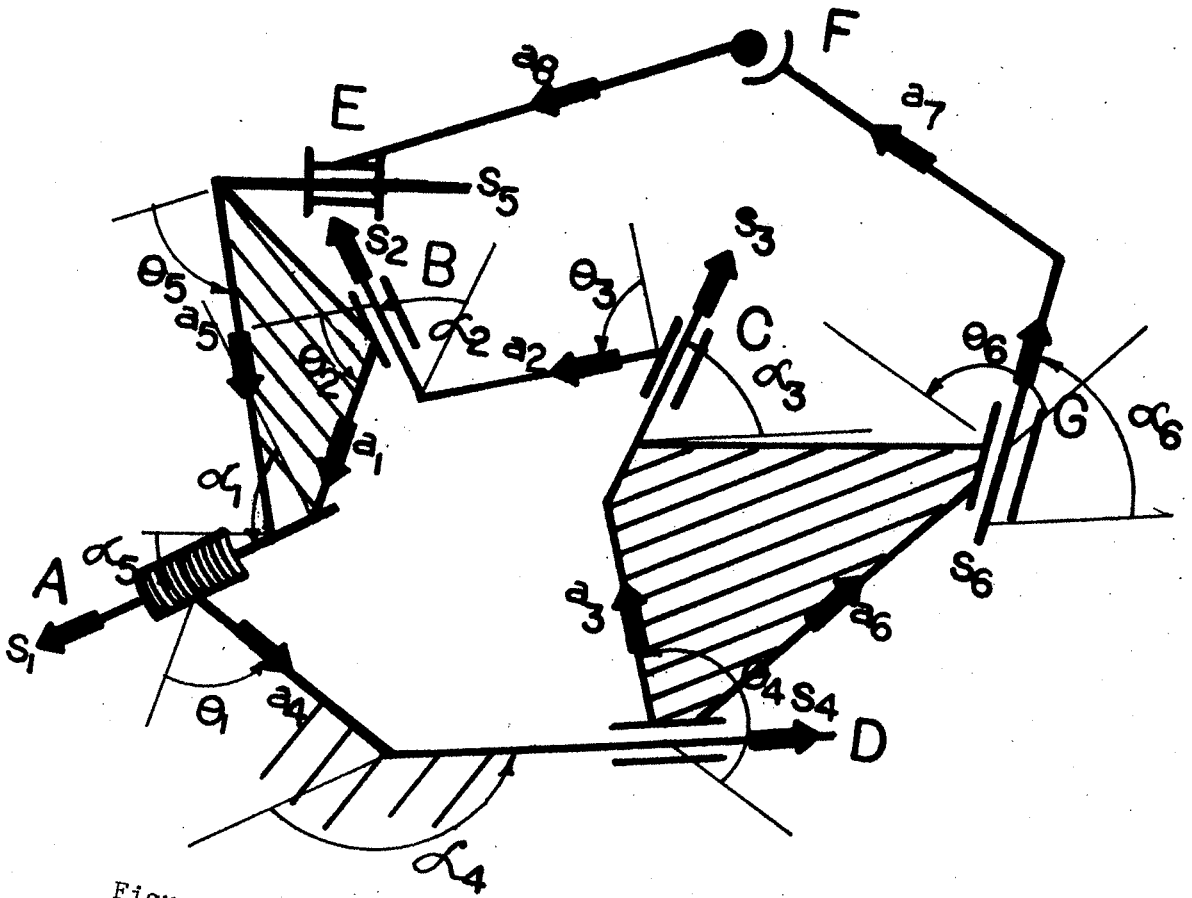


Figure 18. Six-Link, Spatial HCCC-RSC Mechanism

lengths and offset distances are directed segments and form a closed directed polygon in space.  $\alpha_1, \alpha_2, \alpha_3$  and  $\alpha_4$  are the twist angles measured between the pair axes at A and B, B and C, C and D, D and A, in positive sense about links  $a_1, a_2, a_3$  and  $a_4$ .

Angle  $\theta_1$  is measured at the axis of pair A, between links  $a_1$  and  $a_4$  in positive sense about offset  $S_1$ . Similarly, angles  $\theta_2, \theta_3$ , and  $\theta_4$  are measured at the axes of pairs B, C and D, between links  $a_1$  and  $a_2, a_2$  and  $a_3$ , and  $a_3$  and  $a_4$  about offset distances  $S_2, S_3$  and  $S_4$ . Note that rotations  $\theta_1$  are related to offset distance by the pitch of the screw at the helical pair. In loop AEF GD,  $a_5, \alpha_5$  are the link length and twist angle between the pair axes at E and F;  $\alpha_6$  and  $a_6$  are the twist angle and link length between the pair axes at D and G while  $a_7$  and  $a_8$  are perpendicular distances from the spherical pair at F to the pair axes at G and E. The constant offset distance at the revolute pair at A, between links  $a_4$  and  $a_5$  is  $S_1 + S_{c_1}$ , where  $S_{c_1}$  is constant offset of ternary link ABE at A pair. The offset distances at E and G pairs are  $S_5$  and  $S_6$  and are measured between links  $a_5$  and  $a_8$ , and  $a_6$  and  $a_7$  respectively. The offset distance at D, measured between  $a_4$  and  $a_6$  is  $S_4 + S_{c_2}$  where  $S_{c_2}$  is the offset of ternary link GDG at D pair.

Similarly, the rotation angle between links  $a_4$  and  $a_5$  is  $\theta_1 + \theta_{c_1}$ , where  $\theta_{c_1}$  is the included angle of ternary link ABE at pair A; the rotation angle between links  $a_4$  and  $a_6$  is  $\theta_4 + \theta_{c_2}$ , where  $\theta_{c_2}$  is the included angle of ternary link GDG at pair D;  $\theta_5$  measures the angle between links  $a_5$  and  $a_8$  while  $\theta_6$  measures the angle between links  $a_6$  and  $a_7$ . Note that all rotation angles are measured in positive screw sense about common offset distances which are directed segments in space. Loop ABCD is analyzed by separating the two elements of the cylinder pair located at

c, thus dividing loop ABCD into two open loop chains. Similarly, loop AEFGD is divided into two open loop chains by separating two elements of the spherical pair at F. The four chains thus obtained are unfolded along the Y axis as shown in Figures 19 and 20.

The following vectors are defined in Figures 19 and 20.

$$\begin{aligned}
 \bar{Q}_1 &= 0 \\
 \bar{P} &= a_2 \vec{j} \\
 \bar{O} &= (a_1 + a_2) \vec{j} \\
 \bar{R} &= (a_1 + a_2 + a_4) \vec{j} \\
 \bar{Q}_2 &= (a_1 + a_2 + a_3 + a_4) \vec{j} \\
 \bar{u}_1 &= (a_1 + a_2 - a_5 - a_8) \vec{j} \\
 \bar{T} &= (a_1 + a_2 - a_5) \vec{j} \\
 \bar{W} &= (a_1 + a_2 + a_4 + a_6) \vec{j} \\
 \bar{u}_2 &= (a_1 + a_2 + a_4 + a_6 + a_7) \vec{j} \\
 \bar{A} &= \vec{i} \\
 \bar{B} &= \cos \alpha_1 \vec{i} + \sin \alpha_1 \vec{k} \\
 \bar{C}_1 &= \cos(\alpha_1 + \alpha_2) \vec{i} + \sin(\alpha_1 + \alpha_2) \vec{k} \\
 \bar{D} &= \cos \alpha_4 \vec{i} - \sin \alpha_4 \vec{k} \\
 \bar{C}_2 &= \cos(\alpha_3 + \alpha_4) \vec{i} - \sin(\alpha_3 + \alpha_4) \vec{k} \\
 \bar{E} &= \cos \alpha_5 \vec{i} + \sin \alpha_5 \vec{k} \\
 \bar{G} &= \cos(\alpha_4 + \alpha_6) \vec{i} - \sin(\alpha_4 + \alpha_6) \vec{k}
 \end{aligned}$$

Screwing  $\bar{C}_1$  and  $\bar{Q}_1$  about  $\hat{B}$  and  $\hat{A}$ , we obtain the final position of the axis at joint C. The final position may also be obtained by screwing  $\bar{C}_2$  and  $\bar{Q}_2$  about  $\hat{D}$ . Using the pair constraint Equation (2.25) for the cylinder pair,

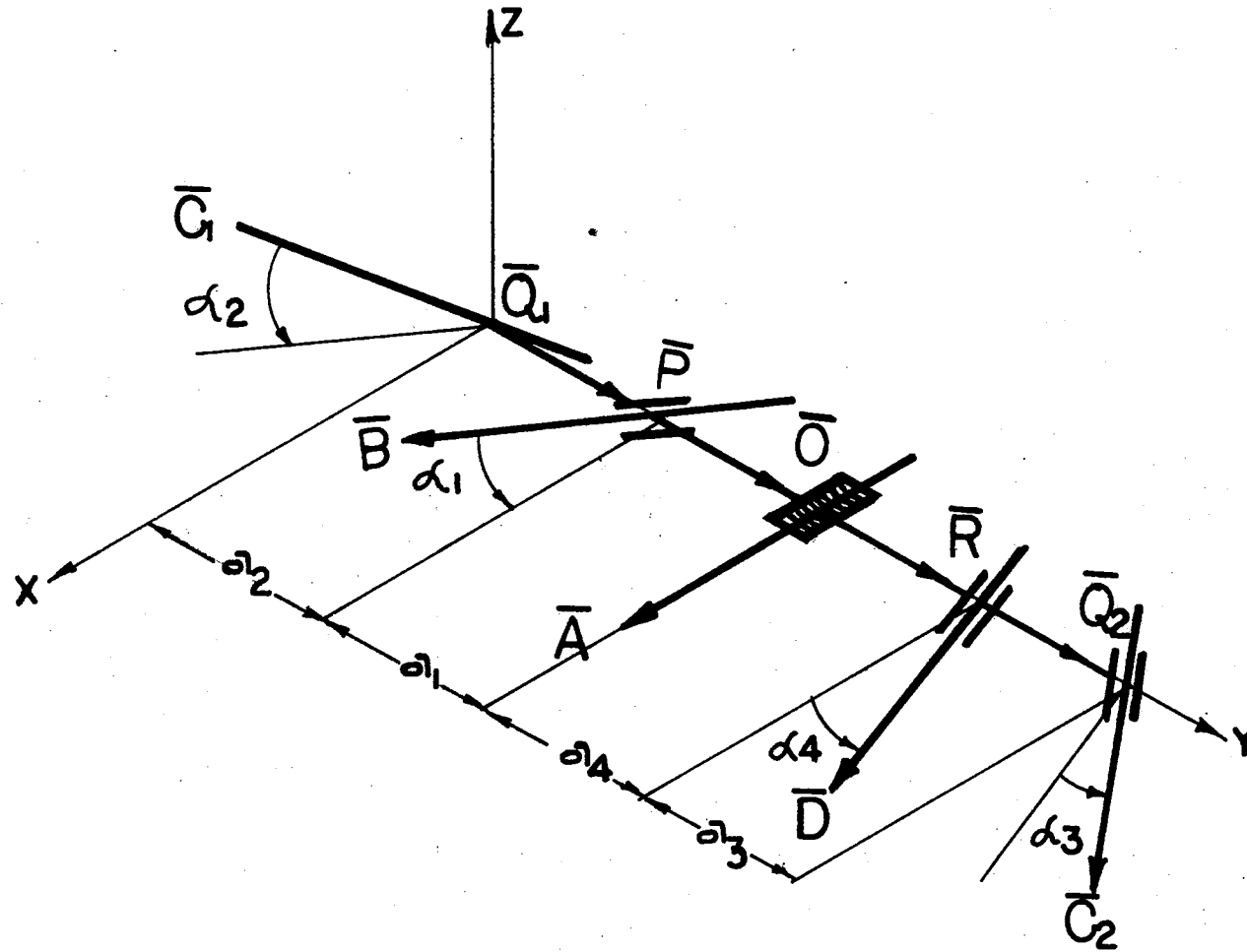


Figure 19. Unfolded Position of First Loop of HCGG-RSG Mechanism

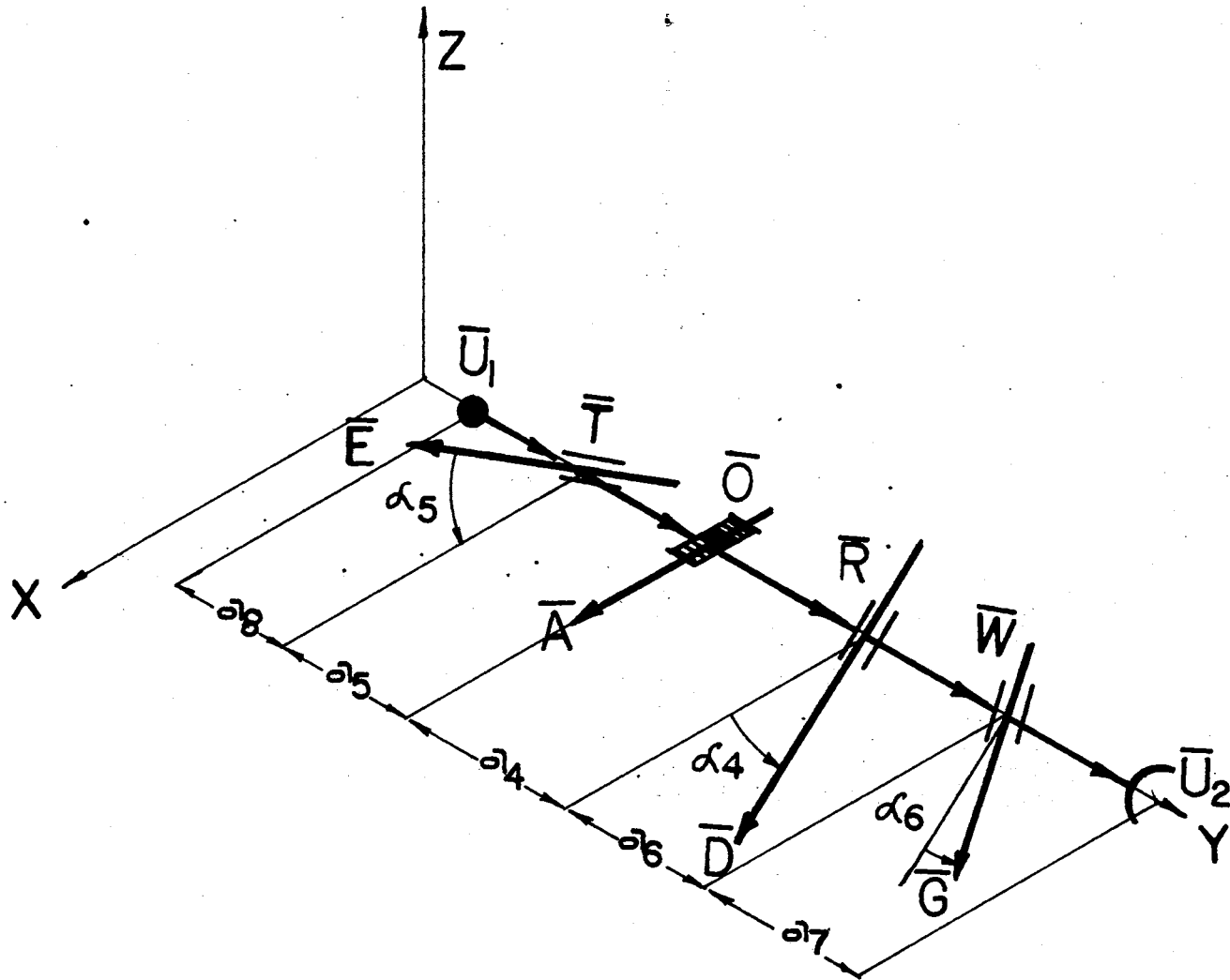


Figure 20. Unfolded Position of Second Loop of HGGG-RSG Mechanism

$$\begin{aligned}
& C\theta_2 [C\theta_1 \bar{L}_1 - S\theta_1 \bar{L}_2 + \bar{L}_3] + C\theta_1 \bar{K}_1 - S\theta_1 \bar{K}_2 + \bar{K}_3 \\
& + S\theta_2 [-C\theta_1 \bar{M}_1 + S\theta_1 \bar{M}_2 - \bar{M}_3] \\
& = \bar{I}P_1 C\theta_4 + \bar{I}P_2 S\theta_4 + \bar{I}P_3 \quad (3.55)
\end{aligned}$$

where

$$\begin{aligned}
\bar{L}_1 &= \bar{J}_1 - (\bar{J}_1 \cdot \bar{A}) \bar{A} \\
\bar{L}_2 &= \bar{A} \times \bar{J}_1 \\
\bar{L}_3 &= (\bar{J}_1 \cdot \bar{A}) \bar{A} \\
\bar{M}_1 &= \bar{J}_2 - (\bar{J}_2 \cdot \bar{A}) \bar{A} \\
\bar{M}_2 &= \bar{A} \times \bar{J}_2 \\
\bar{M}_3 &= (\bar{J}_2 \cdot \bar{A}) \bar{A} \\
\bar{J}_1 &= \bar{C}_1 - (\bar{C}_1 \cdot \bar{B}) \bar{B} \\
\bar{J}_2 &= \bar{B} \times \bar{C}_1 \\
\bar{J}_3 &= (\bar{C}_1 \cdot \bar{B}) \bar{B} \\
\bar{K}_1 &= \bar{J}_3 - (\bar{J}_3 \cdot \bar{A}) \bar{A} \\
\bar{K}_2 &= (\bar{A} \times \bar{J}_3) \\
\bar{K}_3 &= (\bar{J}_3 \cdot \bar{A}) \bar{A} \\
\bar{I}P_1 &= \bar{C}_2 - (\bar{C}_2 \cdot \bar{D}) \bar{D} \\
\bar{I}P_2 &= \bar{D} \times \bar{C}_2 \\
\bar{I}P_3 &= (\bar{C}_2 \cdot \bar{D}) \bar{D}
\end{aligned}$$

Eliminating  $\theta_2$  from Equation (3.55), we obtain

$$X_3 \tan^2 \frac{1}{2}\theta_4 + Y_3 \tan \frac{1}{2}\theta_4 + Z_3 = 0 \quad (3.56)$$

where



$$\begin{aligned}
X_3 &= (\bar{N}_1 \times \bar{N}_2) \cdot (\bar{I}P_3 - \bar{N}_3 - \bar{I}P_1) \\
Y_3 &= 2 (\bar{N}_1 \times \bar{N}_2) \cdot \bar{I}P_2 \\
Z_3 &= (\bar{N}_1 \times \bar{N}_2) \cdot (\bar{I}P_3 + \bar{I}P_1 - \bar{N}_3) \\
\bar{N}_1 &= c\theta_1 \bar{L}_1 - s\theta_1 \bar{L}_2 + \bar{L}_3 \\
\bar{N}_2 &= c\theta_1 \bar{M}_1 - s\theta_1 \bar{M}_2 + \bar{M}_3 \\
\bar{N}_3 &= c\theta_1 \bar{K}_1 - s\theta_1 \bar{K}_2 + \bar{K}_3
\end{aligned}$$

There are a maximum of two values of  $\theta_4$  from Equation (3.56); for each value of  $\theta_4$ , one value of  $\theta_2$  may be computed using Equation (3.55). Similarly if we separate the mechanism at B pair, one value of  $\theta_3$  is obtained from the displacement relationship for each value of  $\theta_1$  and  $\theta_4$ .

The kink length at the helical pair when the input has rotated through  $\theta_1$  is,

$$S_h = S_{\text{helical}} = s_1 + \rho \theta_1$$

Using pair constraint Equation (2.26) for point  $\bar{Q}_1$  and  $\bar{Q}_2$  in chains  $ABQ_1$  and  $DQ_2$  we obtain

$$\begin{aligned}
-\bar{A}(s_1 + \rho \theta_1) - \bar{B}_j s_2 + \bar{Q}_1' \\
= \bar{D} s_4 + \bar{C}_j s_3 + \bar{Q}_2'
\end{aligned} \tag{3.57}$$

where

$$\begin{aligned}
\bar{B}_j &= \Delta_1(\bar{B}, -\bar{A}, \theta_1) \\
\bar{C}_j &= \Delta_1(\bar{C}, \bar{D}, \theta_4) \\
\bar{Q}_1' &= \Delta_4(\bar{Q}_1, \bar{P}_1, \bar{O}, -\bar{B}, -\bar{A}, \theta_2, \theta_1, 0, 0) \\
\bar{Q}_2' &= \Delta_2(\bar{Q}_2, \bar{R}, \bar{D}, \theta_4, 0)
\end{aligned}$$

Unknowns  $S_2$ ,  $S_3$  and  $S_4$  are computed from the three linear equations obtained from Equation (3.57).

The position of the spheric pair U is obtained by screwing  $\bar{U}_1$  about  $\hat{E}$  and  $\hat{A}$  and also by screwing  $\bar{U}_2$  about  $\hat{G}$  and  $\hat{D}$ . Using the pair constraint Equation (2.18) for spheric pair, we get

$$\begin{aligned}
 & c\theta_5 [(\bar{u}'_1 - \bar{t}') - \{(\bar{u}'_1 - \bar{t}') \cdot \bar{E}_j\} \bar{E}_j] \\
 & - s\theta_5 [\bar{E}_j \times (\bar{u}'_1 - \bar{t}')] - \bar{E}_j s_5 \\
 & + \{(\bar{u}'_1 - \bar{t}') \cdot \bar{E}_j\} \bar{E}_j \\
 & = c\theta_6 [(\bar{u}'_2 - \bar{w}') - \{(\bar{u}'_2 - \bar{w}') \cdot \bar{G}_j\} \bar{G}_j] \\
 & + s\theta_6 [\bar{G}_j \times (\bar{u}'_2 - \bar{w}')] + \bar{G}_j s_6 \\
 & + \{(\bar{u}'_2 - \bar{w}') \cdot \bar{G}_j\} \bar{G}_j \quad (3.58)
 \end{aligned}$$

where

$$\begin{aligned}
 \bar{u}'_1 &= \Delta_3(\bar{u}_1, \bar{o}, \bar{A}, \theta_1 + \theta_{c_1}, \text{sit}) \\
 \bar{t}'_1 &= \Delta_3(\bar{t}'_1, \bar{o}, \bar{A}, \theta_1 + \theta_{c_1}, \text{sit}) \\
 \bar{E}_j &= \Delta_1(\bar{E}, \bar{A}, \theta_1 + \theta_{c_1}) \\
 \bar{u}'_2 &= \Delta_3(\bar{u}_2, \bar{R}, \bar{D}, \theta_4 + \theta_{c_2}, s_4 + s_{c_2}) \\
 \bar{w}'_2 &= \Delta_3(\bar{w}, \bar{R}, \bar{D}, \theta_4 + \theta_{c_2}, s_4 + s_{c_2}) \\
 \bar{G}_j &= \Delta_1(\bar{G}, \bar{D}, \theta_4 + \theta_{c_2}) \\
 \text{sit} &= s_{\text{helical}} + s_{c_1}
 \end{aligned}$$

$\theta_{c_1}$ ,  $s_{c_1}$  and  $\theta_{c_2}$ ,  $s_{c_2}$  are parameters of ternary links at pairs A and D.

Equation (3.58) may be rewritten as

$$\begin{aligned} \bar{N}'_1 \cos \theta_5 + \bar{N}'_2 \sin \theta_5 + \bar{N}'_3 \\ = \bar{J}'_1 \cos \theta_6 + \bar{J}'_2 \sin \theta_6 + \bar{J}'_3 + \bar{G}_j S_6 \end{aligned} \quad (3.59)$$

where  $\bar{N}'_1, \bar{N}'_2, \bar{N}'_3, \bar{J}'_1, \bar{J}'_2$  and  $\bar{J}'_3$  are appropriately defined. Equation (3.59) is of the same form as Equation (3.19) and hence may be reduced to the form

$$\sum_{i=0}^4 P_i \tan^i \frac{1}{2} \theta_5 = 0 \quad (3.60)$$

where  $P_i$ 's are functions of  $\bar{N}'_1, \bar{N}'_2, \bar{N}'_3, \bar{J}'_1, \bar{J}'_2$  and  $\bar{J}'_3$  and are known. There are a maximum of four values of  $\theta_5$  from Equation (3.60) for each value of  $\theta_6$ .  $\theta_6$  and  $S_6$  are then computed using

$$\begin{aligned} \cos \theta_6 &= \frac{(\bar{N}'_1 \cos \theta_5 + \bar{N}'_2 \sin \theta_5 + \bar{N}'_3 - \bar{J}'_3) \cdot (\bar{J}'_2 \times \bar{G}_j)}{(\bar{J}'_2 \times \bar{G}_j) \cdot \bar{J}'_1} \\ \sin \theta_6 &= \frac{(\bar{N}'_1 \cos \theta_5 + \bar{N}'_2 \sin \theta_5 + \bar{N}'_3 - \bar{J}'_3) \cdot (\bar{J}'_1 \times \bar{G}_j)}{(\bar{J}'_1 \times \bar{G}_j) \cdot \bar{J}'_2} \\ S_6 &= (\bar{N}'_1 \cos \theta_5 + \bar{N}'_2 \sin \theta_5 + \bar{N}'_3 - \bar{J}'_3) \cdot \bar{G}_j \\ &\quad - \bar{J}'_2 \sin \theta_6 - \bar{J}'_1 \cos \theta_6 \end{aligned}$$

This completes the displacement analysis of the mechanism. For any input link position, the position of all other link pairs may be computed. Let this position be denoted by subscript  $j$ . Using the pair constraint Equation (2.26) for velocity at pair  $C$ , we get

$$(\bar{A}\omega_1 + \bar{B}_j\omega_2) \times \bar{C}_j = -(\bar{D} \times \bar{C}_j)\omega_4 \quad (3.61)$$

from which

$$\omega_2 = -\frac{(\bar{A} \times \bar{C}_j) \cdot \bar{D}}{(\bar{B}_j \times \bar{C}_j)} \omega_1 \quad (3.62)$$

$$\omega_4 = -\frac{(\bar{A} \times \bar{C}_j) \cdot \bar{B}_j}{(\bar{D} \times \bar{C}_j) \cdot \bar{B}_j} \omega_1 \quad (3.63)$$

$\omega_3$  is computed by equating the velocity of B from two sides

$$\omega_3 = -\frac{(\bar{A} \times \bar{B}_j) \cdot \bar{D}}{(\bar{C}_j \times \bar{B}_j) \cdot \bar{D}} \omega_1 \quad (3.64)$$

Using the pair constraint Equation (2.26) for point  $Q_j$  on the cylinder pair axis at C, we get

$$\begin{aligned} & \bar{A}\omega_1 \times (\bar{Q}_j - \bar{O}) + \bar{B}_j\omega_2 \times (\bar{Q}_j - \bar{P}_j) \\ & + \bar{A}_j\dot{\omega}_1 + \bar{B}_j\dot{\omega}_2 \\ & = -(\bar{D}\omega_4 \times (\bar{Q}_j - \bar{R}) - \bar{C}_j\dot{\omega}_3 - \bar{D}_j\dot{\omega}_4) \quad (3.65) \end{aligned}$$

Velocities  $\dot{\omega}_2$ ,  $\dot{\omega}_3$  and  $\dot{\omega}_4$  are computed from the set of three linear equations obtained from vector Equation (3.65).

The velocity analysis of loop AEUGD is performed by equating the velocity of spheric pair U from chains  $AEU_1$  and  $GDU_2$ . We get

$$\begin{aligned}
& \bar{A} \omega_1 \times (\bar{u}_j - \bar{O}) + \bar{E}_j \omega_5 \times (\bar{u}_j - \bar{T}_j) \\
& \quad + \bar{A} \dot{\omega}_1 \\
& = -[\bar{D} \omega_4 \times (\bar{u}_j - \bar{R}_j) + \bar{D} \dot{\omega}_4 + \bar{G}_j \dot{\omega}_6 \\
& \quad + \bar{G}_j \omega_6 \times (\bar{u}_j - \bar{W}_j)] \quad (3.66)
\end{aligned}$$

$\omega_5$ ,  $\omega_6$  and  $\dot{\omega}_6$  are obtained using the three linear equations obtained from vector Equation (3.66). Expressions for computing accelerations at joints are obtained by differentiating velocity expressions. Thus we get

$$\begin{aligned}
& (\bar{A} \omega_1 + \dot{\bar{B}}_j \omega_2 + \bar{B}_j \dot{\omega}_2) \times \bar{C}_j \\
& \quad + (\bar{A} \omega_1 + \bar{B}_j \omega_2) \times \dot{\bar{C}}_j \\
& = -(\bar{D} \times \dot{\bar{C}}_j) \omega_4 - (\bar{D} \times \bar{C}_j) \dot{\omega}_4 \quad (3.67)
\end{aligned}$$

$$\begin{aligned}
- \bar{A} \omega_1 \times \dot{\bar{B}}_j & = (\dot{\bar{C}}_j \omega_3 + \bar{C}_j \dot{\omega}_3 + \bar{D} \dot{\omega}_4) \times \bar{B}_j \\
& \quad + (\bar{C}_j \omega_3 + \bar{D} \omega_4) \times \dot{\bar{B}}_j \quad (3.68)
\end{aligned}$$

$$\begin{aligned}
& \bar{A} \omega_1 \times \dot{\bar{Q}}_j + \dot{\bar{B}}_j \omega_2 \times (\bar{Q}_j - \bar{P}_j) + \bar{B}_j \dot{\omega}_2 \\
& \quad + \bar{B}_j \times (\bar{Q}_j - \bar{P}_j) \dot{\omega}_2 + \bar{B}_j \ddot{\omega}_2 - \bar{A} \omega_1 \ddot{\bar{O}}_j \\
& \quad + \bar{B}_j \omega_2 \times (\dot{\bar{Q}}_j - \dot{\bar{P}}_j) \\
& = -[\bar{D} \dot{\omega}_4 \times (\bar{Q}_j - \bar{R}_j) + \dot{\bar{C}}_j \dot{\omega}_3 \\
& \quad + \bar{D} \omega_4 \times (\dot{\bar{Q}}_j - \dot{\bar{R}}_j) + \bar{C}_j \ddot{\omega}_3 \\
& \quad + \bar{D} \ddot{\omega}_4] \quad (3.69)
\end{aligned}$$

$$\begin{aligned}
& \bar{A} \omega_1 \times (\dot{\bar{u}}_j - \dot{\bar{o}}_j) + \dot{\bar{E}}_j \omega_5 \times (\bar{u}_j - \bar{T}_j) \\
& + \bar{E}_j \dot{\omega}_5 \times (\bar{u}_j - \bar{T}_j) + \bar{E}_j \omega_5 \times (\dot{\bar{u}}_j - \dot{\bar{T}}_j) \\
& = - \left[ \bar{D} \dot{\omega}_4 \times (\bar{u}_j - \bar{R}_j) + \bar{D} \omega_4 \times (\dot{\bar{u}}_j - \dot{\bar{R}}_j) \right. \\
& \quad + \dot{\bar{G}}_j \omega_6 \times (\bar{u}_j - \bar{W}_j) + \bar{G}_j \dot{\omega}_6 \times (\bar{u}_j - \bar{W}_j) \\
& \quad + \bar{G}_j \omega_6 \times (\dot{\bar{u}}_j - \dot{\bar{W}}_j) + \bar{D} \ddot{S}_4 + \dot{\bar{G}}_j \dot{S}_6 \\
& \quad \left. + \bar{G}_j \dot{S}_6 \right] \tag{3.70}
\end{aligned}$$

The angular accelerations  $\dot{\omega}_4$  and  $\dot{\omega}_2$  are computed from Equation (3.67);  $\dot{\omega}_3$  from Equation (3.68);  $\ddot{S}_2, \ddot{S}_4, \ddot{S}_3$  from Equation (3.69); and  $\ddot{S}_6, \dot{\omega}_6$  and  $\dot{\omega}_5$  from Equation (3.70). Table IV presents an example of displacement analysis of HCGG-RSC mechanism.

### 3.5. Kinematic Analysis of RCGCC-CC Mechanism

Figure 21 shows a Stephenson-3 fixed pivot type RCGCC-CC mechanism. A revolute pair is located at joint G while A, B, C, D, E and F are cylinder pairs. The twist angle and link length between the axes at pairs at A and B are  $\alpha_1$  and  $a_1$ ; between pairs at B and C,  $\alpha_2$  and  $a_2$ ; between pairs at C and D,  $\alpha_3$  and  $a_3$ ; between pairs at D and A,  $\alpha_4$  and  $a_4$ ; between pairs at B and E,  $\alpha_5$  and  $a_5$ ; between pairs at E and F,  $\alpha_6$  and  $a_6$ ; between pairs at F and G,  $\alpha_7$  and  $a_7$ ; between pairs at G and A,  $\alpha_8$  and  $a_8$ . Offset distance at pair at A, due to links  $a_1$  and  $a_4$  is  $S_1$ , due to links  $a_1$  and  $a_8$ , is  $S_1 + S_{c_1}$  where  $S_{c_1}$  is constant offset of ternary link ADG at pair A. Rotation angle at pair A, between links  $a_1$  and  $a_4$  is  $\theta_1$ , while due to links  $a_1$  and  $a_8$  it is  $\theta_1 + \theta_{c_1}$  where  $\theta_{c_1}$  is included angle of ternary link ADG at pair A. Similarly,  $S_2, \theta_2$  and  $S_2 + S_{c_2}, \theta_2 + \theta_{c_2}$

TABLE IV

## EXAMPLE ANALYSIS OF HCCG-RSG MECHANISM

The constant parameters of the mechanism are:

$$\alpha_1 = 20^\circ, \alpha_2 = 30^\circ, \alpha_3 = 40^\circ, \alpha_4 = 30^\circ, \alpha_5 = 20^\circ, \alpha_6 = 15^\circ, \theta_{c1} = 10^\circ, \theta_{c2} = 18^\circ, s_{c1} = 0.1$$

$$s_{c2} = 0.4, \beta = 0.022, S_{11} = 0.12, S_5 = -0.2, a_1 = 1.2, a_2 = 2.5, a_3 = 2.8, a_4 = 1.2, a_5 = 1.8$$

$$a_6 = 3.0, a_7 = 2.8, a_8 = 3.5$$

One of the solutions is shown below:

$\theta_1$	$S_1$	$\theta_2$	$\theta_4$	$\theta_5$	$\theta_6$	$S_6$	$S_2$	$S_3$	$S_4$
240	0.212	-4.706	-86.423	32.717	-81.456	-0.219	-0.316	-0.848	2.178
250	0.216	-18.577	-87.911	18.880	-80.526	0.081	0.032	-0.985	2.137
260	0.220	-31.158	-90.720	7.192	-80.969	0.284	0.347	-1.134	2.117
270	0.224	-43.900	-94.450	-3.400	-81.769	0.414	0.712	-1.388	2.111
280	0.228	-53.773	-98.827	-13.336	-82.571	0.486	0.882	-1.462	2.114
290	0.232	-64.168	-103.654	-22.785	-83.245	0.511	1.109	-1.635	2.118
300	0.236	-74.069	-108.776	-31.819	-83.752	0.499	1.309	-1.812	2.120
310	0.240	-83.504	-114.061	-40.449	-84.121	0.454	1.484	-1.986	2.116
320	0.244	-92.472	-119.397	-48.672	-84.426	0.385	1.633	-2.153	2.103
330	0.248	-100.950	-124.679	-56.483	-84.783	0.295	1.756	-2.306	2.077
340	0.252	-108.907	-129.816	-63.894	-85.344	0.189	1.849	-2.437	2.037
350	0.254	-116.309	-134.727	-70.933	-86.297	0.069	1.913	-2.539	1.979

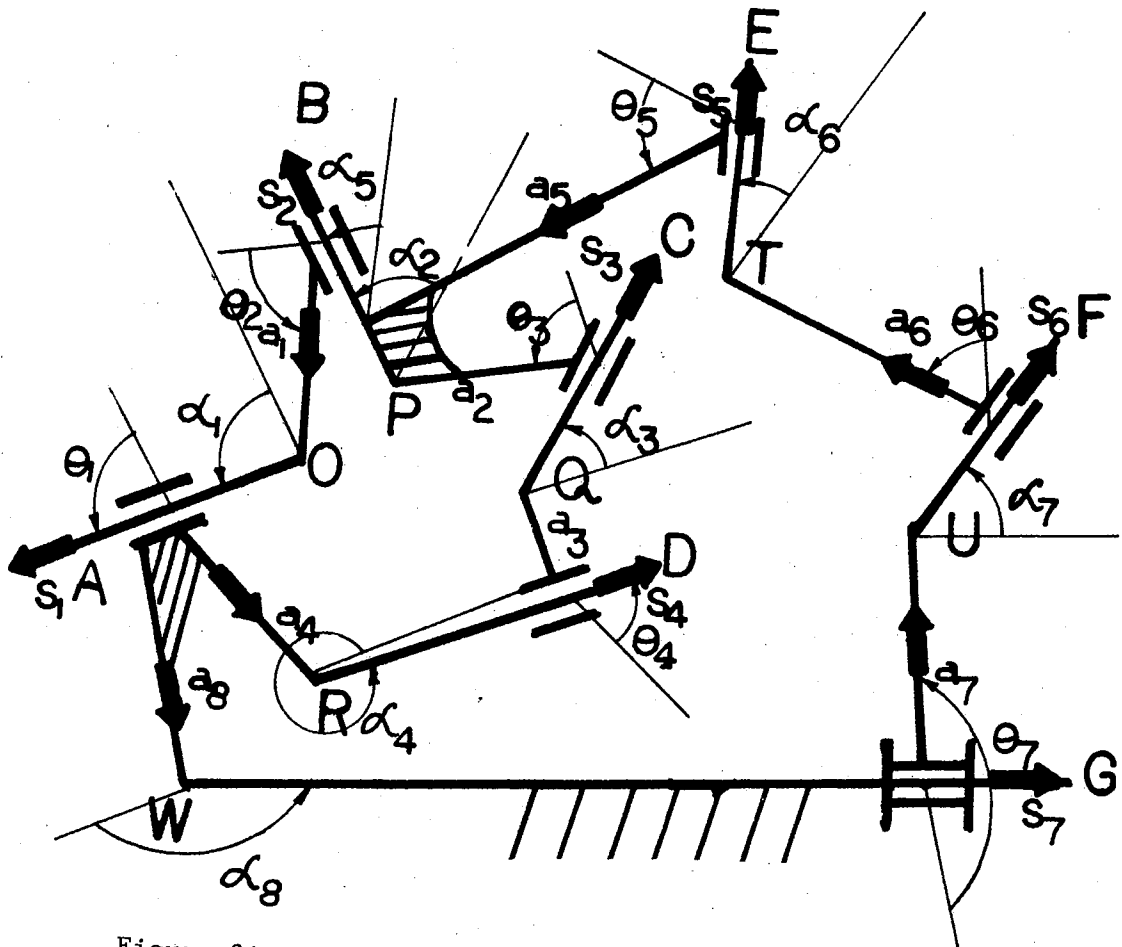


Figure 21. A RCCCG-CC Spatial, Six-Link Mechanism



denote the offset distances and rotations between links  $a_1, a_2$  and  $a_1, a_5$  where  $S_{c_2}$  and  $\theta_{c_2}$  are parameters of ternary links BCE at B pair. Other offsets and rotation angles are  $S_5, \theta_5$  at pair E between links  $a_5$  and  $a_6$ ;  $S_6, \theta_6$  at pair F between links  $a_6$  and  $a_7$ ;  $S_7, \theta_7$  at pair G, between links  $a_7$  and  $a_8$ ;  $S_3$  and  $\theta_3$  at pair C between links  $a_2$  and  $a_3$ ;  $S_4$  and  $\theta_4$  at D pair between links  $a_3$  and  $a_4$ . Note that the link lengths and offset distances have directed sense, and the rotation angles and twist angles are measured in positive screw sense as described in Chapter II.

Since the pair at G is a revolute pair, the offset distance  $S_7$  is a constant. The mechanism is divided into four open loop chains by separating the two elements of each of the cylinder pairs located at C and F. The open loop chains are unfolded along a straight line and are shown in Figure 22 and Figure 23. The following vectors are defined from Figures 22 and 23.

$$\begin{aligned} \bar{A} &= \vec{i} \\ \bar{B} &= \cos \alpha_1 \vec{i} + \sin \alpha_1 \vec{K} \\ \bar{C}_1 &= \cos(\alpha_1 + \alpha_2) \vec{i} + \sin(\alpha_1 + \alpha_2) \vec{K} \\ \bar{E} &= \cos(\alpha_1 + \alpha_5) \vec{i} + \sin(\alpha_1 + \alpha_5) \vec{K} \\ \bar{F}_1 &= \cos(\alpha_1 + \alpha_5 + \alpha_6) \vec{i} + \sin(\alpha_1 + \alpha_5 + \alpha_6) \vec{K} \\ \bar{G} &= \cos \alpha_8 \vec{i} - \sin \alpha_8 \vec{K} \\ \bar{D} &= \cos \alpha_4 \vec{i} - \sin \alpha_4 \vec{K} \\ \bar{C}_2 &= \cos(\alpha_3 + \alpha_4) \vec{i} - \sin(\alpha_3 + \alpha_4) \vec{K} \\ \bar{F}_2 &= \cos(\alpha_7 + \alpha_8) \vec{i} - \sin(\alpha_7 + \alpha_8) \vec{K} \\ \bar{u}_1 &= 0 \\ \bar{T} &= a_6 \vec{j} \\ \bar{P} &= (a_5 + a_6) \vec{j} \end{aligned}$$

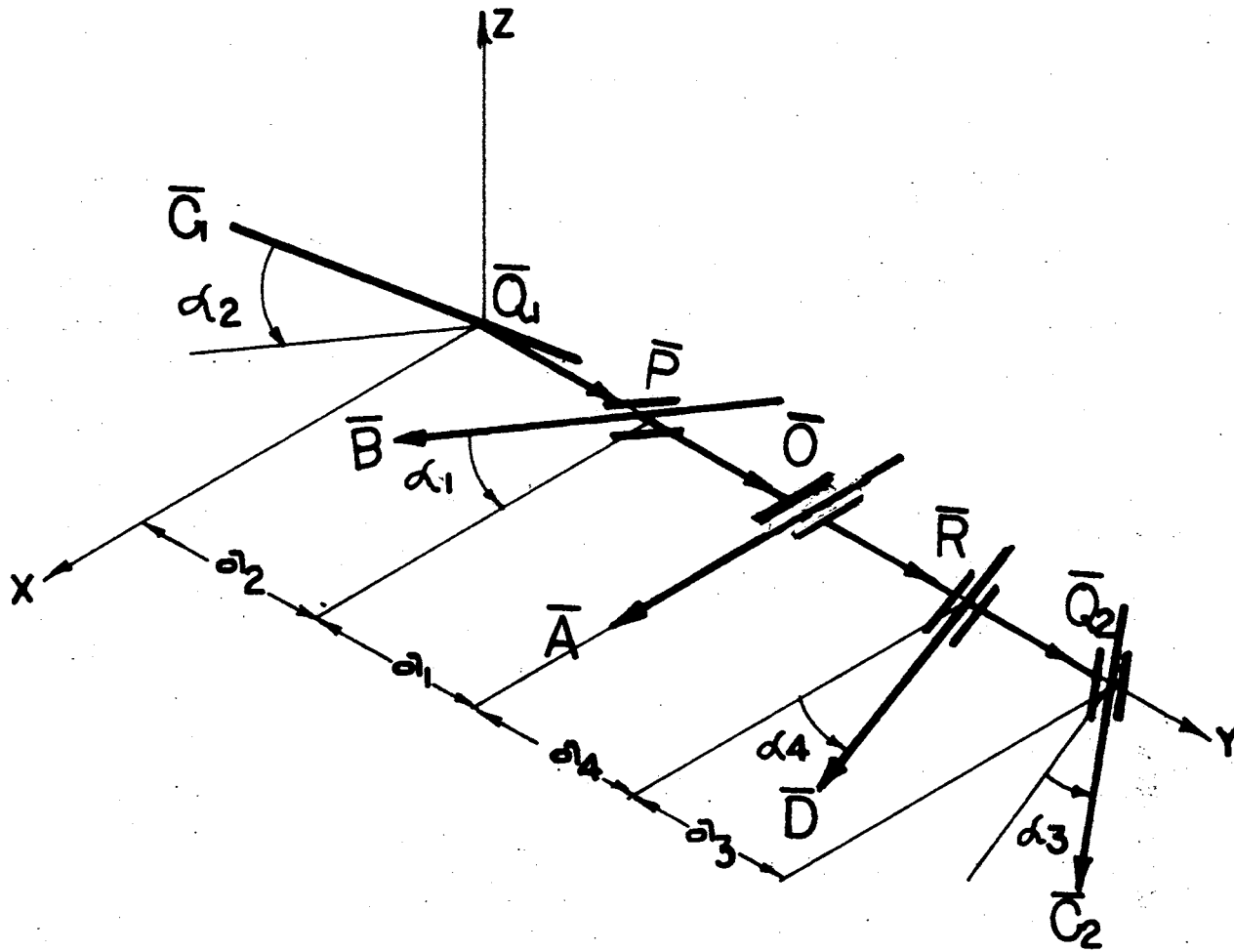


Figure 22. Unfolded Position of First Loop of Spatial RCCG-CC Mechanism

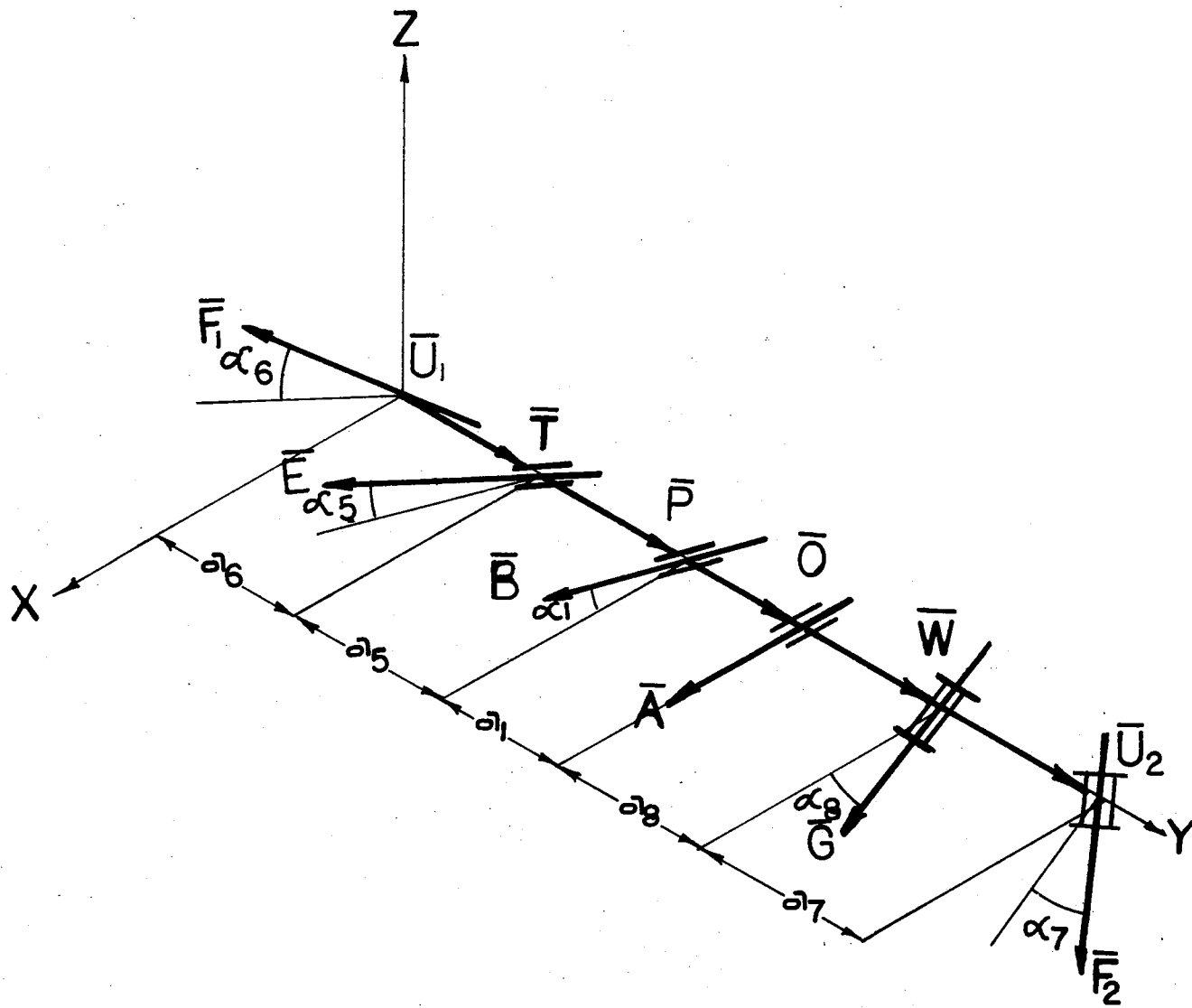


Figure 23. Unfolded Position of Second Loop of Spatial RCCCG-CC Mechanism

$$\begin{aligned}
\bar{O} &= (a_1 + a_5 + a_6) \vec{j} \\
\bar{W} &= (a_1 + a_5 + a_6 + a_8) \vec{j} \\
\bar{u}_2 &= (a_1 + a_5 + a_6 + a_7 + a_8) \vec{j} \\
\bar{Q}_1 &= (a_5 + a_6 - a_2) \vec{j} \\
\bar{R} &= (a_1 + a_5 + a_6 + a_4) \vec{j} \\
\bar{Q}_2 &= (a_1 + a_3 + a_4 + a_5 + a_6) \vec{j}
\end{aligned}$$

Let  $\theta_1$ , rotations at  $\bar{A}$ , be known, and we shall compute rotations and translations at all the joints for this value of  $\theta_1$ . The angular relationships in the loop ABCD in Figure 21 are the same as the angular relationships of the loop ABCD in Figure 16. Hence  $\theta_4$ ,  $\theta_3$  and  $\theta_2$  are computed using Equations (3.56) and (3.55). The angular displacement relationships of loop ABEFG are similar to those described in Section 3.2 for analysis ABEFG of mechanism shown in Figure 14. Hence,  $\theta_5$ ,  $\theta_6$  and  $\theta_7$  are computed using Equations (3.37), (3.38) and (3.39). The angular displacements at all the joints are thus known. To calculate the translations at the pairs, we utilize equations obtained by using constraint Equation (2.26) on  $\bar{Q}_1$  and  $\bar{Q}_2$  for successive screw displacements of chains  $ABQ_1$  and  $DQ_2$  and on  $\bar{U}_1$  and  $\bar{U}_2$  for successive screw displacements of chains  $ABEU_1$  and  $AGU_2$ . We obtain

$$\begin{aligned}
\bar{A}S_1 + \bar{B}jS_2 + \bar{C}jS_3 + \bar{D}S_4 \\
= \bar{Q}_1' - \bar{Q}_2'
\end{aligned} \tag{3.71}$$

$$\begin{aligned}
\bar{A}S_1 + \bar{B}jS_2 + \bar{C}jS_3 + \bar{E}jS_5 + \bar{F}jS_6 \\
+ \bar{G}jS_7 = \bar{u}_1' - \bar{u}_2' - \bar{B}jSc_2 - \bar{A}Sc_1
\end{aligned} \tag{3.72}$$

where

$$\begin{aligned}
\bar{B}_j &= \Delta_1(\bar{B}, -\bar{A}, \theta_1) \\
\bar{C}_j &= \Delta_2(\bar{C}_1, -\bar{B}, -\bar{A}, \theta_2, \theta_1) \\
\bar{E}_j &= \Delta_2(\bar{E}, -\bar{B}, -\bar{A}, \theta_2 + \theta_{c_2}, \theta_1) \\
\bar{F}_j &= \Delta_2(\bar{F}, \bar{G}, \bar{A}, \theta_7, \theta_{c_1}) \\
\bar{G}_j &= \Delta_1(\bar{G}, \bar{A}, \theta_{c_1}) \\
\bar{Q}'_2 &= \Delta_3(\bar{Q}_2, \bar{R}, \bar{D}, \theta_4, 0) \\
\bar{Q}'_1 &= \Delta_4(\bar{Q}_1, \bar{P}, \bar{O}, -\bar{B}, -\bar{A}, \theta_2, \theta_1, 0, 0) \\
\bar{u}'_2 &= \Delta_4(\bar{u}_2, \bar{W}, \bar{O}, \bar{G}, \bar{A}, \theta_7, \theta_{c_1}, 0, 0) \\
\bar{u}''_1 &= \Delta_4(\bar{u}_1, \bar{T}, \bar{P}, -\bar{E}, -\bar{B}, \theta_5, \theta_2 + \theta_{c_2}, 0, 0) \\
\bar{u}'_1 &= \Delta_3(\bar{u}''_1, \bar{O}, -\bar{A}, \theta_1, 0, 0)
\end{aligned}$$

where  $\theta_{c_2}$ ,  $\theta_{c_1}$ ,  $S_{c_2}$  and  $S_{c_1}$  are parameters of ternary links. Since G is a revolute pair,  $S_7 = \text{Constant}$ . Translations  $S_1$ ,  $S_2$ ,  $S_3$ ,  $S_4$ ,  $S_5$  and  $S_6$  are computed from six linear equations obtained from two vector Equations (3.71) and (3.72). Velocity and acceleration analysis of the mechanism is conducted by equating the velocity and accelerations at cylinder pairs located at C and F. Table V shows an example of displacement analysis of an RCCC-RSC mechanism. Tables VI and VII show examples of velocities and acceleration analysis of RCCC-RSC mechanism shown in Table V.

TABLE V

## KINEMATIC ANALYSIS OF RCGG-RSG MECHANISM

The constant parameters of the mechanism are:

$$\alpha_1 = 20^\circ, \alpha_2 = 30^\circ, \alpha_4 = 30^\circ, \alpha_5 = 20^\circ, \alpha_6 = 15^\circ, s_{c1} = 0.1, s_{c2} = 0.4, \theta_{c1} = 0, s_1 = 0.35$$

$$\omega_1 = 0.1, a_1 = 1.2, a_2 = 2.5, a_3 = 2.8, a_4 = 1.8, a_6 = 3.0, a_7 = 2.8, a_8 = 3.5, s_8 = 0.7$$

One of the solutions is given below:

$\theta_1$	$\theta_2$	$\theta_4$	$\theta_5$	$\theta_6$	$S_6$	$S_2$	$S_3$	$S_4$
250	-18.58	-87.91	52.54	-62.93	-1.16	1.52	-1.73	2.39
260	-31.16	-90.72	35.97	-53.77	-0.92	1.72	-1.86	2.50
270	-45.33	-94.45	22.89	-48.44	-0.74	2.12	-2.20	2.58
280	-53.77	-98.83	11.53	-44.86	-0.61	2.11	-2.11	2.65
290	-64.17	-103.65	1.29	-42.29	-0.52	2.29	-2.24	2.70
300	-74.07	-108.78	-8.20	-40.35	-0.45	2.44	-2.36	2.73
310	-83.51	-114.06	-17.14	-38.88	-0.42	2.57	-2.47	2.74
320	-92.47	-119.40	-25.62	-37.80	-0.40	2.67	-2.56	2.73
330	-100.95	-124.68	-33.69	-37.07	-0.41	2.74	-2.62	2.70
340	-108.91	-129.82	-41.38	-36.73	-0.42	2.77	-2.66	2.64
350	-116.31	-134.73	-48.69	-36.83	-0.44	2.77	-2.65	2.56
360	-123.14	-139.36	-55.62	-37.40	-0.46	2.74	-2.61	2.44
10	-129.37	-143.65	-62.15	-38.52	-0.49	2.68	-2.52	2.31
20	-135.02	-147.59	-68.29	-40.22	-0.51	2.59	-2.40	2.16
30	-140.10	-151.18	-74.03	-42.54	-0.53	2.48	-2.25	1.99
40	-144.67	-154.42	-79.35	-45.52	-0.55	2.36	-2.08	1.81
50	-148.77	-157.35	-84.26	-49.20	-0.57	2.23	-1.89	1.62
60	-152.45	-160.00	-88.73	-53.64	-0.59	2.11	-1.70	1.43
70	-155.77	-162.39	-92.73	-58.98	-0.62	1.99	-1.51	1.24
80	-158.78	-164.57	-96.15	-65.49	-0.66	1.88	-1.32	1.05
90	-167.38	-166.56	-98.64	-73.93	-0.70	2.23	-1.65	0.83
100	-164.06	168.39	-99.27	-88.16	-0.88	1.70	-0.97	0.65

TABLE VI

## VELOCITY ANALYSIS OF RCGG-RSG MECHANISM

$\theta_1$	$\omega_2$	$\omega_3$	$\omega_4$	$\omega_5$	$\omega_6$	$\dot{s}_2$	$\dot{s}_3$	$\dot{s}_4$	$\dot{s}_6$
250	-0.13	-0.07	-0.02	-0.09	-0.05	0.37	0.81	0.29	-0.09
260	-0.12	-0.06	-0.03	-0.08	-0.05	0.34	0.80	0.31	-0.13
270	-0.11	-0.06	-0.04	-0.07	-0.05	0.32	0.77	0.32	-0.17
280	-0.11	-0.06	-0.05	-0.07	-0.05	0.29	0.75	0.33	-0.21
290	-0.10	-0.05	-0.05	-0.07	-0.05	0.27	0.72	0.33	-0.24
300	-0.10	-0.05	-0.05	-0.07	-0.04	0.25	0.68	0.33	-0.26
310	-0.09	-0.04	-0.05	-0.07	-0.04	0.23	0.64	0.32	-0.28
320	-0.09	-0.03	-0.05	-0.07	-0.04	0.21	0.59	0.30	-0.29
330	-0.08	-0.03	-0.05	-0.07	-0.04	0.19	0.54	0.28	-0.30
340	-0.08	-0.02	-0.05	-0.07	-0.04	0.17	0.49	0.25	-0.29
350	-0.07	-0.01	-0.05	-0.06	-0.04	0.15	0.43	0.22	-0.28
360	-0.07	0.00	-0.04	-0.06	-0.04	0.13	0.38	0.19	-0.27
10	-0.06	0.01	-0.04	-0.06	-0.04	0.12	0.32	0.16	-0.25
20	-0.05	0.02	-0.04	-0.06	-0.04	0.10	0.27	0.12	-0.23
30	-0.05	0.03	-0.03	-0.05	-0.04	0.09	0.23	0.09	-0.20
40	-0.04	0.03	-0.03	-0.05	-0.04	0.08	0.19	0.04	-0.18
50	-0.03	0.04	-0.03	-0.05	-0.05	0.07	0.15	0.01	-0.16
60	-0.03	0.05	-0.03	-0.05	-0.05	0.06	0.12	-0.01	-0.15
70	-0.03	0.05	-0.02	-0.04	-0.05	0.05	0.09	-0.03	-0.13
80	-0.03	0.06	-0.02	-0.04	-0.05	0.05	0.07	-0.03	-0.12
90	-0.03	0.06	-0.02	-0.04	-0.06	0.04	0.05	-0.04	-0.11
100	-0.02	0.06	-0.02	-0.03	-0.06	0.04	0.03	-0.05	-0.10

TABLE VII

## ACCELERATION ANALYSIS OF RCGG-GSR MECHANISM

$\theta_1$	$\dot{\omega}_2$	$\dot{\omega}_3$	$\dot{\omega}_4$	$\dot{\omega}_6$	$\ddot{s}_2$	$\ddot{s}_3$	$\ddot{s}_6$
250	-0.12	0.32	-0.03	0.02	0.23	0.50	-0.25
260	-0.12	-0.40	-0.04	0.05	0.23	0.51	-0.27
270	-0.11	-0.27	-0.04	0.07	0.23	0.51	-0.28
280	-0.10	-0.23	-0.05	0.08	0.22	0.50	-0.29
290	-0.10	-0.21	-0.05	0.09	0.22	0.50	-0.30
300	-0.09	-0.20	-0.05	0.09	0.21	0.49	-0.30
310	-0.09	-0.19	-0.05	0.09	0.20	0.48	-0.30
320	-0.08	-0.17	-0.05	0.09	0.19	0.47	-0.30
330	-0.08	-0.16	-0.05	0.09	0.18	0.45	-0.29
340	-0.07	-0.15	-0.05	0.08	0.17	0.43	-0.28
350	-0.07	-0.14	-0.05	0.08	0.16	0.41	-0.27
360	-0.06	-0.13	-0.04	0.07	0.15	0.39	-0.25
10	-0.06	-0.13	-0.04	0.07	0.14	0.36	-0.23
20	-0.05	-0.12	-0.04	0.06	0.13	0.34	-0.22
30	-0.05	-0.11	0.03	0.05	0.12	0.31	-0.20
40	-0.04	-0.11	-0.03	0.05	0.11	0.29	-0.18
50	-0.04	-0.11	-0.03	0.04	0.10	0.27	-0.17
60	-0.03	-0.11	-0.02	0.04	0.10	0.25	-0.15
70	-0.03	-0.11	-0.02	0.04	0.09	0.23	-0.14
80	-0.03	-0.13	-0.02	0.03	0.09	0.21	-0.13
90	-0.03	-0.17	-0.02	0.03	0.08	0.20	-0.12
100	-0.02	-0.39	-0.02	0.03	0.08	0.19	-0.11



## CHAPTER IV

### DEVELOPMENT OF TOOLS FOR SYNTHESIS OF SPATIAL, TWO-LOOP MECHANISMS

The central problem in dimensional synthesis is to find the dimensions of a mechanism which will provide a completely or incompletely specified motion to one or more links of the mechanism. The motion of links may be specified in terms of finitely separated, infinitesimally separated, or multiply separated positions. In what follows, the procedures for dimensional synthesis of spatial, two-loop, six-link mechanisms are developed. The general procedure developed here, however, is applicable to the dimensional synthesis of any spatial, spherical or planar mechanisms.

#### 4.1. Location of Lines in the Rigid Body in Motion

The synthesis procedures described herein require one to be able to express positions of lines and points in the rigid body in any  $j^{\text{th}}$  position when the body moves from the  $i^{\text{th}}$  to the  $j^{\text{th}}$  position.

Let the rigid body displacement be denoted by a screw, that is, a line  $LL'$ , where a rotational displacement  $\theta_{ij}$  about line  $LL'$  and translation  $t_{ij}$  along line  $LL'$  will move the body from the  $i^{\text{th}}$  to the  $j^{\text{th}}$  position. The line  $LL'$  in an  $xyz$  coordinate system is completely specified by a unit vector  $\bar{S}_{ij}$  parallel to  $LL'$ , and  $\bar{R}_{ij}$ , a vector from the

origin to an arbitrary point on the line.

Let there be a line  $MM'$ , in the  $i^{\text{th}}$  position of the rigid body, denoted by a unit vector  $\bar{A}_i$  parallel to line  $MM'$  and  $\bar{P}_i$  a vector from the origin to a point  $P$  on the line  $MM'$  in the  $i^{\text{th}}$  position. Then the  $j^{\text{th}}$  position of the line can be obtained by screwing it by screw of the rigid body associated with the  $i^{\text{th}}$  and  $j^{\text{th}}$  positions of the rigid body. The screws are denoted by  $\wedge$  on the unit vectors parallel to the screws. The direction  $\bar{A}_j$  of line  $MM'$  in the  $j^{\text{th}}$  position is obtained by rotating  $\bar{A}_i$  about  $\bar{S}_{ij}$  by an angle  $\theta_{ij}$  as follows

$$\bar{A}_j = (1 - \cos \theta_{ij}) (\bar{A}_i \cdot \bar{S}_{ij}) \bar{S}_{ij} + \bar{A}_i \cos \theta_{ij} + \sin \theta_{ij} (\bar{S}_{ij} \times \bar{A}_i) \quad (4.1)$$

$\bar{P}_j$ , the vector from the origin to point  $P$  in the  $j^{\text{th}}$  position is obtained by screwing  $\bar{P}_i$  by screw  $\hat{S}_{ij}$ . Hence,

$$\bar{P}_j = [(\bar{P}_i - \bar{R}_{ij}) \cdot \bar{S}_{ij}] \bar{S}_{ij} (1 - \cos \theta_{ij}) + \bar{R}_{ij} + \bar{S}_{ij} t_{ij} + \cos \theta_{ij} (\bar{P}_i - \bar{R}_{ij}) + \sin \theta_{ij} [\bar{S}_{ij} \times (\bar{P}_i - \bar{R}_{ij})] \quad (4.2)$$

Note that  $\bar{S}_{ij}$  (a unit vector with two independent components),  $\bar{R}_{ij}$  (an arbitrary point on  $LL'$ , with two independent components),  $\theta_{ij}$  and  $t_{ij}$  are six independent parameters associated with finite displacement of the rigid body from the  $i^{\text{th}}$  to the  $j^{\text{th}}$  position. It is also to be observed that  $\bar{A}_j$  and  $\bar{P}_j$  are expressed linearly in terms of  $\bar{A}_i$  and  $\bar{P}_i$  if the screw displacement parameters are known.

Let the displacement of the rigid body at the  $i^{\text{th}}$  position be infini-

tesimal, and let  $\tau$  be the independent parameter of motion. Then derivatives of axis  $\bar{A}_i$  and vector  $\bar{P}_i$  with respect to  $\tau$  may be evaluated by differentiating Equation (4.1) and Equation (4.2) and letting  $\theta_{ij} \rightarrow 0$ , to get

$$\begin{aligned}\cos \theta_{ij} &= 1 \\ \sin \theta_{ij} &= 0\end{aligned}$$

$$\frac{d\bar{A}_i}{d\tau} = (\bar{S}_i \times \bar{A}_i) \frac{d\theta_i}{d\tau} \quad (4.3)$$

and

$$\frac{d\bar{P}_i}{d\tau} = \bar{S}_i \times (\bar{P}_i - \bar{R}_i) \frac{d\theta_i}{d\tau} + \bar{S}_i \frac{dt_i}{d\tau} \quad (4.4)$$

Second order derivatives are obtained by differentiating Equations (4.3) and (4.4) as follows

$$\begin{aligned}\frac{d^2\bar{A}_i}{d\tau^2} &= \left[ \frac{d\bar{S}_i}{d\tau} \times \bar{A}_i \right] \frac{d\theta_i}{d\tau} + (\bar{S}_i \times \bar{A}_i) \frac{d^2\theta_i}{d\tau^2} \\ &\quad + (\bar{S}_i \times \frac{d\bar{A}_i}{d\tau}) \frac{d\theta_i}{d\tau} \\ &= \left[ \frac{d\bar{S}_i}{d\tau} \times \bar{A}_i \right] + \bar{S}_i \times (\bar{S}_i \times \bar{A}_i) \frac{d\theta_i}{d\tau} \\ &\quad + (\bar{S}_i \times \bar{A}_i) \frac{d^2\theta_i}{d\tau^2} \quad (4.5)\end{aligned}$$

and also

$$\begin{aligned}\frac{d^2\bar{P}_i}{d\tau^2} &= \bar{S}_i \times (\bar{P}_i - \bar{R}_i) \frac{d^2\theta_i}{d\tau^2} + \frac{d\bar{S}_i}{d\tau} \times (\bar{P}_i - \bar{R}_i) \frac{d\theta_i}{d\tau} \\ &\quad + \bar{S}_i \times \left( \frac{d\theta_i}{d\tau} \left( \frac{d\bar{P}_i}{d\tau} - \frac{d\bar{R}_i}{d\tau} \right) + \frac{d^2t_i}{d\tau^2} \right) \\ &\quad + \frac{d\bar{S}_i}{d\tau} \frac{dt_i}{d\tau} \quad (4.6)\end{aligned}$$

where  $d\bar{P}_i/d\tau$  is given by Equation (4.4). In general, the  $n^{\text{th}}$  derivative of line  $PP'$  may be expressed as

$$\frac{d^n \bar{A}_i}{d\tau^n} = \frac{d^{n-1}}{d\tau^{n-1}} \left\{ (\bar{S}_i \times \bar{A}_i) \frac{d\theta_i}{d\tau} \right\} \quad (4.7)$$

$$\frac{d^n \bar{P}_i}{d\tau^n} = \frac{d^{n-1}}{d\tau^{n-1}} \left\{ \bar{S}_i \times (\bar{P}_i - \bar{R}_i) \frac{d\theta_i}{d\tau} + \bar{S}_i \frac{d\tau_i}{d\tau} \right\} \quad (4.8)$$

It is observed that six independent motion parameters are required to specify each infinitesimally separated position of the moving link. For example, for the 2nd infinitesimally separated position, the independent parameters are

$$\frac{d^2\theta}{d\tau^2}, \frac{d^2t}{d\tau^2}, \frac{d\bar{S}}{d\tau}, \frac{d\bar{R}}{d\tau}$$

Note that derivatives of points and lines in infinitesimally separated position at  $i^{\text{th}}$  finitely separated position in the rigid body are linearly expressed in terms of position coordinates of such points and lines in the rigid body in the  $i^{\text{th}}$  position.

Let the rigid body move from the  $i^{\text{th}}$  to the  $j^{\text{th}}$  finitely separated position and then undergo a series of infinitesimal motions at the  $j^{\text{th}}$  position. Then from the above discussion, it follows that derivatives of a line in the  $j^{\text{th}}$  position may be expressed linearly in terms of its position in the  $i^{\text{th}}$  position, screws associated with displacement from the  $i^{\text{th}}$  to the  $j^{\text{th}}$  position and higher order displacements of the rigid body in the  $j^{\text{th}}$  position.

Let a rigid body  $\Sigma_1$  be attached to another body  $\Sigma_2$  by a pair which

permits screw motion. Let the screw displacement of rigid body  $\Sigma_1$  be denoted by  $\hat{S}_{ij}$  when the bodies  $\Sigma_1$  and  $\Sigma_2$  move from the  $i^{\text{th}}$  to the  $j^{\text{th}}$  position. Let the screw displacement at pair be denoted by  $\hat{H}_{ij}$ , that is a unit vector  $\bar{H}_{ij}$  parallel to screw axis, a vector  $\bar{T}_{ij}$ , locating a point on the screw axis,  $\phi_{ij}$ , rotation about the screw axis,  $h_{ij}$ , translation along the screw axis. The body  $\Sigma_2$  may be moved from its  $i^{\text{th}}$  position to the  $j^{\text{th}}$  position by first screwing it by screw  $\hat{H}_{ij}$  and then about  $\hat{S}_{ij}$ . Let  $MM'$  be a line in body  $\Sigma_2$ . Then the  $j^{\text{th}}$  position of line  $MM'$  is obtained by screwing  $MM'$  in the  $i^{\text{th}}$  position about  $\hat{H}_{ij}$  and  $\hat{S}_{ij}$  in succession. Thus, line  $MM'$  in the  $j^{\text{th}}$  position is expressed in terms of screws  $\hat{S}_{ij}$ ,  $\hat{H}_{ij}$  and coordinates of the line in the  $i^{\text{th}}$  position. The same procedure holds for expressing the  $j^{\text{th}}$  position of a point in terms of its  $i^{\text{th}}$  position. In case the  $i^{\text{th}}$  and  $j^{\text{th}}$  positions are infinitesimally separated,  $\hat{S}_{ij}$  and  $\hat{H}_{ij}$  become instantaneous screws. Higher order infinitesimal motion is expressed as a differential of first order infinitesimal motion.

#### 4.2. Chain of Rigid Bodies and

##### Pair Constraints

Let two rigid bodies  $\Sigma_1$  and  $\Sigma_2$  be connected by a kinematic pair. Let  $\hat{S}_1$  and  $\hat{S}_2$  be screws associated with the motion of bodies  $\Sigma_1$  and  $\Sigma_2$ ; then as described in Section 2.2., the geometry of the pair places certain constraints on the motion of bodies  $\Sigma_1$  and  $\Sigma_2$ , or alternatively on  $\hat{S}_1$  and  $\hat{S}_2$ . It is known from Halphen's theorem that successive screw displacements are equivalent to one single screw. Therefore, screws  $\hat{S}_1$  and  $\hat{S}_2$  may represent the resultant motion of two chains, while bodies  $\Sigma_1$  and  $\Sigma_2$  represent two chains of rigid bodies. The pair constraint equa-

tions described in Chapter II shall be used in the next section to perform the dimensional synthesis of spatial mechanisms.

#### 4.3. Synthesis of Dyads

Figure 24 shows a binary link, connecting the rigid body to the fixed frame of reference. A and B are two cylindrical pairs as shown in Figure 24. Let the rigid body move from the  $i^{\text{th}}$  to the  $j^{\text{th}}$  position. Let the screw displacement associated with the finitely separated position of the rigid body be denoted by a unit vector  $\bar{S}_{ij}$ , parallel to the screw axis; vector  $\bar{U}_{ij}$  from origin to a point U on the screw axis;  $u_{ij}$ , translations along the screw axis; and  $\theta_{ij}$ , rotations about the screw axis. Let  $\bar{A}_i$  and  $\bar{B}_i$  be unit vectors parallel to cylinder pair axes A and B in the  $i^{\text{th}}$  position; let vectors  $\bar{Q}_i$  and  $\bar{P}_i$  locate points on the axes of the cylinder pair at A and B. Let the cylinder pair at A experience a translation  $q_{ij}$  and a rotation  $\phi_{ij}$ ; and cylinder pair B experience a translation  $r_{ij}$  and rotation  $\gamma_{ij}$  when the rigid body moves from its  $i^{\text{th}}$  to  $j^{\text{th}}$  position.

Now consider the cylinder pair at B on rigid body  $\Sigma$ , then its  $j^{\text{th}}$  position is given by

$$(\bar{B}_j)_\Sigma = [\bar{B}_i - (\bar{B}_i \cdot \bar{S}_{ij}) \bar{S}_{ij}] \cos \theta_{ij} + (\bar{B}_i \cdot \bar{S}_{ij}) \bar{S}_{ij} + (\bar{S}_{ij} \times \bar{B}_i) \sin \theta_{ij} \quad (4.9)$$

$$(\bar{P}_j)_\Sigma = [(\bar{P}_i - \bar{U}_{ij}) - \{(\bar{P}_i - \bar{U}_{ij}) \cdot \bar{S}_{ij}\} \bar{S}_{ij}] \cos \theta_{ij} + \bar{S}_{ij} \times (\bar{P}_i - \bar{U}_{ij}) \sin \theta_{ij} + \bar{U}_{ij} + \bar{S}_{ij} u_{ij} + \{(\bar{P}_i - \bar{U}_{ij}) \cdot \bar{S}_{ij}\} \bar{S}_{ij} \quad (4.10)$$

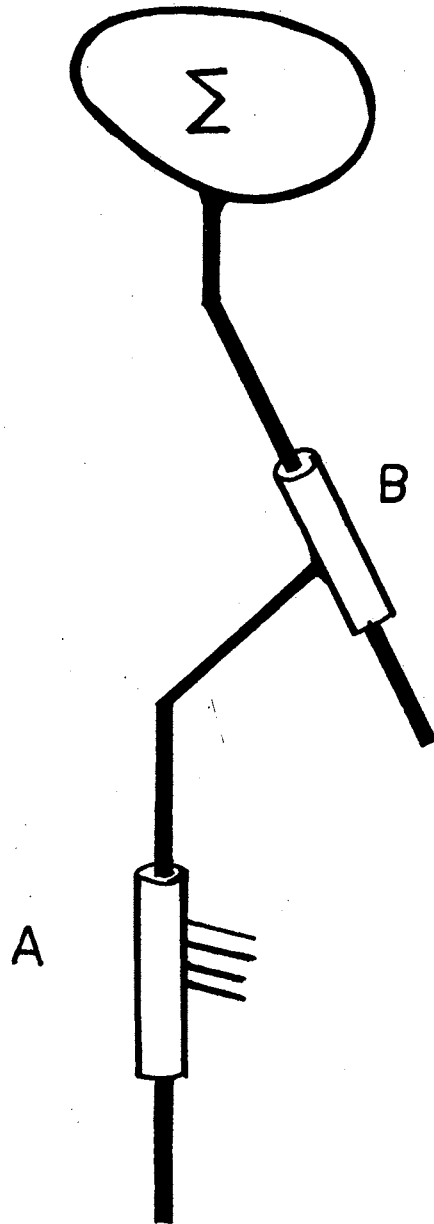


Figure 24. A Rigid Body Connected to Ground Via a C-C Dyad

The  $j^{\text{th}}$  position of cylinder joint B may also be obtained by considering the joint B on the link connected to joint A and screwing it by the screw displacement of joint A. Then

$$(\bar{B}_j)_{\text{Link AB}} = [\bar{B}_i - (\bar{B}_i \cdot \bar{A}_i) \bar{A}_i] \cos \phi_{ij} + (\bar{B}_i \cdot \bar{A}_i) \bar{A}_i + (\bar{A}_i \times \bar{B}_i) \sin \phi_{ij} \quad (4.11)$$

$$(\bar{P}_j)_{\text{Link AB}} = [(\bar{P}_i - \bar{Q}_i) - \{(\bar{P}_i - \bar{Q}_i) \cdot \bar{A}_i\} \bar{A}_i] \cos \phi_{ij} + \bar{A}_i \times (\bar{P}_i - \bar{Q}_i) \sin \phi_{ij} + \bar{A}_i \bar{Q}_i + \{(\bar{P}_i - \bar{Q}_i) \cdot \bar{A}_i\} \bar{A}_i + \bar{Q}_i \quad (4.12)$$

Pair constraint equation, which for cylinder pair from Chapter II gives

$$(\bar{P}_j)_{\Sigma} = (\bar{P}_j)_{\text{Link AB}} + (\bar{B}_j) r_{ij} \quad (4.13)$$

$$(\bar{B}_j)_{\Sigma} = (\bar{B}_j)_{\text{Link AB}} \quad (4.14)$$

Using Equation (4.14) for the  $j^{\text{th}}$  position of the axis at B, we find

$$\begin{aligned} & [\bar{B}_i - (\bar{B}_i \cdot \bar{S}_{ij}) \bar{S}_{ij}] \cos \theta_{ij} + (\bar{S}_{ij} \times \bar{B}_i) \sin \theta_{ij} \\ & + (\bar{B}_i \cdot \bar{S}_{ij}) \bar{S}_{ij} \\ & = [\bar{B}_i - (\bar{B}_i \cdot \bar{A}_i) \bar{A}_i] \cos \phi_{ij} \\ & + (\bar{A}_i \times \bar{B}_i) \sin \phi_{ij} + (\bar{B}_i \cdot \bar{A}_i) \bar{A}_i \end{aligned} \quad (4.15)$$

Eliminating  $\phi_{ij}$ , we may express  $\theta_{ij}$  as

$$\tan \frac{\theta_{ij}}{2} = - \frac{\bar{A}_i \cdot (\bar{S}_{ij} \times \bar{B}_i)}{(\bar{A}_i \times \bar{S}_{ij}) \cdot (\bar{S}_{ij} \times \bar{B}_i)} \quad (4.16)$$

Similarly eliminating  $\theta_{ij}$ , we may express  $\phi_{ij}$  as



$$\tan \frac{\phi_{ij}}{2} = \frac{\bar{A}_i \cdot (\bar{S}_{ij} \times \bar{B}_i)}{(\bar{B}_i \times \bar{A}_i) \cdot (\bar{A}_i \times \bar{S}_{ij})} \quad (4.17)$$

Using Equation (4.13) for  $\bar{P}_j$  obtained from Equations (4.10) and (4.11)

$$\begin{aligned} & [(\bar{P}_i - \bar{U}_{ij}) - \{(\bar{P}_i - \bar{U}_{ij}) \cdot \bar{S}_{ij}\} \bar{S}_{ij}] \cos \theta_{ij} + \bar{U}_{ij} \\ & + \bar{S}_{ij} \times (\bar{P}_i - \bar{U}_{ij}) \sin \theta_{ij} + \{(\bar{P}_i - \bar{U}_{ij}) \cdot \bar{S}_{ij}\} \bar{S}_{ij} + \bar{S}_{ij} u_{ij} \\ & = [(\bar{P}_i - \bar{Q}_i) - \{(\bar{P}_i - \bar{Q}_i) \cdot \bar{A}_i\} \bar{A}_i] \cos \phi_{ij} + \bar{Q}_i \\ & + \bar{A}_i \times (\bar{P}_i - \bar{Q}_i) \sin \phi_{ij} + \{(\bar{P}_i - \bar{Q}_i) \cdot \bar{A}_i\} \bar{A}_i \\ & + \bar{A}_i q_{ij} \\ & + [\{ \bar{B}_i - (\bar{B}_i \cdot \bar{S}_{ij}) \cdot \bar{S}_{ij} \} \cos \theta_{ij} + \bar{S}_{ij} \times \bar{B}_i \sin \theta_{ij} \\ & + (\bar{B}_i \cdot \bar{S}_{ij}) \bar{S}_{ij}] r_{ij} \quad (4.18) \end{aligned}$$

Vector Equation (4.18) provides three scalar equations. Eliminating  $q_{ij}$  and  $u_{ij}$  from Equation (4.18)

$$\begin{aligned} \frac{r_{ij}}{2} &= \frac{\bar{B}_i - (\bar{B}_i \cdot \bar{A}_i) \bar{A}_i}{1 - (\bar{B}_i \cdot \bar{A}_i)^2} \cdot (\bar{Q}_i - \bar{P}_i) \\ &- \frac{\bar{B}_i - (\bar{B}_i \cdot \bar{S}_{ij}) \bar{S}_{ij}}{1 - (\bar{B}_i \cdot \bar{S}_{ij})^2} \cdot (\bar{U}_{ij} - \bar{P}_i) \quad (4.19) \end{aligned}$$

Similarly, other translations are

$$\begin{aligned} \frac{u_{ij}}{2} &= - \frac{\bar{S}_{ij} - (\bar{S}_{ij} \cdot \bar{B}_i) \bar{B}_i}{1 - (\bar{S}_{ij} \cdot \bar{B}_i)^2} \cdot (\bar{P}_i - \bar{U}_{ij}) \\ &+ \frac{\bar{S}_{ij} - (\bar{S}_{ij} \cdot \bar{A}_i) \bar{A}_i}{1 - (\bar{S}_{ij} \cdot \bar{A}_i)^2} \cdot (\bar{Q}_i - \bar{U}_{ij}) \quad (4.20) \end{aligned}$$

$$\frac{q_{ij}}{2} = \frac{\bar{A}_i - (\bar{A}_i \cdot \bar{S}_{ij})\bar{S}_{ij}}{1 - (\bar{A}_i \cdot \bar{S}_{ij})^2} \cdot (\bar{U}_{ij} - \bar{Q}_i) - \frac{\bar{A}_i - (\bar{A}_i \cdot \bar{B}_i)\bar{B}_i}{1 - (\bar{A}_i \cdot \bar{B}_i)^2} \cdot (\bar{P}_i - \bar{U}_{ij}) \quad (4.21)$$

The rotation angles  $\gamma_{ij}$  at the pair B are obtained by screwing the screw axis of the rigid body by the screw at pair B and then by the screw at pair A in succession. This gives

$$\tan \frac{\gamma_{ij}}{2} = \frac{\bar{A}_i \cdot (\bar{S}_{ij} \times \bar{B}_i)}{(\bar{S}_{ij} \times \bar{B}_i) \cdot (\bar{B}_i \times \bar{A}_i)} \quad (4.22)$$

Note that the screw axes at pairs A and B and the screw axis of body form a screw triangle geometry. The relations (4.16) - (4.21) are given using screw triangle geometry in [25]. This forms an alternate derivation of the screw triangle relationships. A method for dimensional synthesis of dyads containing revolute, cylinder, prismatic and helical pairs using these relations is given in [25] and hence is not discussed in the present work. Expressions similar to Equations (4.16) - (4.21) may be derived for infinitesimally separated positions of a rigid body using infinitesimal pair constraint conditions.

However, when one or both of A and B pairs are spherical pairs, the screw axis at pairs is not completely defined.

Let B be a spheric pair and A be a revolute, a cylinder, a prism or a helical pair. Let the coordinates of the spheric point in the first position be  $(R_x, R_y, R_z)$ . Then finding the displaced position of B from

the screw displacement of the rigid body; and from the screw displacement of pair A and using the pair constraint Equation (2.18), we obtain (dropping the subscript i for initial position)

$$\begin{aligned}
 & [(\bar{R}_1 - \bar{U}_j) \cdot \bar{S}_j] \bar{S}_j (1 - \cos \theta_j) + \cos \theta_j (\bar{R}_1 - \bar{U}_j) \\
 & + \sin \theta_j (\bar{S}_j \times (\bar{R}_1 - \bar{U}_j)) + \bar{U}_j + \bar{S}_j u_j \\
 & = [(\bar{R}_1 - \bar{Q}_1) \cdot \bar{A}] \bar{A} (1 - \cos \phi_j) + \bar{Q}_1 + \bar{A} q_j \\
 & + \cos \phi_j (\bar{R}_1 - \bar{Q}_1) \\
 & + \sin \phi_j \bar{A} \times (\bar{R}_1 - \bar{Q}_1) \tag{4.23}
 \end{aligned}$$

where  $j$  denotes the parameter associated with displacement from the initial position to the  $j^{\text{th}}$  position;  $q_j = \rho \theta_j$  for the helical pair where  $\rho$  is the pitch of the screw;  $q_j$  is zero for the revolute pair;  $q_j$  is the variable for the cylinder pair and the prismatic pair;  $\theta_j$  is zero for the prismatic pair.

Consider a dimensional synthesis problem when a rigid body  $\Sigma$  is to be guided through specified positions via a G-S link. Then unit vector  $\bar{S}_j$ , vector  $\bar{U}_j$ , rotations  $\theta_j$  and translations  $u_j$  are known quantities;  $\theta_j$  and  $q_j$  are unknown variables in Equation (4.23) and may be eliminated. In addition to these variables, Equation (4.23) contains seven unknown mechanism parameters,  $R_x, R_y, R_z, Q_x, Q_y, A_x$  and  $A_y$  ( $Q_z$  is assigned an arbitrary value, since  $\bar{Q}$  locates an arbitrary point on the pair axis at A,  $A_z$  is a dependent variable on  $A_x$  and  $A_y$  by the relation  $A_z = (1 - A_x^2 - A_y^2)^{1/2}$ ).

Let the pair located at A be a revolute pair and synthesis problem is to coordinate motions of the input link with positions of the rigid

body. Then in addition to the screws of the rigid body, the rotations at the revolute pair at A are known and the translations  $q_j$  at the revolute pair are zero. Since vector Equation (4.23) provides three equations and contains seven unknown mechanism parameters, the revolute-sphere binary link may be synthesized for three positions of the rigid body coordinated with motions of the input link. For this there are a single infinity of solutions.

For infinitesimal displacements a similar procedure is followed; that is, the infinitesimal position of the spheric pair is found from both sides and is equated. Then for the first infinitesimally separated position using pair constraint Equation (2.19),

$$\bar{A} \frac{d\phi}{d\tau} \times (\bar{R}_1 - \bar{Q}_1) + \bar{A} \frac{dq}{d\tau} = -\bar{S} \times \frac{d\theta}{d\tau} (\bar{U} - \bar{R}) \quad (4.24)$$

Let  $\theta$  be independent parameter describing the motion. Then

$$\bar{A} \frac{d\phi}{d\theta} \times (\bar{R}_1 - \bar{Q}_1) + \bar{A} \frac{dq}{d\theta} = -\bar{S} \times (\bar{U} - \bar{R}) \quad (4.25)$$

where  $q$  is translation at pair A.

$dq/d\theta$  is 0, for revolute pair

$dq/d\theta = \rho (d\ell/d\theta)$  for helical pair

$dq/d\theta$  is zero for prismatic pair.

Let A be a revolute pair and synthesis problem is to guide the rigid body through infinitesimally separated positions, then Equation (4.25) reduces to

$$\bar{A} \cdot \{ \bar{S} \times (\bar{U} - \bar{R}) \} = 0 \quad (4.26)$$

$$(\bar{R}_1 - \bar{Q}_1) \cdot \{ \bar{S} \times (\bar{U} - \bar{R}_1) \} = 0 \quad (4.27)$$

If the synthesis problem is to guide a rigid body through infinitesimally separated position coordinated with infinitesimal motion of input crank, then,

$$\bar{A} \frac{d\phi}{d\theta} \times (\bar{R}_1 - \bar{Q}) = \bar{S} \times (\bar{U} - \bar{R}_1) \quad (4.28)$$

provides three equation for each infinitesimally separated position and note that  $d\phi/d\theta$  is known for such a problem.

A synthesis equation for the  $n^{\text{th}}$  infinitesimally separated position may be obtained by differentiating Equation (4.24) as

$$\frac{d^{n-1}}{d\tau^{n-1}} \left\{ \left[ \bar{A} \frac{d\phi}{d\tau} \times (\bar{R}_1 - \bar{Q}) \right] + \bar{A} \frac{dq}{d\tau} - \bar{S} \times \frac{d\theta}{d\tau} (\bar{U} - \bar{R}_1) \right\} = 0 \quad (4.29)$$

Taking  $\theta$  as independent parameter of motion

$$\frac{d^{n-1}}{d\theta^{n-1}} \left[ \left\{ \bar{A} \frac{d\phi}{d\theta} \times (\bar{R}_1 - \bar{Q}) \right\} + \bar{A} \frac{dq}{d\theta} - \bar{S} \times (\bar{U} - \bar{R}_1) \right] = 0 \quad (4.30)$$

where  $d\bar{Q}/d\theta = \bar{A} dq/d\theta$

$$\frac{d^n \bar{R}_1}{d\theta^n} = \frac{d^{n-1}}{d\theta^{n-1}} \left\{ -\bar{S} \times (\bar{U} - \bar{R}_1) \right\} \quad (4.31)$$

for rigid body guidance problem. Derivatives of  $\bar{s}$  and  $\bar{u}$  are known quantities.

If A is a spheric pair and B is a helical, cylinder, involute or prismatic pair, then it is convenient to take inversion about the moving body; that is, motion of the fixed body relative to the moving body is the inverse of the motion of the moving body relative to the fixed body. Thus, in the inverse case, the moving body becomes the fixed frame, and the fixed frame of the original problem becomes the moving body. Thus the problem of synthesis of an S-X dyad, where X denotes a helical, cylinder, involute or prismatic pair reduces to synthesis of X-S dyad which was discussed above.

Let both A and B be spherical pairs. Let spherical points denoting A and B be vectors  $\bar{Q}$  and  $\bar{R}$ , then the  $j^{\text{th}}$  position of the moving spheric point is

$$\begin{aligned} \bar{R}_j = & [(\bar{R}_1 - \bar{U}_j) \cdot \bar{S}_j] \bar{S}_j (1 - \cos \theta_j) + \bar{S}_j u_j \\ & + \sin \theta_j (\bar{S}_j \times (\bar{R}_1 - \bar{U}_j)) + \cos \theta_j (\bar{R}_1 - \bar{U}_j) \\ & + \bar{U}_j \end{aligned} \quad (4.32)$$

and

$$(\bar{R}_j - \bar{Q})^T (\bar{R}_j - \bar{Q}) = (\bar{R}_1 - \bar{Q})^T (\bar{R}_1 - \bar{Q}) \quad (4.33)$$

is the synthesis equation to be used.  $\bar{R}$  and  $\bar{Q}$  are column vectors in Equation (4.33). For infinitesimally separated position synthesis, derivatives of  $\bar{R}$  are found from the rigid body motion and differentials of Equation (4.33) are used for synthesis.

#### 4.4. Synthesis of Triads

Figure 25 shows a rigid body connected to the fixed frame of

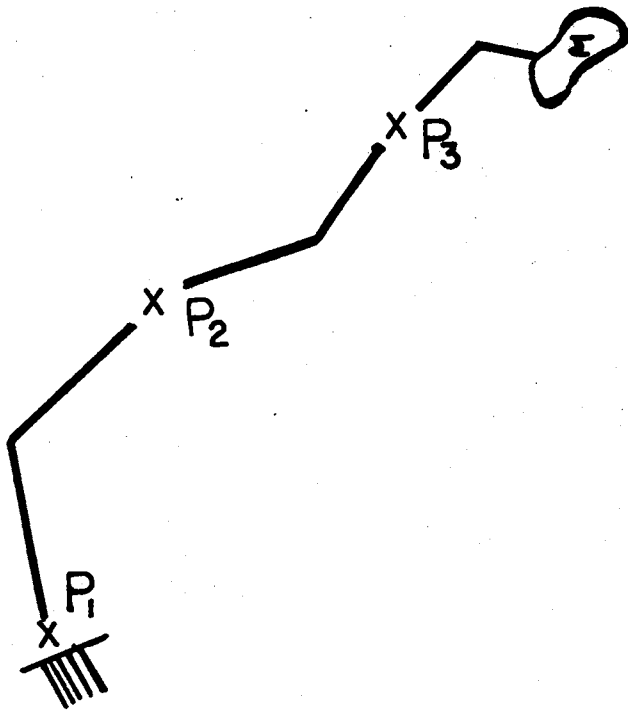


Figure 25. A Rigid Body Connected to the Ground Via a Triad

reference via a triad. Joints  $P_1$ ,  $P_2$  and  $P_3$  shown in Figure 25 are a combination of revolute, cylinder, helical, prismatic and spheric pairs. Let the screw at pair  $p_1$  be denoted by  $\bar{A}$  (unit vector),  $\bar{Q}$  (location vector),  $q$  (translation),  $\phi$  (rotation); at pair  $p_2$  by  $\bar{B}$ ,  $\bar{R}$ ,  $r$ ,  $\alpha$ ; at pair  $p_3$  by  $\bar{C}$ ,  $\bar{T}$ ,  $t$ , and  $\gamma$ : Let the finitely separated screw of the rigid body be denoted by  $\bar{S}$ ,  $\bar{U}$ ,  $u$  and  $\theta$ . Then the following equation must hold.

$$\hat{A} \hat{B} \hat{C} = \hat{S} \quad (4.34)$$

However, if we define  $\hat{A} \hat{B} = \hat{H}$  using Halphen's theorem, then

$$\hat{H} \hat{C} = \hat{S} \quad (4.35)$$

Consequently,  $\hat{A} \hat{B} = \hat{H}$  and  $\hat{H} \hat{C} = \hat{S}$  break up into two screw triangles or screw triangle chains [26]. Reference [26] also deals with corresponding infinitesimal treatment. If we choose not to introduce the unknown screw  $H$ , then alternatively the chain may be divided at  $P_3$  or  $P_2$  and the displaced positions of the pair axis and/or point from two sides may be located. Then using the pair constraint conditions described in Section 2.1 provide the synthesis equations for a synthesis problem.

Next consider four cases of rigid body guidance problem via the triad.

#### 4.4.1. C-C-R Triad

Consider the C-C-R triad shown in Figure 26. The rigid body moving through specified finitely and infinitesimally separated positions is attached to the fixed frame via a triad consisting of cylinder-cylinder and revolute pair. The displaced position of the revolute pair via successive screw displacement at two C pairs is,



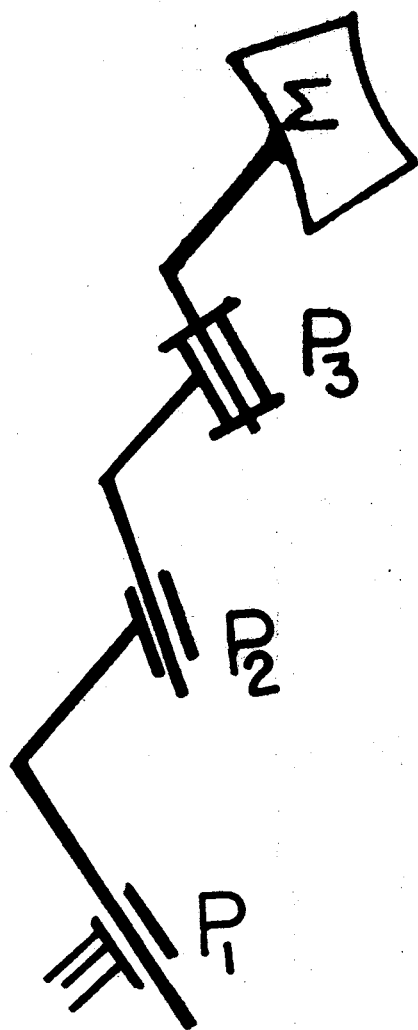


Figure 26. A Rigid Body Connected to the Ground Via a C-C-R Triad

$$\bar{C}_j = \cos \phi [\bar{C}' - (\bar{C}' \cdot \bar{A}) \bar{A}] + \sin \phi_j (\bar{A} \times \bar{C}') + (\bar{C}' \cdot \bar{A}) \bar{A} \quad (4.36)$$

where

$$\bar{C}' = \cos \gamma [\bar{C} - (\bar{C} \cdot \bar{B}) \bar{B}] + \sin \gamma (\bar{B} \times \bar{C}) + (\bar{C} \cdot \bar{B}) \bar{B} \quad (4.37)$$

and

$$\bar{T}_j = \cos \phi [(\bar{T}' - \bar{Q}) - \{(\bar{T}' - \bar{Q}) \cdot \bar{A}\} \bar{A}] + \sin \phi [\bar{A} \times (\bar{T}' - \bar{Q})] + \bar{Q} + \bar{A} \bar{Q} + \{(\bar{T}' - \bar{Q}) \cdot \bar{A}\} \bar{A} \quad (4.38)$$

where

$$\bar{T}' = \cos \gamma [(\bar{T} - \bar{R}) - \{(\bar{T} - \bar{R}) \cdot \bar{B}\} \bar{B}] + \sin \gamma [\bar{B} \times (\bar{T} - \bar{R})] + \bar{R} + \bar{B} \bar{R} + \{(\bar{T} - \bar{R}) \cdot \bar{B}\} \bar{B} \quad (4.39)$$

The displaced position of the revolute pair from specified rigid body motion is

$$\bar{C}_j = \cos \theta [\bar{C} - (\bar{C} \cdot \bar{S}) \bar{S}] + \sin \theta (\bar{S} \times \bar{C}) + (\bar{C} \cdot \bar{S}) \bar{S} \quad (4.40)$$

and

$$\bar{T}_j = \cos \theta [(\bar{T} - \bar{U}) - \{(\bar{T} - \bar{U}) \cdot \bar{S}\} \bar{S}] + \bar{U} + \bar{S} \bar{U} + \sin \theta [\bar{S} \times (\bar{T} - \bar{U})] + \{(\bar{T} - \bar{U}) \cdot \bar{S}\} \bar{S} \quad (4.41)$$

Using the pair constraint Equation (2.21) for the revolute pair we get

$$\begin{aligned} \cos\phi [\bar{c}' - (\bar{c}' \cdot \bar{A})\bar{A}] + \sin\phi (\bar{A} \times \bar{c}') + (\bar{c}' \cdot \bar{A})\bar{A} \\ = \cos\theta [\bar{c} - (\bar{c} \cdot \bar{S})\bar{S}] + \sin\theta (\bar{S} \times \bar{c}) + (\bar{c} \cdot \bar{S})\bar{S} \end{aligned} \quad (4.42)$$

$$\begin{aligned} \cos\phi [(\bar{T}' - \bar{Q}) - \{(\bar{T}' - \bar{Q}) \cdot \bar{A}\}\bar{A}] + \sin\phi [\bar{A} \times (\bar{T}' - \bar{Q})] \\ + \{(\bar{T}' - \bar{Q}) \cdot \bar{A}\}\bar{A} + \bar{Q} + \bar{A}q \\ = \cos\theta [(\bar{T} - \bar{U}) - \{(\bar{T} - \bar{U}) \cdot \bar{S}\}\bar{S}] + \bar{U} + \bar{S}u \\ + \sin\theta [\bar{S} \times (\bar{T} - \bar{U})] + \{(\bar{T} - \bar{U}) \cdot \bar{S}\}\bar{S} \end{aligned} \quad (4.43)$$

Equations (4.42) and (4.43) are the synthesis equations to be used for rigid body guidance problem via C-C-R triad,  $\gamma, \phi, q$  and  $r$  may be eliminated from five equations obtained from Equations (4.42) and (4.43) to get one equation for each precision position. Synthesis equations for this problem may also be obtained by separating the triad at pair  $p_2$ , then finding the displaced position of the cylinder pair at  $p_2$  from two sides and using the constraint Equation (2.25) of the cylinder pair.

Similar procedure is employed for derivations of equations for infinitesimal position synthesis. Derivative pair constraint equations are used on infinitesimal displacements of points and/or lines obtained from two sides. For C-C-R triad, for first infinitesimally separated position, we get

$$\left[ \bar{A} \frac{d\phi}{d\tau} + \bar{B} \frac{dr}{d\tau} \right] \times \bar{c} = (\bar{S} \times \bar{c}) \frac{d\theta}{d\tau} \quad (4.44)$$

and

$$\begin{aligned} \bar{A} \times (\bar{T} - \bar{Q}) \frac{d\theta}{d\tau} + \bar{A} \frac{dq}{d\tau} + \bar{B} \times (\bar{T} - \bar{R}) \frac{dr}{d\tau} + \bar{B} \frac{dz}{d\tau} \\ = \bar{S} \times (\bar{T} - \bar{U}) \frac{d\theta}{d\tau} + \bar{S} \frac{du}{d\tau} \end{aligned} \quad (4.45)$$

where  $\tau$  is the independent parameter of motion. Equations for higher order infinitesimal displacements synthesis are obtained by differentiating Equations (4.44) and (4.45).

#### 4.4.2. G-C-S Triad

Figure 27 shows a rigid body  $\Sigma$  attached to fixed frame of reference via G-C-S triad. Finding the displaced position of spherical pair by successive screw displacements at G-C pairs and also from specified rigid body motion and then using the pair constraint equations, obtain Equation (4.43) for finitely separated positions, and Equation (4.45) for infinitesimally separated positions as the synthesis equations.

#### 4.4.3. G-S-C Triad

Figure 28 shows a rigid body  $\Sigma$  attached to fixed frame of reference via G-S-C triad. The displaced position of spherical pair at  $p_2$  is found from successive screw displacements of rigid body and pair  $p_3$  and also from screw displacements of pair  $p_1$ . Then using the pair constraint Equation (2.18), we get for finitely separated position of rigid body,

$$\begin{aligned} \cos \theta [(\bar{R} - \bar{Q}) - \{(\bar{R} - \bar{Q}) \cdot \bar{A}\} \bar{A}] + \sin \theta \bar{A} \times (\bar{R} - \bar{Q}) \\ + \{(\bar{R} - \bar{Q}) \cdot \bar{A}\} \bar{A} + \bar{A} q + \bar{Q} \\ = \cos \theta [(\bar{R}' - \bar{U}) - \{(\bar{R}' - \bar{U}) \cdot \bar{S}\} \bar{S}] + \bar{U} + \bar{S} u \\ + \sin \theta (\bar{S} \times (\bar{R}' - \bar{U})) + \{(\bar{R}' - \bar{U}) \cdot \bar{S}\} \bar{S} \end{aligned} \quad (4.46)$$

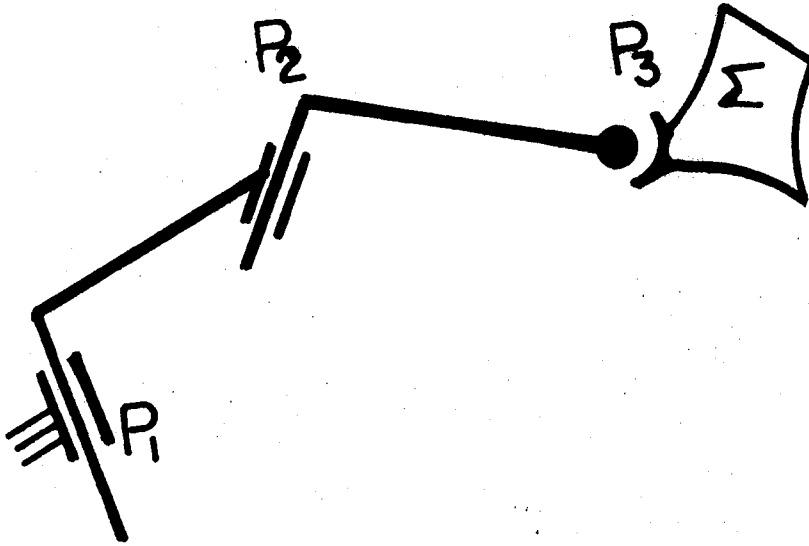


Figure 27. A Rigid Body Connected to the Ground Via a G-C-S Triad

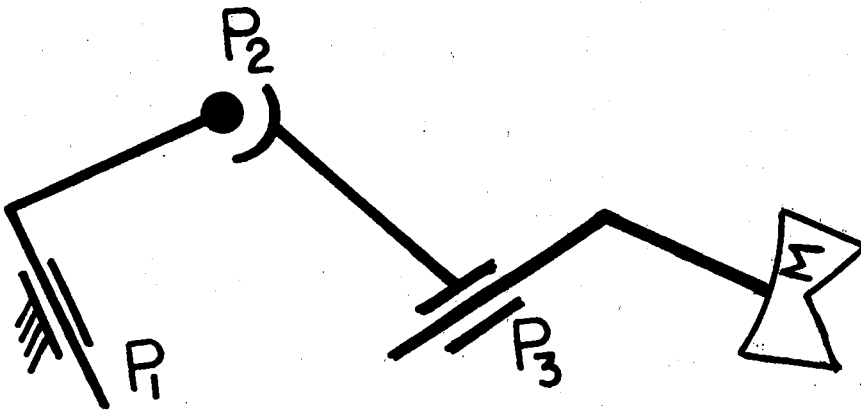


Figure 28. A Rigid Body Connected to the Ground Via a G-S-C Triad

where

$$\begin{aligned}\bar{R}' &= \cos \alpha [(\bar{R}-\bar{T}) - \{(\bar{R}-\bar{T}) \cdot \bar{C}\} \bar{C}] \\ &\quad + \sin \alpha \bar{C} \times (\bar{R}-\bar{T}) + \bar{T} + \bar{C}t \\ &\quad + \{(\bar{R}-\bar{T}) \cdot \bar{C}\} \bar{C}\end{aligned}\quad (4.47)$$

for infinitesimally separated positions,

$$\begin{aligned}\bar{A} \times (\bar{R}-\bar{Q}) \frac{d\phi}{d\tau} + \bar{A} \frac{dq}{d\tau} &= \\ &= \bar{C} \times (\bar{R}-\bar{T}) \frac{d\alpha}{d\tau} + \bar{C} \frac{dt}{d\tau} \\ &\quad + \bar{S} \times (\bar{R}-\bar{U}) \frac{d\theta}{d\tau} + \bar{S} \frac{du}{d\tau}\end{aligned}\quad (4.48)$$

#### 4.4.4. C-S-S Triad

Figure 29 shows a rigid body attached to C-S-S triad. Locate the displaced position of  $p_2$  by screwing initial  $p_2$  by screw of pair  $p_1$  and position of  $p_3$  by screwing it by screw of specified rigid body motion. Synthesis equations are obtained by using the constant length conditions between two spheric pairs as follows.

$$\begin{aligned}\bar{R}_j &= \cos \phi [(\bar{R}-\bar{Q}) - \{(\bar{R}-\bar{Q}) \cdot \bar{A}\} \bar{A}] + \bar{Q} + \bar{A}q \\ &\quad + \sin \phi \{ \bar{A} \times (\bar{R}-\bar{Q}) \} + \{(\bar{R}-\bar{Q}) \cdot \bar{A}\} \bar{A} \\ \bar{T}_j &= \cos \theta [(\bar{T}-\bar{U}) - \{(\bar{T}-\bar{U}) \cdot \bar{S}\} \bar{S}] + \bar{U} + \bar{S}u \\ &\quad + \sin \theta \{ \bar{S} \times (\bar{T}-\bar{U}) \} + \{(\bar{T}-\bar{U}) \cdot \bar{S}\} \bar{S}\end{aligned}\quad (4.49)$$

Constant length condition is expressed as

$$(\bar{R}_j - \bar{T}_j)^T (\bar{R}_j - \bar{T}_j) = (\bar{R} - \bar{T})^T (\bar{R} - \bar{T}) \quad (4.50)$$

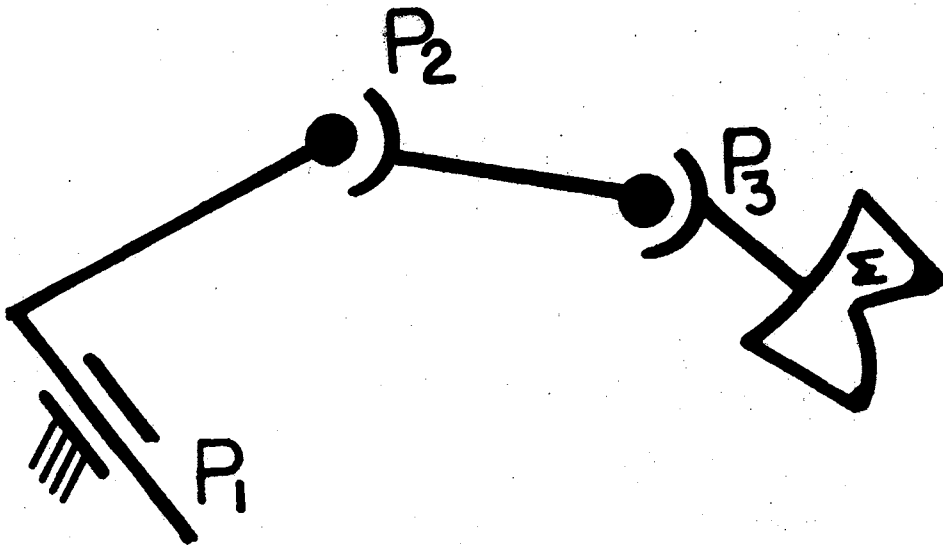


Figure 29. A Rigid Body Connected to the Ground via a C-S-S Triad

where  $\bar{R}_j$  and  $\bar{T}_j$  are column vectors.

#### 4.4.5. Constraints Due to Space Ternary Links

Consider a ternary link floating in space. It has three joints  $p_1$ ,  $p_2$ , and  $p_3$  to which three screw chains  $S_1$ ,  $S_2$ ,  $S_3$  are connected. Constraints that a ternary link places on the total motion of the mechanism may be mathematically expressed as

$$\begin{aligned} P_1(\hat{H}) &= P_1(\hat{S}_1) \\ P_2(\hat{H}) &= P_2(\hat{S}_2) \\ P_3(\hat{H}) &= P_3(\hat{S}_3) \end{aligned}$$

where  $\hat{H}$  is screw associated with ternary link;  $\hat{S}_1$ ,  $\hat{S}_2$ ,  $\hat{S}_3$  are resultant screws of the chains  $S_1$ ,  $S_2$  and  $S_3$ .

With the above discussion as background, general synthesis procedure may be laid down as follows:

1. Separate the mechanism in two or more chains at certain critical pairs in the initial position.
2. Obtain the displaced position (finite or infinitesimal) of these pairs from two sides in terms of initial position coordinates of the mechanism.
3. Impose constraint conditions described in Section 4.2., on two positions of these critical pairs.
4. Eliminate unwanted variables from the equations obtained in Step 3.

Note that cylinder, revolute, helical and prismatic pairs are specified using a unit vector parallel to the pair axis, a vector



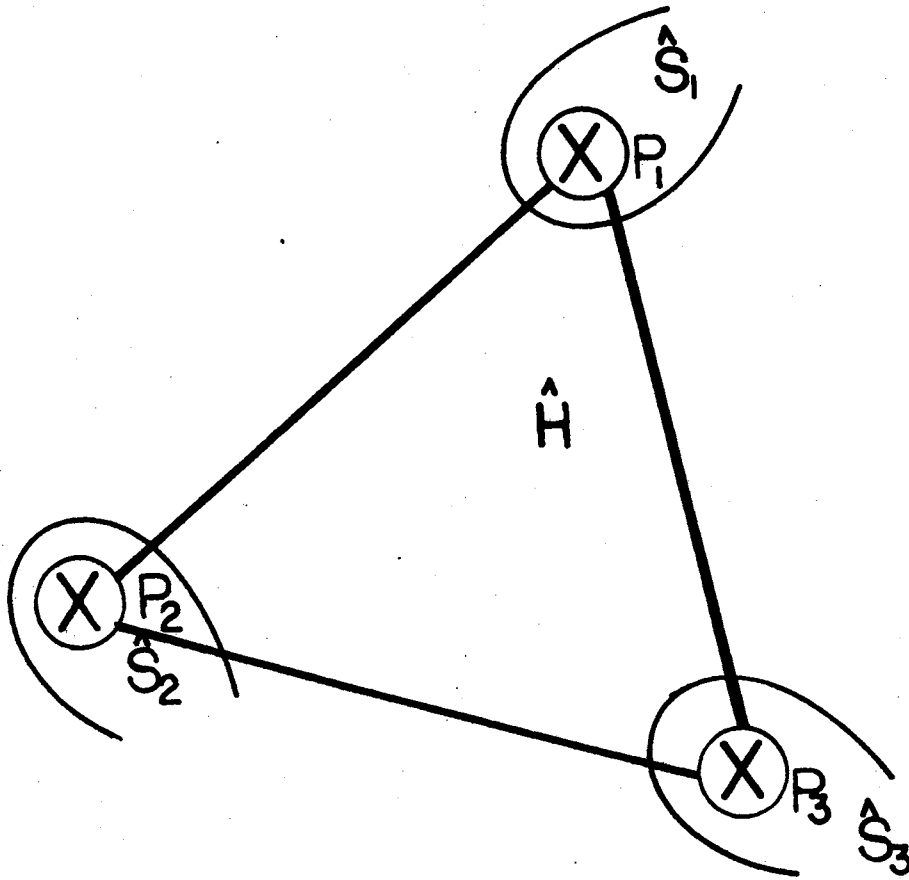


Figure 30. Screw Constraints on a Ternary Link in Space

locating an arbitrary point on the axis. Since the point along the axis is arbitrary, it may be taken as the point where pair axis intersects X-Y plane (Z component is assumed zero). Spherical pairs are specified by three coordinates of the spheric point in its initial position. In synthesis equations, these parameters of the mechanism are unknown and are computed using synthesis equations which also contain specified motion parameters.

## CHAPTER V

### SYNTHESIS OF TWO-LOOP, SPATIAL, SIX-LINK MECHANISMS

In this chapter, the mathematical tools developed in Chapter IV are applied to spatial mechanism synthesis problems. The screw triangle geometry method is also extended to the synthesis of six-link, spatial mechanisms.

#### 5.1. Synthesis of Watt's RSSR-RSR Mechanism

Figure 31 shows a Watt's RSSR-RSR mechanism. Revolute pairs are located at joints 1, 4, 5 and 6; and spherical pairs are located at joints 2, 3 and 7. The mechanism in its initial position is specified by specification of pairs in the initial position. Revolute pairs are specified by a unit vector parallel to the pair axis and a vector locating any arbitrary point on the axis. Let  $\bar{A}$ ,  $\bar{B}$ ,  $\bar{E}$  and  $\bar{F}$  be unit vectors parallel to the pair axes at joints 1, 4, 5 and 6; and let vectors  $\bar{P}$ ,  $\bar{T}$ ,  $\bar{U}$ , and  $\bar{V}$  locate arbitrary points on these pair axes. Similarly, spherical pairs are specified by vectors locating the spheric points in their initial position. Let  $\bar{Q}$ ,  $\bar{R}$ , and  $\bar{W}$  be the vectors locating spherical pairs at 2, 3 and 7 in their initial position.

Let the rigid body to be guided through specified finitely or infinitesimally separated positions be attached to the coupler link joining the revolute pairs at joints 5 and 6. Finite screws associated with specified

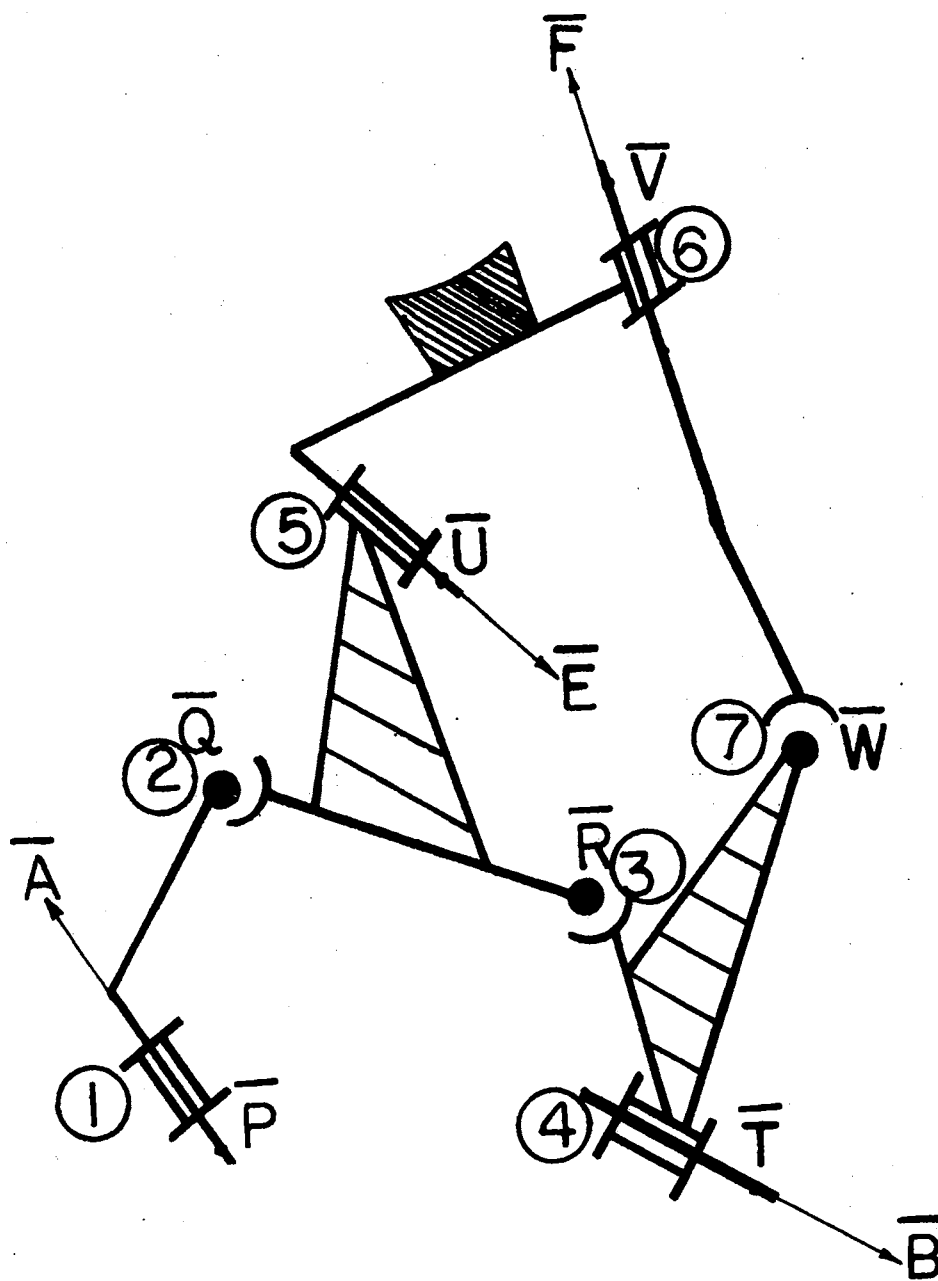


Figure 31. A Watt's Type Six-Link RSSR-RSR Mechanism for Spatial Rigid Body Guidance

rigid body displacements are  $\bar{S}_j$  (unit vector),  $\bar{X}_j$  (location vector), translations  $x_j$ , and rotation  $\theta_j$ , where it is to be understood that this screw takes the rigid body from its initial to its  $j^{\text{th}}$  position.

The dimensional synthesis problem is to find the mechanism parameters,  $\bar{A}$ ,  $\bar{B}$ ,  $\bar{E}$ ,  $\bar{F}$ ,  $\bar{P}$ ,  $\bar{T}$ ,  $\bar{U}$ ,  $\bar{V}$ ,  $\bar{Q}$ ,  $\bar{R}$  and  $\bar{W}$ , where this mechanism will guide the rigid body through specified positions. Note that since displacements of the rigid body are specified,  $\bar{S}_j$ ,  $\bar{X}_j$ ,  $x_j$ ,  $\theta_j$ ,  $j = 1, \dots, n$  are specified quantities.

Let  $\alpha_j$ ,  $\beta_j$ ,  $\gamma_j$ , and  $\delta_j$  be the rotations at revolute pairs at 1, 4, 6 and 5, when the mechanism moves from its first to its  $j^{\text{th}}$  position. The mechanism is separated at three spherical pairs and then providing known screw displacements of specified rigid motion and unknown screw displacements at revolute pairs, the  $j^{\text{th}}$  position of three spherical pairs is located as follows.

$$\bar{Q}_j = \hat{S} \hat{E} \bar{Q} = \hat{A} \bar{Q} \quad (5.1)$$

$$\bar{R}_j = \hat{S} \hat{E} \bar{R} = \hat{B} \bar{R} \quad (5.2)$$

$$\bar{W}_j = \hat{S} \hat{F} \bar{W} = \hat{B} \bar{W} \quad (5.3)$$

where the symbol  $(\wedge)$  denotes the screw and notation  $\hat{Z}\bar{X}$  signifies that vector  $\bar{X}$  is screwed by screw  $\hat{Z}$ . Then screwing  $\bar{Q}$  by  $\hat{A}$  and also by  $\hat{E}$  and  $\hat{S}$  in succession and equating the two final positions, we obtain

$$\begin{aligned} \bar{Q}_j &= \cos \theta_j [(\bar{Q}' - \bar{x}_j) - \{(\bar{Q}' - \bar{x}_j) \cdot \bar{S}_j\} \bar{S}_j] + \bar{x}_j \\ &\quad + \{(\bar{Q}' - \bar{x}_j) \cdot \bar{S}_j\} \bar{S}_j + \sin \theta_j \bar{S}_j \times (\bar{Q}' - \bar{x}_j) + \bar{S}_j \times \bar{x}_j \\ &= \cos \alpha_j [(\bar{Q} - \bar{P}) - \{(\bar{Q} - \bar{P}) \cdot \bar{A}\} \bar{A}] + \bar{P} \\ &\quad + \sin \alpha_j \{ \bar{A} \times (\bar{Q} - \bar{P}) \} + \{(\bar{Q} - \bar{P}) \cdot \bar{A}\} \bar{A} \end{aligned} \quad (5.4)$$

where,

$$\begin{aligned}\bar{Q}' &= \cos \delta_j [(\bar{Q} - \bar{U}) - \{(\bar{Q} - \bar{U}) \cdot \bar{E}\} \bar{E}] + \bar{U} \\ &+ \sin \delta_j [\bar{E} \times (\bar{Q} - \bar{U})] + \{(\bar{Q} - \bar{U}) \cdot \bar{E}\} \bar{E}\end{aligned}\quad (5.5)$$

Similarly, screwing  $\bar{R}$  by  $\hat{B}$  and also, by  $\hat{E}$  and  $\hat{S}$  in succession and equating the locations of  $\bar{R}$  in the  $j^{\text{th}}$  position, we find:

$$\begin{aligned}\bar{R}_j &= \cos \theta_j [(\bar{R}' - \bar{x}_j) - \{(\bar{R}' - \bar{x}_j) \cdot \bar{s}_j\} \bar{s}_j] + \bar{s}_j \times \\ &+ \sin \theta_j [\bar{s}_j \times (\bar{R}' - \bar{x}_j)] + \{(\bar{R}' - \bar{x}_j) \cdot \bar{s}_j\} \bar{s}_j + \bar{x}_j \\ &= \cos \beta_j [(\bar{R} - \bar{T}) - \{(\bar{R} - \bar{T}) \cdot \bar{B}\} \bar{B}] + \bar{T} \\ &+ \sin \beta_j [\bar{B} \times (\bar{R} - \bar{T})] + \{(\bar{R} - \bar{T}) \cdot \bar{B}\} \bar{B}\end{aligned}\quad (5.6)$$

where

$$\begin{aligned}\bar{R}' &= \cos \delta_j [(\bar{R} - \bar{U}) - \{(\bar{R} - \bar{U}) \cdot \bar{E}\} \bar{E}] + \bar{U} \\ &+ \sin \delta_j [\bar{E} \times (\bar{R} - \bar{U})] + \{(\bar{R} - \bar{U}) \cdot \bar{E}\} \bar{E}\end{aligned}\quad (5.7)$$

Similar procedure is applied to locate the  $j^{\text{th}}$  position of the spheric point at 7, that is,  $\bar{W}$  is screwed by  $\hat{B}$  and also by  $\hat{F}$  and  $\hat{S}$  in succession to get,

$$\begin{aligned}
\bar{W}_j &= \cos\theta_j [(\bar{W}' - \bar{x}_j) - \{(\bar{W}' - \bar{x}_j) \cdot \bar{s}_j\} \bar{s}_j] \\
&\quad + \sin\theta_j \{ \bar{s}_j \times (\bar{W}' - \bar{x}_j) \} + \{(\bar{W}' - \bar{x}_j) \cdot \bar{s}_j\} \bar{s}_j \\
&\quad + \bar{x}_j + \bar{s}_j \times \\
&= \cos\beta_j [(\bar{W} - \bar{T}) - \{(\bar{W} - \bar{T}) \cdot \bar{B}\} \bar{B}] + \bar{T} \\
&\quad + \sin\beta_j \{ \bar{B} \times (\bar{W} - \bar{T}) \} + \{(\bar{W} - \bar{T}) \cdot \bar{B}\} \bar{B}
\end{aligned} \tag{5.8}$$

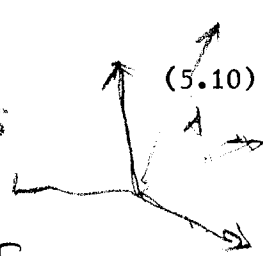
$$\begin{aligned}
\bar{W}' &= \cos\gamma_j [(\bar{W} - \bar{V}) - \{(\bar{W} - \bar{V}) \cdot \bar{F}\} \bar{F}] + \bar{V} \\
&\quad + \sin\gamma_j [\bar{F} \times (\bar{W} - \bar{V})] + \{(\bar{W} - \bar{V}) \cdot \bar{F}\} \bar{F}
\end{aligned} \tag{5.9}$$

Vector Equations (5.4), (5.6) and (5.8) provide 9 scalar equations for each specified position of the rigid body; but for each position, four unknown rotations at the revolute pairs, namely  $\alpha_j$ ,  $\beta_j$ ,  $\gamma_j$  and  $\delta_j$ , are introduced into these equations. These unknowns may be eliminated from Equations (5.4), (5.6) and (5.8). Since  $\bar{A}$ ,  $\bar{B}$ ,  $\bar{E}$  and  $\bar{F}$  are unit vectors, they have only two independent unknown components; vectors  $\bar{P}$ ,  $\bar{T}$ ,  $\bar{U}$  and  $\bar{V}$  locate arbitrary points along the axis of revolute pairs, 3rd components of such vectors may then be assigned arbitrary value. Vectors  $\bar{Q}$ ,  $\bar{R}$  and  $\bar{W}$  locating spheric points contribute three unknowns each. Hence, there are a total of 25 unknown mechanism parameters in Equations (5.4), (5.6) and (5.8). The maximum of six positions of rigid body may be specified for guidance via a RSSR-RSR six-link mechanism.

To obtain design equations for infinitesimally separated positions, the mechanism is again divided at three spherical pairs and derivatives

$$\frac{(\bar{A} \times \bar{E}) \cdot \bar{A} \times (\bar{Q} \cdot \bar{P})}{0}$$

of  $\bar{R}$ ,  $\bar{Q}$ , and  $\bar{W}$  from two sides are equated to get,

$$\begin{aligned} 1) \quad & \bar{S} \times (\bar{Q} - \bar{X}) \frac{d\theta}{d\tau} + \bar{E} \times (\bar{Q} - \bar{U}) \frac{d\delta}{d\tau} + \bar{S} \frac{dx}{d\tau} \\ & = \left\{ \frac{(\bar{A} \times \bar{E}) \cdot \bar{A}}{(\bar{A} \times \bar{Q}) - \bar{A} \times \bar{P}} \bar{A} \times (\bar{Q} - \bar{P}) \frac{d\alpha}{d\tau} \right\} \end{aligned} \quad (5.10)$$


$$\begin{aligned} & \bar{S} \times (\bar{R} - \bar{X}) \frac{d\theta}{d\tau} + \bar{E} \times (\bar{R} - \bar{U}) \frac{d\delta}{d\tau} + \bar{S} \frac{dx}{d\tau} \\ & = \bar{B} \times (\bar{R} - \bar{T}) \frac{d\beta}{d\tau} \end{aligned} \quad (5.11)$$

$$\begin{aligned} & \bar{S} \times (\bar{W} - \bar{X}) \frac{d\theta}{d\tau} + \bar{F} \times (\bar{W} - \bar{V}) \frac{d\gamma}{d\tau} + \bar{S} \frac{dx}{d\tau} \\ & = \bar{B} \times (\bar{W} - \bar{T}) \frac{d\beta}{d\tau} \end{aligned} \quad (5.12)$$

Taking  $\theta$  as independent parameter of motion and then eliminating  $d\alpha/d\theta$ ,  $d\beta/d\theta$ ,  $d\gamma/d\theta$  and  $d\delta/d\theta$ , the following five equations are obtained:

$$(\bar{A} \times \bar{E}) \cdot \left\{ \bar{S} \times (\bar{Q} - \bar{X}) \right\} + (\bar{A} \times \bar{E}) \cdot \bar{S} \frac{dx}{d\theta} = 0 \quad (5.13)$$

$$(\bar{E} \times \bar{B}) \cdot \left\{ \bar{S} \times (\bar{R} - \bar{X}) \right\} + (\bar{E} \times \bar{B}) \cdot \bar{S} \frac{dx}{d\theta} = 0 \quad (5.14)$$

$$(\bar{B} \times \bar{F}) \cdot \left\{ \bar{S} \times (\bar{W} - \bar{X}) \right\} + (\bar{B} \times \bar{F}) \cdot \bar{S} \frac{dx}{d\theta} = 0 \quad (5.15)$$



$$\frac{\bar{A} \cdot \{ \bar{S} \times (\bar{Q} - \bar{X}) \} + \bar{A} \cdot \bar{S} \frac{d\bar{x}}{d\theta}}{\bar{A} \cdot \{ \bar{E} \times (\bar{Q} - \bar{U}) \}} = \frac{\bar{B} \cdot \{ \bar{S} \times (\bar{R} - \bar{X}) \} + \bar{B} \cdot \bar{S} \frac{d\bar{x}}{d\theta}}{\bar{B} \cdot \{ \bar{E} \times (\bar{R} - \bar{U}) \}}$$

(5.16)

$$\frac{\bar{E} \cdot \{ \bar{S} \times (\bar{R} - \bar{X}) \} + \bar{E} \cdot \bar{S} \frac{d\bar{x}}{d\theta}}{\bar{E} \cdot \{ \bar{B} \times (\bar{R} - \bar{T}) \}} = \frac{\bar{F} \cdot \{ \bar{S} \times (\bar{W} - \bar{X}) \} + \bar{F} \cdot \bar{S} \frac{d\bar{x}}{d\theta}}{\bar{F} \cdot \{ \bar{B} \times (\bar{W} - \bar{T}) \}}$$

(5.17)

Synthesis equations for higher order infinitesimal synthesis may be obtained by differentiating Equations (5.13) to (5.17). Where derivatives  $d\bar{A}^n/d\theta^n = 0$  and  $d\bar{B}^n/d\theta^n = 0$ , since  $\bar{A}$  and  $\bar{B}$  are direction vectors of fixed axes,  $d^n\bar{E}/d\theta^n$ ,  $d^n\bar{F}/d\theta^n$  and other derivatives may be obtained using the method outlined in Chapter IV. This completes the design procedure for the design of a RSSR-RSR Watt's type mechanism for rigid body guidance through finitely or infinitesimally separated positions.

## 5.2. Extension of Screw Triangle Geometry to Synthesis of Spatial, Two-Loop, Six-Link Mechanisms

In this section, the concept of screw triangle is extended to synthesis of spatial, six-link, two-loop mechanisms. In Section 4.3., under the discussion on synthesis of C-C dyads, it was shown that three screws denoted by  $\hat{A}$ ,  $\hat{B}$ , and  $\hat{S}$  form a spatial triangle, where  $\hat{A}$  is the screw displacement at cylinder pair fixed to the ground,  $\hat{B}$  is the screw

displacement at the moving cylinder pair, and  $\hat{S}$  is the screw displacement of the rigid body attached to the C-C dyad. The relations for finitely separated position of the rigid body are given by Equations (4.16) to (4.22). In fact, these relations are applicable to any three screws  $\hat{A}$ ,  $\hat{B}$  and  $\hat{S}$ , since three general screws form a screw triangle in space. Then let this screw triangle be designated by  $\Delta(\hat{A} \hat{B} \hat{S})$ . Let  $\theta$ ,  $t$  and  $\bar{X}$  followed by the subscript of the screw denote the rotation about the screw axis, the translation along the screw axis, and the location vector locating a point on the screw axis. Note that pair axes and screw axes associated with screw displacements at cylindrical, revolute, helical and prismatic joints are coincident. Prismatic, revolute, cylinder and helical pairs require specification of 4 unknowns each (2 for specification of direction of axis, 2 for locating a point on the axis).

The following three steps provide synthesis equations for a mechanism for a particular synthesis problem.

1. The geometry of the mechanism imposes constraints on the screws associated with displacements of coupler links and screws associated with displacements at pairs. These constraints occur because some of the screws are common to more than one screw triangle. These constraint conditions are, therefore, expressed as relations expressing equivalence of rotations and translations of the common screw from two screw geometry relations.

2. Geometry of the pair places constraints on the screws associated with screw displacements at pairs, for example, for a pair A

$$t_A = \rho \theta_A \quad (5.18)$$

where  $\rho$  is finite constant for helical pairs

- $\rho$  is zero for revolute pairs  
 $\rho = \infty, \theta_A = 0, t_A \neq 0$  for prism pairs  
 $\rho$  is variable for cylinder pairs.

The translations and rotations at the pair are expressed in terms of screw triangle relations and then constrained by Equation (5.18).

3. If motion of one or more links, or displacements at pairs, are specified, then such values are known in the screw triangle geometry relations.

In the following, the screw displacements at pairs are denoted by the symbol  $(\wedge)$  on the unit vector parallel to the pair axis.

#### 5.2.1. Stephenson-3 Fixed Pivot Type Mechanism

Figure 32 shows a Stephenson-3 fixed pivot type mechanism.  $\bar{A}, \bar{B}, \bar{C}, \bar{D}, \bar{E}, \bar{F}$  and  $\bar{G}$  are unit vectors parallel to the pair axes A, B, C, D, E, F and G respectively. Let the screw associated with the coupler link BCE be  $\hat{H}_j$  and associated with EF by  $\hat{I}_j$  when the mechanism moves from the first to the  $j^{\text{th}}$  position. Then the following constraint conditions are obtained from the geometry of the mechanism.

$$\hat{A}_j \hat{B}_j = \hat{H}_j \quad (5.19)$$

$$\hat{C}_j \hat{D}_j = \hat{H}_j \quad (5.20)$$

$$\hat{H}_j \hat{E}_j = \hat{I}_j \quad (5.21)$$

$$\hat{G}_j \hat{F}_j = \hat{I}_j \quad (5.22)$$

Conditions in Equations (5.19) - (5.22) are expressed as

$$[\theta_{H_j}] \Delta(\hat{A}_j \hat{B}_j \hat{H}_j) = [\theta_{H_j}] \Delta(\hat{C}_j \hat{D}_j \hat{H}_j) \quad (5.23)$$

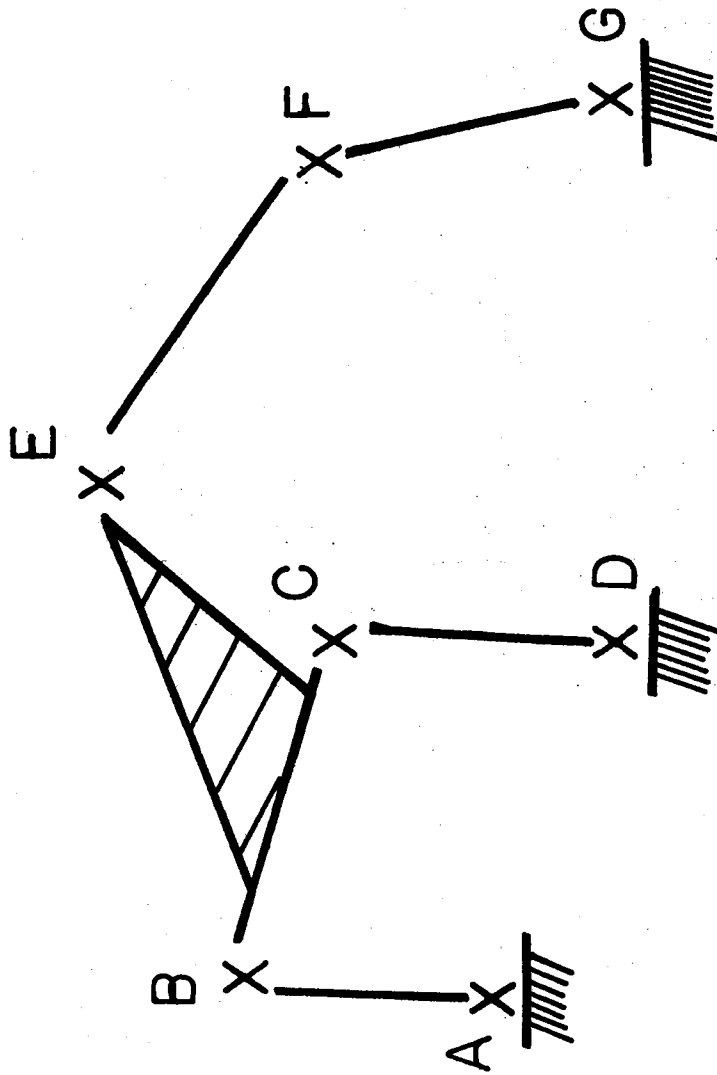


Figure 32. Stephenson-3 Fixed Type Mechanism

$$[\theta_{Hj}] \Delta (\hat{A}_j \hat{B}_j \hat{H}_j) = [\theta_{Hj}] \Delta (\hat{H}_j \hat{E}_j \hat{I}_j) \quad (5.24)$$

$$\checkmark [t_{Hj}] \Delta (\hat{A}_j \hat{B}_j \hat{H}_j) = [t_{Hj}] \Delta (\hat{C}_j \hat{D} \hat{H}_j) \quad (5.25)$$

$$4 \quad [t_{Hj}] \Delta (\hat{A}_j \hat{B}_j \hat{H}_j) = [t_{Hj}] \Delta (\hat{H}_j \hat{E}_j \hat{I}_j) \quad (5.26)$$

$$\checkmark [\theta_{Ij}] \Delta (\hat{H}_j \hat{E}_j \hat{I}_j) = [\theta_{Ij}] \Delta (\hat{G}_j \hat{F}_j \hat{I}_j) \quad (5.27)$$

$$\checkmark [t_{Ij}] \Delta (\hat{H}_j \hat{E}_j \hat{I}_j) = [t_{Ij}] \Delta (\hat{G} \hat{F}_j \hat{I}_j) \quad (5.28)$$

In addition to the conditions expressed by Equations (5.23) - (5.28) due to mechanism geometry, additional constraint due to pair geometry may be placed using Equation (5.18).

If screws  $\hat{I}_j$  are specified, then

$$[\theta_{Ij}]_{\text{specified}} = [\theta_{Ij}] \Delta (\hat{H}_j \hat{E}_j \hat{I}_j) \quad (5.29)$$

$$[t_{Ij}]_{\text{specified}} = [t_{Ij}] \Delta (\hat{H}_j \hat{E}_j \hat{I}_j) \quad (5.30)$$

If the mechanism is to be used for function generation, e.g., coordination of motion of links AB and FG, then screws at joint A and G are specified and constraints due to motion are

$$[\theta_{Aj}] \Delta (\hat{A}_j \hat{B}_j \hat{H}_j) = [\theta_{Aj}]_{\text{specified}} \quad (5.31)$$

$$[t_{Aj}] \Delta (\hat{A}_j \hat{B}_j \hat{H}_j) = [t_{Aj}]_{\text{specified}} \quad (5.32)$$

$$[\theta_{Gj}] \Delta (\hat{G}_j \hat{F}_j \hat{I}_j) = [\theta_{Gj}]_{\text{specified}} \quad (5.33)$$

$$[t_{Gj}] \Delta (\hat{G}_j \hat{F}_j \hat{I}_j) = [t_{Gj}]_{\text{specified}} \quad (5.34)$$

Consider the problem of multiple coordination where motion of links AB, CD and FG is coordinated then in addition to constraints expressed by Equations (5.31) - (5.34), the following constraints are obtained due to specification of motion:

$$[\theta_{Dj}] \Delta (\hat{D}_j \hat{C}_j \hat{H}_j) = [\theta_{Dj}] \text{ specified} \quad (5.35)$$

$$[t_{Dj}] \Delta (\hat{D}_j \hat{C}_j \hat{H}_j) = [t_{Dj}] \text{ specified} \quad (5.36)$$

Table VIII presents the summary of the number of precision positions, unknowns, and equations to be used for RCGC-GCC Stephenson-2 mechanism for various types of synthesis problems. Note that when the rigid body displacements are incompletely specified, corresponding incompletely specified screws must be used. A screw triangle circuit for Stephenson-2 mechanism is shown in Figure 33.

Now consider the case of multiple coordinations of links where motion of links AB, CD and FG are coordinated. Assume that screw displacement at A, D and G are known. Equating  $\hat{H}_j$ , obtained from two sides,

$$\hat{A}_j \hat{B}_j = \hat{H}_j = \hat{D}_j \hat{C}_j \quad (5.37)$$

Manipulation of Equation (5.37) provides

$$\hat{B}_j \hat{C}_j^{-1} = \hat{A}_j^{-1} \hat{D}_j = \hat{K}_j \quad (5.38)$$

Since  $\hat{A}$  and  $\hat{D}$  are known, screw  $\hat{K}_j$  may be computed using  $\hat{K}_j = \hat{A}_j^{-1} \hat{D}_j$ .

The unknown axes at B and C are calculated using the following relations from screw triangle geometry.

$$\tan \frac{\theta_{Kj}}{2} = - \frac{\bar{B} \cdot (\bar{K}_j \times \bar{C})}{(\bar{B} \times \bar{K}_j) \cdot (\bar{K}_j \times \bar{C})} \quad (5.39)$$

TABLE VIII

SYNTHESIS OF RCCG-CCC STEPHENSON MECHANISM FOR VARIETY OF MOTION PROGRAMS

Type of Problem	Specifications	Unknowns	Equations To Be Used	No. of Equations For p, Precision Positions	No. of Unknowns For p, Precision Positions	No. of Precision Positions
1. Rigid Body Guidance Coupler EF	$\bar{I}_j, \bar{X}_{I_j}, \theta_{I_j}, t_{I_j}$	$\bar{A}, \bar{B}, \bar{C}, \bar{D}, \bar{E}, \bar{F}, \bar{G}, \bar{H}, \bar{X}_A, \bar{X}_B, \bar{X}_C, \bar{X}_D, \bar{X}_E, \bar{X}_F, \bar{X}_G, \bar{X}_H$	(3.23) - (3.30) and $(t_{A_j}) \Delta(\hat{A}\hat{B}\hat{H})=0$	$9(p-1)$	$28 + 4(p-1)$	5* 8 free parameters
2. Function Generation AB - GF	$\bar{A}, \bar{G}, \bar{X}_A, \bar{X}_B, \theta_{A_j}, \theta_{G_j}, t_{G_j}$	$\bar{B}, \bar{C}, \bar{D}, \bar{E}, \bar{F}, \bar{H}_j, \bar{I}_j, \bar{X}_B, \bar{X}_C, \bar{X}_D, \bar{X}_E, \bar{X}_F, \bar{X}_{H_j}, \bar{X}_{I_j}$	(3.23) - (3.28) (3.31) - (3.34) $(t_{A_j}) \Delta(\hat{A}\hat{B}\hat{H})=0$	$13(p-1)$	$20 + 8(p-1)$	5
3. Input + Rigid Body [A-EF]	$\bar{A}, \bar{I}_j, \bar{X}_A, \theta_{I_j}, \theta_{A_j}, t_{I_j}$	$\bar{B}, \bar{C}, \bar{D}, \bar{E}, \bar{F}, \bar{G}, \bar{H}, \bar{X}_B, \bar{X}_C, \bar{X}_D, \bar{X}_E, \bar{X}_F, \bar{X}_G$	(3.23) - (3.32) $(t_{A_j}) \Delta(\hat{A}\hat{B}\hat{H})=0$	$11(p-1)$	$24 + 8(p-1)$	9
4. Incompletely Specified Rigid Body Position Coupler EF	n parameters of incompletely specified screw for each precision position	$\bar{A}, \bar{B}, \bar{C}, \bar{D}, \bar{E}, \bar{F}, \bar{G}, \bar{X}_A, \bar{X}_B, \bar{X}_C, \bar{X}_D, \bar{X}_E, \bar{X}_F, \bar{X}_G$	(3.23) - (3.30) $(t_{A_j}) \Delta(\hat{A}\hat{B}\hat{H})=0$	$9(p-1)$	$28 + (4+n)(p-1)$	

\*Note C-C dyad. FG places the constraint on number of precision positions.

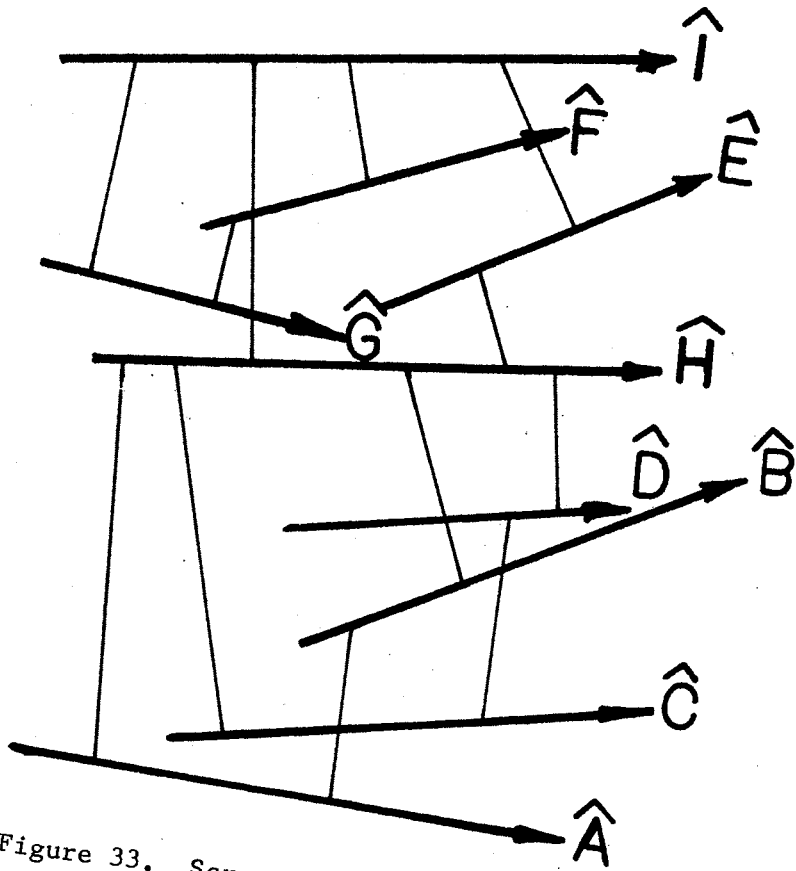


Figure 33. Screw Triangle Circuit Formed by Constraints of the Stephenson-3 Fixed Type Mechanism



$$\begin{aligned} \frac{t_{Kj}}{2} = & - \frac{\bar{K}_j - (\bar{K}_j \cdot \bar{C}) \bar{C}}{1 - (\bar{K}_j \cdot \bar{C})^2} \cdot (\bar{X}_C - \bar{X}_{Kj}) \\ & + \frac{\bar{K}_j - (\bar{K}_j \cdot \bar{B}) \bar{B}}{1 - (\bar{K}_j \cdot \bar{B})^2} \cdot (\bar{X}_B - \bar{X}_{Kj}) \end{aligned} \quad (5.40)$$

Since Equation (5.39) contains four unknowns (2 unknowns contributed by  $\bar{B}$  and  $\bar{C}$  unit vectors), a maximum of 4 values of  $\theta_k$  may be specified which in turn limits the specification of four displacements screws at A and D. From Equation (5.40), the unknowns  $\bar{X}_C$  and  $\bar{X}_B$  are computed. The rotations and translations at pair B are computed using the relations

$$\tan \frac{\theta_{Bj}}{2} = \frac{\bar{B} \cdot (\bar{K}_j \times \bar{C})}{(\bar{C} \times \bar{B}) \cdot (\bar{B} \times \bar{K}_j)} \quad (5.41)$$

$$\begin{aligned} \frac{t_{Bj}}{2} = & \frac{\bar{B} - (\bar{B} \cdot \bar{K}_j) \bar{K}_j}{1 - (\bar{B} \cdot \bar{K}_j)^2} \cdot (\bar{X}_{Kj} - \bar{X}_B) \\ & - \frac{\bar{B} - (\bar{B} \cdot \bar{C}) \bar{C}}{1 - (\bar{B} \cdot \bar{C})^2} \cdot (\bar{X}_C - \bar{X}_B) \end{aligned}$$

(5.42)

Screws associated with coupler links are given by Equation (5.19) and may be computed using the method shown in Chapter IV. Similarly, from Equations (5.21) and (5.22),

$$\hat{G}_j^{-1} \hat{H}_j = \hat{F}_j \hat{E}_j^{-1} = \hat{L}_j \quad (5.43)$$

Since  $\hat{G}_j$  and  $\hat{H}_j$  are known screws,  $\hat{L}_j$  becomes a known screws. Then from

screw triangle relations of  $\hat{F}$ ,  $\hat{E}$  and  $\hat{L}$ ,  $\bar{F}$ ,  $\bar{E}$ ,  $\bar{X}_F$  and  $\bar{X}_E$  are computed as shown above. An example of synthesis of RCCC-CCC mechanism for multiple coordination is shown in Table IX.

### 5.2.2. Synthesis of Watt's Six-Link, Two-Loop, Spatial Mechanisms

Figure 34 shows a Watt's-2 fixed type mechanism. A and D are fixed pivots; B, C, E, F and G are moving pivots of the mechanism. Let the screws associated with coupler links BCE, EF and FG be denoted by  $\hat{H}_j$ ,  $\hat{L}_j$  and  $\hat{I}_j$  when the mechanism moves from the initial to the  $j^{\text{th}}$  position. Following constraints are obtained from the geometry of the mechanism.

$$\hat{A}_j \hat{B}_j = \hat{H}_j \quad (5.44)$$

$$\hat{D}_j \hat{C}_j = \hat{H}_j \quad (5.45)$$

$$\hat{H}_j \hat{E}_j = \hat{L}_j \quad (5.46)$$

$$\hat{D}_j \hat{G}_j = \hat{I}_j \quad (5.47)$$

$$\hat{I}_j \hat{F}_j = \hat{L}_j \quad (5.48)$$

Conditions in Equations (5.44) - (5.48) are expressed as

$$[\theta_{H_j}] \Delta(\hat{A} \hat{B} \hat{H}) = [\theta_{H_j}] \Delta(\hat{D} \hat{C} \hat{H}) \quad (5.49)$$

$$[t_{H_j}] \Delta(\hat{A} \hat{B} \hat{H}) = [t_{H_j}] \Delta(\hat{D} \hat{C} \hat{H}) \quad (5.50)$$

$$[\theta_{H_j}] \Delta(\hat{H} \hat{E} \hat{L}) = [\theta_{H_j}] \Delta(\hat{A} \hat{B} \hat{H}) \quad (5.51)$$

$$[t_{H_j}] \Delta(\hat{H} \hat{E} \hat{L}) = [t_{H_j}] \Delta(\hat{A} \hat{B} \hat{H}) \quad (5.52)$$

$$[\theta_{L_j}] \Delta(\hat{H} \hat{E} \hat{L}) = [\theta_{L_j}] \Delta(\hat{I} \hat{F} \hat{L}) \quad (5.53)$$

TABLE IX  
SYNTHESIS OF STEPHENSON'S SIX-LINK MECHANISMS FOR  
MULTIPLE FUNCTION GENERATION

PP	Rotations At Pair A	Rotations At Paid D	Rotations At Pair G	Translations At Pair D	Translations At Pair G
2	$-20^\circ$	-15.4244	162.623	-0.3816	3.608
3	$-40^\circ$	-33.880	135.527	-2.9096	-9.488
4	$40^\circ$	29.92219	-179.229	6.9520	-2.235
5	$60^\circ$	81.5526	-30.949	-1.2713	-12.004

One of the many solutions is given below.

$$\bar{A}^* = 0.7322i + 0.6112j + 0.3006k$$

$$\bar{E} = -0.5032j - 0.7324j + 0.5889k$$

$$\bar{B} = -0.1965i - 0.2832j + 0.9387k$$

$$\bar{F} = 0.9167i - 0.0010j + 0.3996k$$

$$\bar{C} = -0.3284i - 0.4966j + 0.8034k$$

$$\bar{G}^* = 0.6002i + 0.5001j + 0.6242k$$

$$\bar{D}^* = 0.5442i + 0.1228j + 0.8299k$$

$$\bar{X}_A^* = 1.2876i + 1.1457j$$

$$\bar{X}_E = 1.5492i - 1.9298j$$

$$\bar{X}_B = 3.6428i + 2.6418j$$

$$\bar{X}_F = -4.1121i - 1.2833j$$

$$\bar{X}_C = -1.8276i + 4.2632j$$

$$\bar{X}_G^* = 1.6439i + 1.7451j$$

$$\bar{X}_D^* = 1.7864i + 1.6280j$$

\* are known vectors.

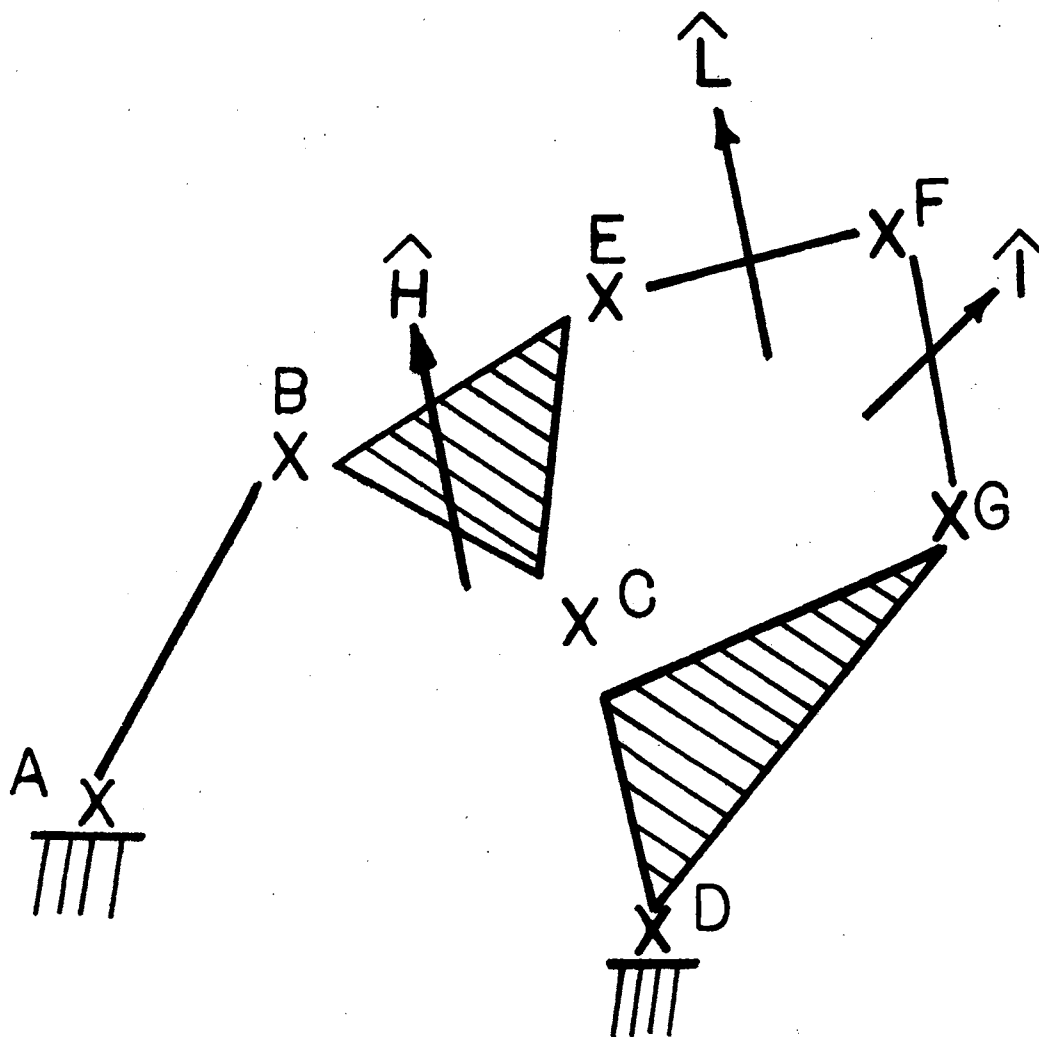


Figure 34. Watt's-2 Fixed Pivot Type Mechanism

$$[t_{L_j}] \Delta(\hat{H} \hat{E} \hat{L}) = [t_{L_j}] \Delta(\hat{I} \hat{F} \hat{L}) \quad (5.54)$$

$$[\theta_{I_j}] \Delta(\hat{L} \hat{F} \hat{I}) = [\theta_{I_j}] \Delta(\hat{D} \hat{G} \hat{I}) \quad (5.55)$$

$$[t_{I_j}] \Delta(\hat{L} \hat{F} \hat{I}) = [t_{I_j}] \Delta(\hat{D} \hat{G} \hat{I}) \quad (5.56)$$

$$[t_{D_j}] \Delta(\hat{D} \hat{C} \hat{H}) = [t_{D_j}] \Delta(\hat{D} \hat{G} \hat{I}) \quad (5.57)$$

$$[\theta_{D_j}] \Delta(\hat{D} \hat{C} \hat{H}) = [\theta_{D_j}] \Delta(\hat{D} \hat{G} \hat{I}) \quad (5.58)$$

If screws  $\hat{L}_j$  are specified screws, then

$$[\theta_{L_j}] \Delta(\hat{I} \hat{F} \hat{L}) = \text{specified value} \quad (5.59)$$

$$[t_{L_j}] \Delta(\hat{I} \hat{F} \hat{L}) = \text{specified value} \quad (5.60)$$

Let A be a revolute pair. Then the pair constraint condition is

$$[t_{A_j}] \Delta(\hat{A} \hat{B} \hat{H}) = 0 \quad (5.61)$$

Table X gives a brief summary of the number of unknowns, the number of equations for each precision position for various types of synthesis problems. Figure 35 shows a screw triangle circuit for this type of Watt's mechanism.

Now consider the synthesis problem where a rigid body to be guided is attached to link EF in Figure 35 and input rotations which are to be coordinated with rigid body motion are provided at the revolute pair at A. (i.e., Screws  $\hat{L}_j$  of coupler link EF and screws  $\hat{A}_j$  of input link AB are known.) Combining Equation (5.44) and Equation (5.46) and eliminating screw  $\hat{H}_j$

$$\hat{B}_j \hat{E}_j = \hat{A}_j^{-1} \hat{L}_j = \hat{N}_j$$

(5.62)

TABLE X

## SYNTHESIS OF WATT'S MECHANISM FOR VARIETY OF MOTION PROGRAMS

Type of Problem	Specifications	Unknowns	Equations To Be Used	No. of Equations For p, Precision Positions	No. of Unknowns For p, Precision Positions	No. of Precision Positions
1. Rigid Body Guidance Coupler EF	$\bar{L}_j, \theta_{L_j}, \bar{X}_{L_j}, t_{L_j}$	$\bar{A}, \bar{B}, \bar{C}, \bar{D}, \bar{E}, \bar{F}, \bar{G}, \bar{X}_A, \bar{X}_B, \bar{X}_C, \bar{X}_D, \bar{X}_E, \bar{X}_F, \bar{X}_G, \bar{I}_j, \bar{H}_j, \bar{X}_{I_j}, \bar{X}_{H_j}$	(5.49) - (5.61)	13(p-1)	28 + 8(p-1)	6 3 free parameters
2. Incompletely Specified Positions of Rigid Body	Incompletely Specified Screws in Terms of n Parameters for Each pp.	In Addition to Above Unknowns, (6-n) Parameters for Each pp.	(5.49) - (5.61)	13(p-1)	28 + (14-n)(p-1)	
3. Input at A and Rigid Body EF	$\bar{A}, \theta_{A_j}, \bar{L}_j, \bar{X}_{L_j}, \theta_{L_j}^-, t_{L_j}$	$\bar{B}, \bar{C}, \bar{D}, \bar{E}, \bar{F}, \bar{G}, \bar{X}_B, \bar{X}_C, \bar{X}_D, \bar{X}_E, \bar{X}_F, \bar{X}_G, \bar{I}_j, \bar{H}_j, \bar{X}_{I_j}, \bar{X}_{H_j}$	(5.49) - (5.61) $(\theta_{A_j})_{\text{specific}} = (\theta_{A_j}) \Delta(\hat{A}\hat{B}\hat{H})$	14(p-1)	24 + 8(p-1)	5
4. Input + Incompletely Specified Positions of Rigid Body	$\bar{A}, \theta_{A_j}$ , and Incompletely Specified Screws in Terms of n Parameters for Each Precision Position	In Addition to Above Unknowns, (6-n) Unknown Parameters of Screws for Each Precision Position	(5.49) - (5.61) $(\theta_{A_j})_{\text{specific}} = (\theta_{A_j}) \Delta(\hat{A}\hat{B}\hat{H})$	14(p-1)	24 + (14-n)(p-1)	

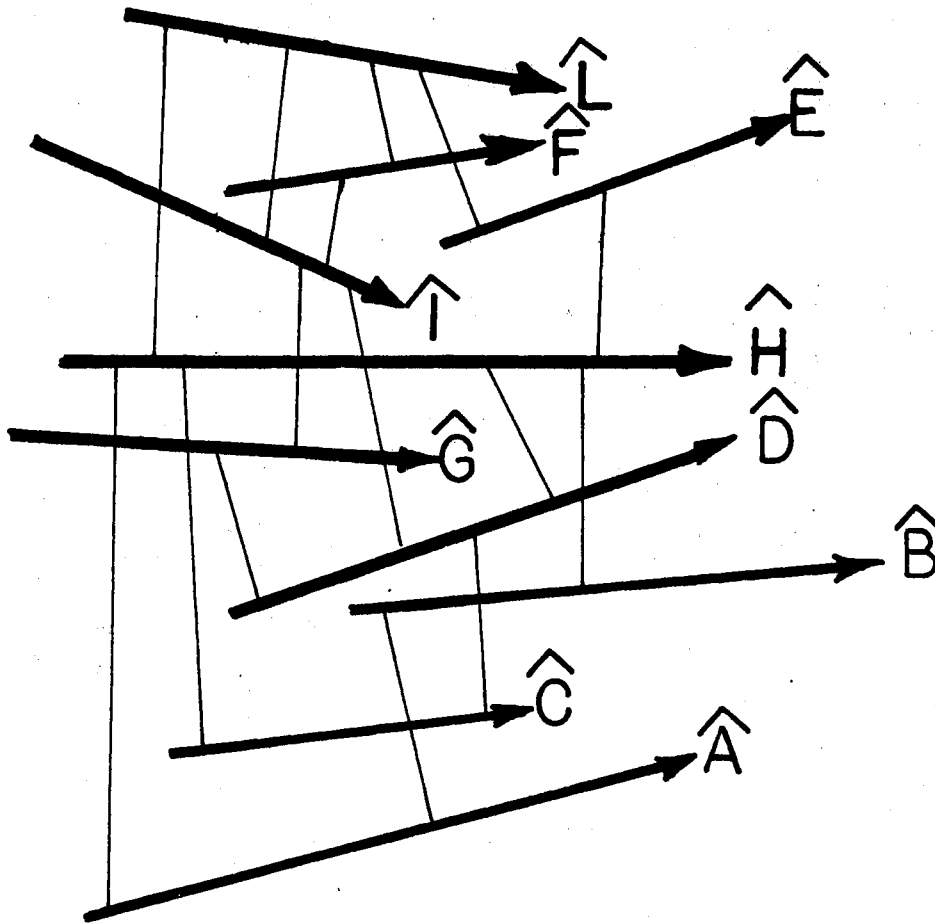


Figure 35. Screw Triangle Circuit Formed by Constraints of the Watt's-2 Fixed Type Mechanism

Since  $\hat{A}^{-1}$  and  $\hat{L}_j$  are known screws, screw  $\hat{N}_j$  may be computed using the method described in Chapter IV. From screw triangle formed by screws  $\hat{B}_j$ ,  $\hat{C}_j$  and  $\hat{N}_j$ , the following relations are obtained.

$$\tan \frac{\theta_{Nj}}{2} = - \frac{\bar{B} \cdot (\bar{N}_j \times \bar{E})}{(\bar{B} \times \bar{N}_j) \cdot (\bar{N}_j \times \bar{E})} \quad j=1 \dots 4 \quad (5.63)$$

$$\begin{aligned} \frac{t_{Nj}}{2} = & \frac{\bar{N}_j - (\bar{N}_j \cdot \bar{E}) \bar{E}}{1 - (\bar{N}_j \cdot \bar{E})^2} \cdot (\bar{X}_E - \bar{X}_{Nj}) \\ & + \frac{\bar{N}_j - (\bar{N}_j \cdot \bar{B}) \bar{B}}{1 - (\bar{N}_j \cdot \bar{B})^2} \cdot (\bar{X}_B - \bar{X}_{Nj}) \end{aligned} \quad j=1 \dots 4 \quad (5.64)$$

The unknowns  $\bar{B}$  and  $\bar{E}$  (4 unknowns) are computed from Equation (5.63) written four times. Once  $\bar{B}$  and  $\bar{E}$  are known,  $\bar{X}_E$  and  $\bar{X}_B$  (4 unknowns) are computed from 4 linear equations obtained by writing Equation (5.64) four times. Rotations and translations at B pair are computed next using relations

$$\tan \frac{\theta_{Bj}}{2} = \frac{\bar{B} \cdot (\bar{N}_j \times \bar{E})}{(\bar{E} \times \bar{B}) \cdot (\bar{B} \times \bar{N}_j)} \quad (5.65)$$

$$\begin{aligned} \frac{t_{Bj}}{2} = & \frac{\bar{B} - (\bar{B} \cdot \bar{N}_j) \bar{N}_j}{1 - (\bar{B} \cdot \bar{N}_j)^2} \cdot (\bar{X}_{Nj} - \bar{X}_{Bj}) \\ & - \frac{\bar{B} - (\bar{B} \cdot \bar{E}) \bar{E}}{1 - (\bar{B} \cdot \bar{E})^2} \cdot (\bar{X}_E - \bar{X}_{Bj}) \end{aligned} \quad (5.66)$$



Thus, screws at B are completely known and screws of coupler link BEC are calculated using

$$\hat{A} \hat{B} = \hat{H} \quad (5.67)$$

From screw triangle formed by screws  $\hat{D}_j$ ,  $\hat{C}_j$  and  $\hat{H}_j$ , the following relations are obtained,

$$\tan \frac{\theta_{Hj}}{2} = - \frac{\bar{D} \cdot (\bar{H}_j \times \bar{C})}{(\bar{D} \times \bar{H}_j) \cdot (\bar{H}_j \times \bar{C})} \quad (5.68)$$

$$\begin{aligned} \frac{t_{Hj}}{2} = & - \frac{\bar{H}_j - (\bar{H}_j \cdot \bar{C}) \bar{C}}{1 - (\bar{H}_j \cdot \bar{C})^2} \cdot (\bar{x}_C - \bar{x}_{Hj}) \\ & + \frac{\bar{H}_j - (\bar{H}_j \cdot \bar{D}) \bar{D}}{1 - (\bar{H}_j \cdot \bar{D})^2} \cdot (\bar{x}_D - \bar{x}_{Hj}) \end{aligned} \quad (5.69)$$

$j = 1, \dots, 4$

$\bar{C}$  and  $\bar{D}$  (4 unknowns) are calculated using four equations obtained from Equation (5.68). Once  $\bar{C}$  and  $\bar{D}$  are unknown,  $\bar{x}_C$  and  $\bar{x}_D$  (4 unknowns) are computed 4 linear equations obtained from Equation (5.69). Rotation and translations are computed using

$$\tan \frac{\theta_{Dj}}{2} = \frac{\bar{D} \cdot (\bar{H}_j \times \bar{C})}{(\bar{C} \times \bar{D}) \cdot (\bar{D} \times \bar{H}_j)} \quad (5.70)$$

$$\begin{aligned} \frac{t_{Dj}}{2} = & \frac{\bar{D} - (\bar{D} \cdot \bar{H}_j) \bar{H}_j}{1 - (\bar{D} \cdot \bar{H}_j)^2} \cdot (\bar{x}_{Hj} - \bar{x}_D) \\ & - \frac{\bar{D} - (\bar{D} \cdot \bar{C}) \bar{C}}{1 - (\bar{D} \cdot \bar{C})^2} \cdot (\bar{x}_C - \bar{x}_D) \end{aligned} \quad (5.71)$$

Thus, screws at pair D are completely known. From Equations (5.47) and (5.48) eliminating screws  $\hat{I}_j$ , we find

$$\hat{G}_j \hat{F}_j = \hat{D}_j^{-1} \hat{L}_j = \hat{P}_j \quad (5.72)$$

Since screws  $\hat{D}_j$  and  $\hat{L}_j$  are known, screws  $\hat{P}_j$  are computed using product rule. From screw triangle formed by screws  $\hat{G}_j$ ,  $\hat{F}_j$  and  $\hat{P}_j$ , we have

$$\tan \frac{\theta_{pj}}{2} = - \frac{\bar{G} \cdot (\bar{P}_j \times \bar{F})}{(\bar{G} \times \bar{P}_j) \cdot (\bar{P}_j \times \bar{F})} \quad (5.73)$$

$j=1 \dots 4$

$$\frac{t_{pj}}{2} = - \frac{\bar{P}_j - (\bar{P}_j \cdot \bar{F}) \bar{F}}{1 - (\bar{P}_j \cdot \bar{F})^2} \cdot (\bar{X}_F - \bar{X}_{Pj})$$

$$+ \frac{\bar{P}_j - (\bar{P}_j \cdot \bar{G}) \bar{G}}{1 - (\bar{P}_j \cdot \bar{G})^2} \cdot (\bar{X}_G - \bar{X}_{Pj})$$

$j=1 \dots 4$

(5.74)

$\bar{G}$  and  $\bar{F}$  (4 unknowns) are computed using Equation (5.73). Once  $\bar{G}$  and  $\bar{F}$  are known,  $\bar{X}_F$  and  $\bar{X}_G$  are computed from linear Equation (5.74). This completes the synthesis of RCCC-CCC Watt's-2 fixed type mechanism for input and rigid motion coordination for five precision positions.

An example of such a synthesis problem is presented in Table XI and Figure 35 shows a screw triangle circuit of the mechanism. Tables XII, XIII, and XIV present constraints of other six-link mechanisms shown in Figures 36, 38, and 40 due to its geometry and corresponding screw triangle circuits are shown in Figures 37, 39, and 41.

TABLE XI

EXAMPLE SYNTHESIS OF WATT'S RCCC-CCC MECHANISM FOR  
COORDINATED MOTIONS OF INPUT-LINK  
AND RIGID BODY

---

Prescribed Input Link and Rigid Body Precision Positions:

$$A = 0.5i - 0.5j + 0.7071k$$

Precision Position 2

$$\bar{L} = 0.7714i - 0.4948j + 0.4002k$$

$$\bar{X}_L = -0.9420j + 2.6504k$$

$$\theta_A = 20.0 \qquad \theta_L = 107.3792 \qquad t_L = 8.2293$$

Precision Position 3

$$\bar{L} = 0.8651i - 0.3565j + 0.3528k$$

$$\bar{X}_L = -.4147j + 1.9545k$$

$$\theta_A = 40^\circ \qquad \theta_L = 122.3592 \qquad t_L = 9.0261$$

Precision Position 4

$$\bar{L} = 0.9248i - 0.2271j + 0.3052k$$

$$\bar{X}_L = 0.0712j + 1.6860k$$

$$\theta_A = 60^\circ \qquad \theta_L = 139.0513 \qquad t_L = 9.4950$$

Precision Position 5

$$\bar{L} = 0.9605i - 0.1059j + 0.2575k$$

$$\bar{X}_L = 0.4639j + 1.7449k$$

$$\theta_A = 80^\circ \qquad \theta_L = 156.7363 \qquad t_L = 9.6834$$

One of the solutions is presented below.

TABLE XI (Continued)

$$\hat{A}^{-1} \hat{L} = \hat{K}_j$$

PP	$K_x$	$K_y$	$X_{K_y}$	$X_{K_z}$	$\theta_k$	$t_k$
2	0.63106	-0.64226	-2.57312	4.23306	100.0990	7.83855
3	0.62906	-0.63539	-3.19300	4.83986	105.69330	8.26299
4	0.62687	-0.61513	-3.43288	5.65049	110.85740	8.30442

$$\bar{B} = -0.8621i + 0.1128j + 1.4940k$$

$$\bar{E} = 0.6287i - 0.6333j + 0.4513k$$

$$\bar{X}_B = -4.2853i + 1.2863j$$

$$\bar{X}_E = -2.8618i + 1.2872j + 1.8756k$$

PP	$\theta_B$	$t_B$
2	-1.7905	0.9707
3	-0.4074	1.9882
4	3.3247	2.9689
5	8.8783	3.9543

$$\hat{H} = \hat{A} \hat{B}$$

PP	$H_x$	$H_y$	$X_{H_y}$	$X_{H_z}$	$\theta_k$	$t_H$
2	0.57021	0.50025	-1.9256	2.5380	20.12442	-0.1734
3	0.50767	0.50179	-2.3110	1.9834	40.01239	-0.0843
4	0.46133	0.48061	-2.5947	1.2293	60.00	0.1926
5	0.43109	0.44176	-2.8363	0.3032	80.18425	0.5801

$$\bar{C} = -0.2861i + 0.8210j + 0.4941k$$

$$\bar{D} = 0.7682i + 0.3296j + 0.5488k$$

$$\bar{X}_C = 0.6212i + 0.5421j$$

$$\bar{X}_D = 1.4569i + 0.8365j$$

PP	$\theta_D$	$t_D$
2	17.4500	-0.9404
3	33.1872	-1.6757
4	48.3693	-2.0997
5	63.9220	-2.1965

$$\hat{D}_j^{-1} \hat{L}_j = \hat{N}_j$$

PP	$N_x$	$N_y$	$X_{N_y}$	$X_{N_z}$	$\theta_N$	$t_N$
2	0.66396	-0.58602	-1.77878	3.81051	96.68796	6.78250
3	0.71181	-0.51917	-1.34189	3.67684	99.31876	6.48781
4	0.76252	-0.44444	-0.51892	3.58475	102.29490	6.22593
5	0.80925	-0.37042	0.42377	3.49244	104.99460	6.05623

$$\bar{F} = 0.5618i + 0.7371j + 0.3756k$$

$$\bar{G} = 0.1163i + 0.3341j + -.9353k$$

$$\bar{X}_F = -3.2568i + 1.9564j$$

$$\bar{X}_G = 0.2811i + 0.7684j$$


---

TABLE XII

## CONSTRAINTS ON THE SCREWS OF WATT'S-3 FIXED PIVOT TYPE MECHANISM

---

 Mechanism Constraints on Screws

$$\begin{aligned}\hat{A}_j \hat{B}_j &= \hat{H}_j \\ \hat{D}_j \hat{C}_j &= \hat{H}_j \\ \hat{D}_j \hat{E}_j &= \hat{I}_j \\ \hat{G}_j \hat{F}_j &= \hat{I}_j\end{aligned}$$

Equations Obtained From Constraint Conditions

$$\begin{aligned}[\theta_{H_j}] \Delta(\hat{A} \hat{B} \hat{H}) &= [\theta_{H_j}] \Delta(\hat{D} \hat{C} \hat{H}) \\ [t_{H_j}] \Delta(\hat{A} \hat{B} \hat{H}) &= [t_{H_j}] \Delta(\hat{D} \hat{C} \hat{H}) \\ [\theta_{D_j}] \Delta(\hat{D} \hat{C} \hat{H}) &= [\theta_{D_j}] \Delta(\hat{D} \hat{E} \hat{I}) \\ [t_{D_j}] \Delta(\hat{D} \hat{C} \hat{H}) &= [t_{D_j}] \Delta(\hat{D} \hat{E} \hat{I}) \\ [\theta_{I_j}] \Delta(\hat{D} \hat{E} \hat{I}) &= [\theta_{I_j}] \Delta(\hat{G} \hat{F} \hat{I}) \\ [t_{I_j}] \Delta(\hat{D} \hat{E} \hat{I}) &= [t_{I_j}] \Delta(\hat{G} \hat{F} \hat{I}) \\ [\theta_{E_j}] \Delta(\hat{E} \hat{D} \hat{H}) &= [\theta_{E_j}] \Delta(\hat{E} \hat{F} \hat{I}) \\ [t_{E_j}] \Delta(\hat{E} \hat{D} \hat{H}) &= [t_{E_j}] \Delta(\hat{E} \hat{F} \hat{I})\end{aligned}$$


---

TABLE XIII

## CONSTRAINTS ON THE SCREWS OF STEPHENSON-2 FIXED PIVOT TYPE-1 MECHANISM

---

 Constraint Condition From the Geometry of the Mechanism

$$\begin{aligned}\hat{A}_j \hat{B}_j &= \hat{L}_j \\ \hat{L}_j \hat{C}_j &= \hat{H}_j \\ \hat{E}_j \hat{D}_j &= \hat{H}_j \\ \hat{E}_j \hat{F}_j &= \hat{I}_j \\ \hat{L}_j \hat{G}_j &= \hat{I}_j\end{aligned}$$

Equations Obtained From Constraint Conditions

$$\begin{aligned}[\theta_{L_j}] \Delta(\hat{A} \hat{B} \hat{L}) &= [\theta_{L_j}] \Delta(\hat{L} \hat{C} \hat{H}) \\ [\theta_{L_j}] \Delta(\hat{A} \hat{B} \hat{L}) &= [\theta_{L_j}] \Delta(\hat{L} \hat{G} \hat{I}) \\ [t_{L_j}] \Delta(\hat{A} \hat{B} \hat{L}) &= [t_{L_j}] \Delta(\hat{L} \hat{G} \hat{I}) \\ [t_{L_j}] \Delta(\hat{A} \hat{B} \hat{L}) &= [t_{L_j}] \Delta(\hat{L} \hat{C} \hat{H}) \\ [\theta_{H_j}] \Delta(\hat{L} \hat{C} \hat{H}) &= [\theta_{H_j}] \Delta(\hat{E} \hat{D} \hat{H}) \\ [t_{H_j}] \Delta(\hat{L} \hat{C} \hat{H}) &= [t_{H_j}] \Delta(\hat{E} \hat{D} \hat{H}) \\ [\theta_{I_j}] \Delta(\hat{E} \hat{F} \hat{I}) &= [\theta_{I_j}] \Delta(\hat{L} \hat{G} \hat{I}) \\ [t_{I_j}] \Delta(\hat{E} \hat{F} \hat{I}) &= [t_{I_j}] \Delta(\hat{L} \hat{G} \hat{I})\end{aligned}$$


---

TABLE XIV

## CONSTRAINTS ON THE SCREWS OF STEPHENSON-2 FIXED PIVOT TYPE-2 MECHANISM

---

 Constraints Due to Mechanism Geometry

$$\begin{aligned}\hat{A}_j \hat{B}_j &= \hat{H}_j \\ \hat{D}_j \hat{C}_j &= \hat{H}_j \\ \hat{D}_j \hat{G}_j &= \hat{I}_j \\ \hat{A}_j \hat{E}_j &= \hat{L}_j \\ \hat{L}_j \hat{F}_j &= \hat{I}_j\end{aligned}$$

Equations Obtained From the Constraint Conditions

$$\begin{aligned}[\theta_{H_j}] \Delta(\hat{A} \hat{B} \hat{H}) &= [\theta_{H_j}] \Delta(\hat{D} \hat{C} \hat{H}) \\ [t_{H_j}] \Delta(\hat{A} \hat{B} \hat{H}) &= [t_{H_j}] \Delta(\hat{D} \hat{C} \hat{H}) \\ [\theta_{I_j}] \Delta(\hat{D} \hat{G} \hat{I}) &= [\theta_{I_j}] \Delta(\hat{L} \hat{F} \hat{I}) \\ [t_{I_j}] \Delta(\hat{D} \hat{G} \hat{I}) &= [t_{I_j}] \Delta(\hat{L} \hat{F} \hat{I}) \\ [\theta_{L_j}] \Delta(\hat{A} \hat{E} \hat{L}) &= [\theta_{L_j}] \Delta(\hat{L} \hat{F} \hat{I}) \\ [t_{L_j}] \Delta(\hat{A} \hat{E} \hat{L}) &= [t_{L_j}] \Delta(\hat{L} \hat{F} \hat{I}) \\ [\theta_{A_j}] \Delta(\hat{A} \hat{B} \hat{H}) &= [\theta_{A_j}] \Delta(\hat{A} \hat{E} \hat{L}) \\ [t_{A_j}] \Delta(\hat{A} \hat{B} \hat{H}) &= [t_{A_j}] \Delta(\hat{A} \hat{E} \hat{L}) \\ [\theta_{D_j}] \Delta(\hat{D} \hat{C} \hat{H}) &= [\theta_{D_j}] \Delta(\hat{D} \hat{G} \hat{I}) \\ [t_{D_j}] \Delta(\hat{D} \hat{C} \hat{H}) &= [t_{D_j}] \Delta(\hat{D} \hat{G} \hat{I})\end{aligned}$$


---



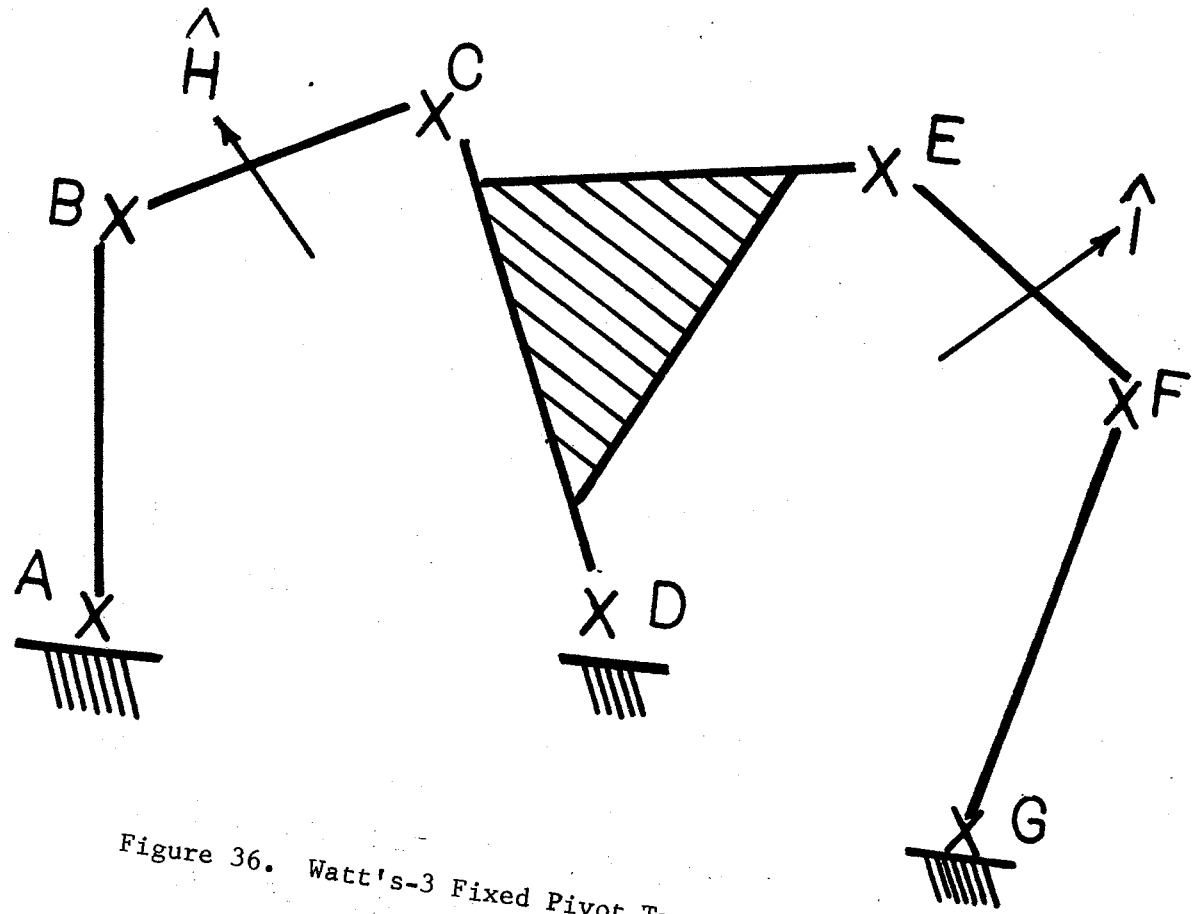


Figure 36. Watt's-3 Fixed Pivot Type Mechanism

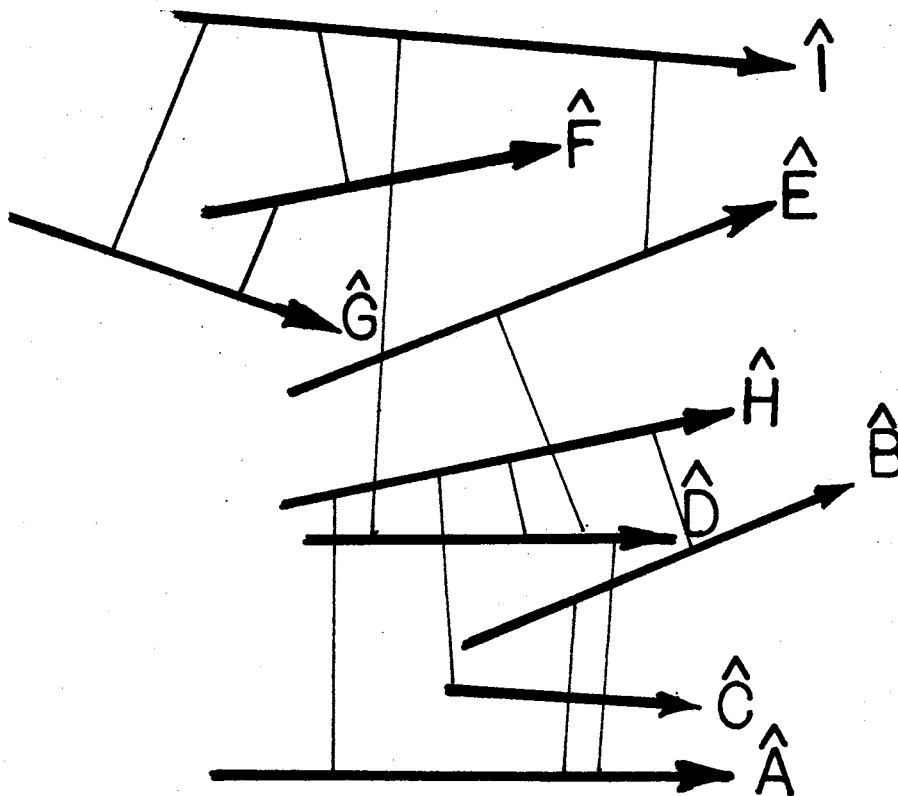


Figure 37. Screw Triangle Circuit for Watt's-3 Fixed Pivot Mechanism

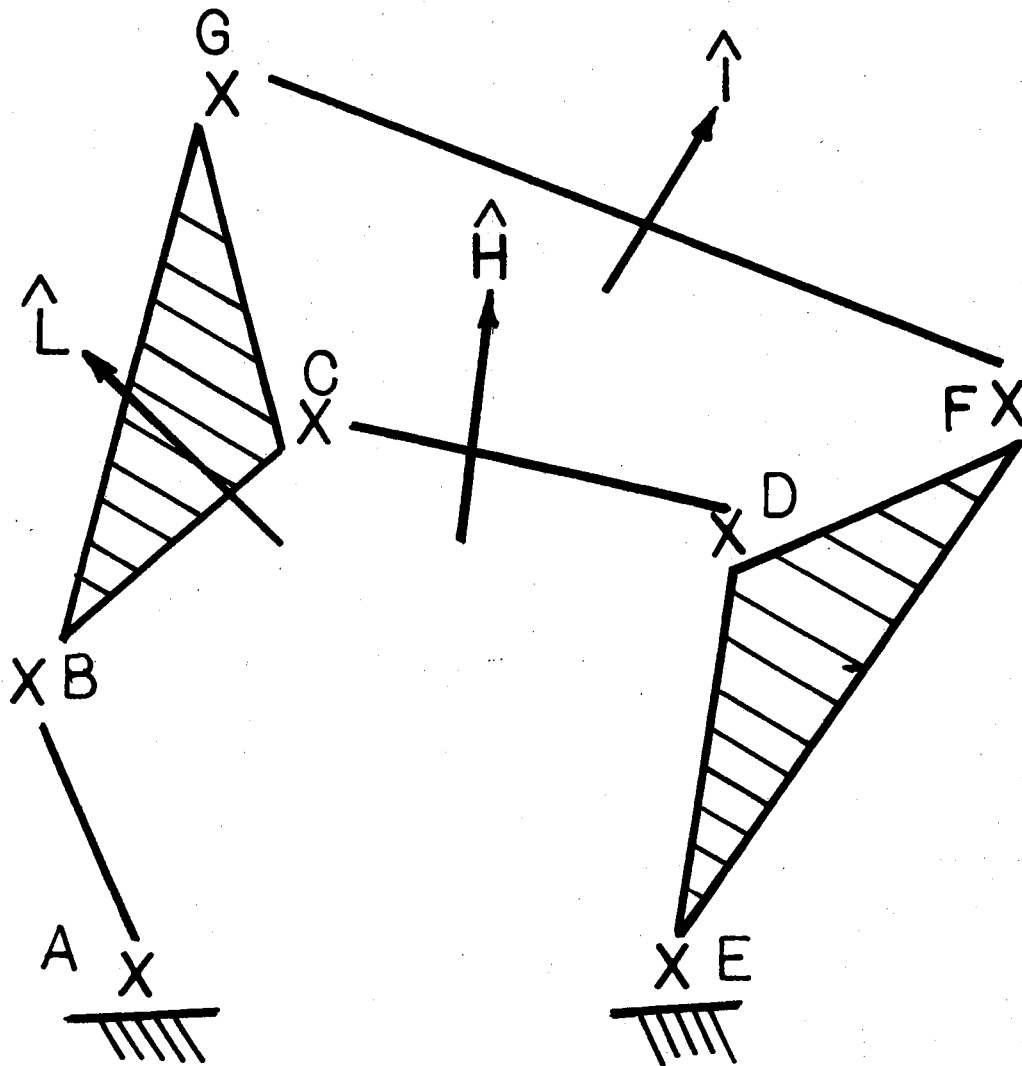


Figure 38. Stephenson-2 Fixed Pivot Type-1 Mechanism

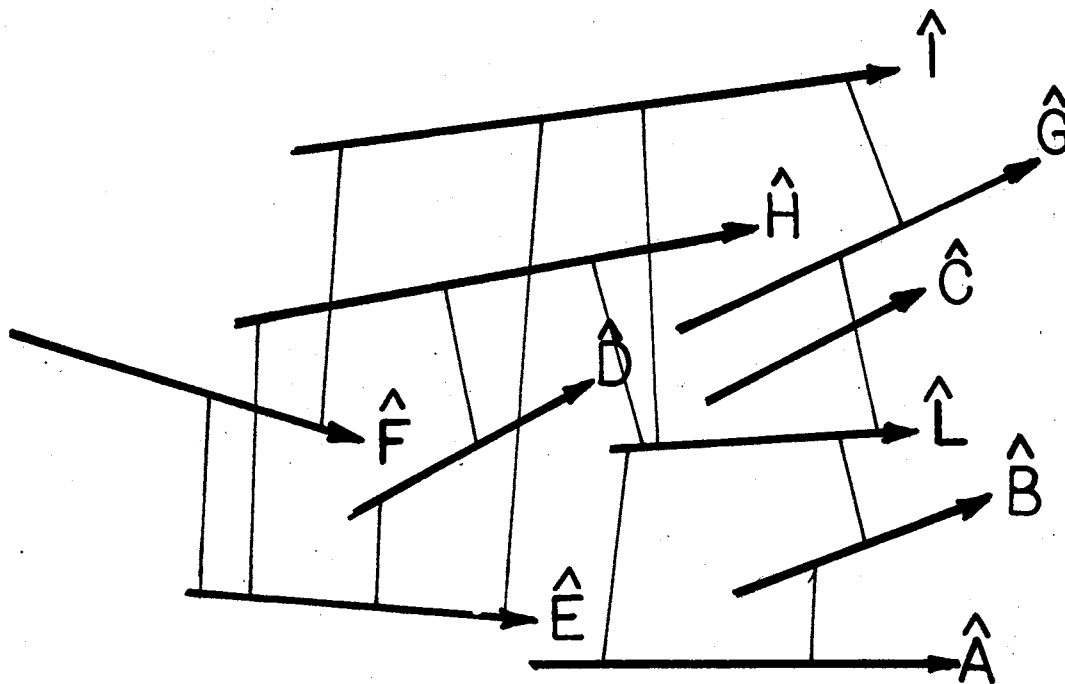


Figure 39. Screw Triangle Circuit for Stephenson-2 Fixed Pivot Type-1 Mechanism

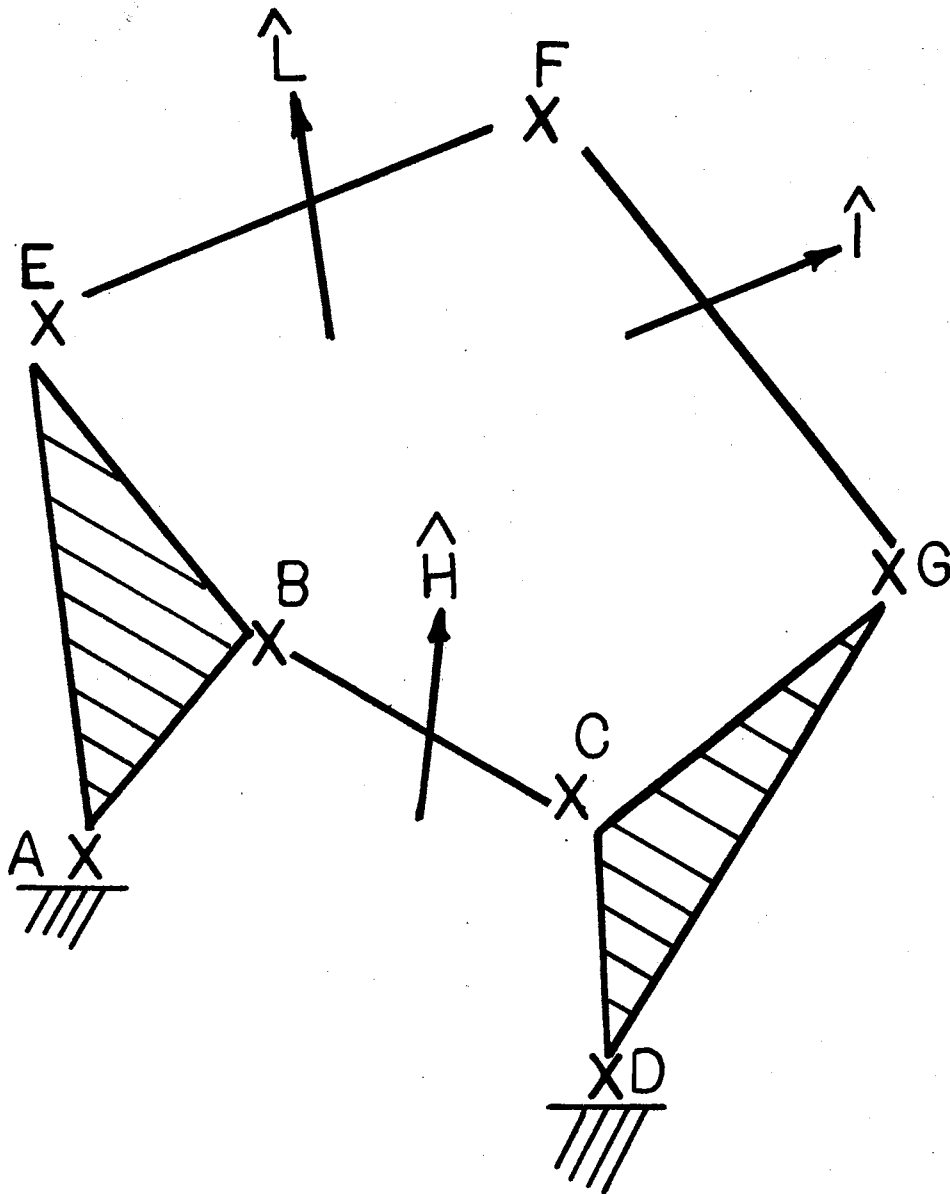


Figure 40. Stephenson-2 Fixed Pivot Type-2 Mechanism

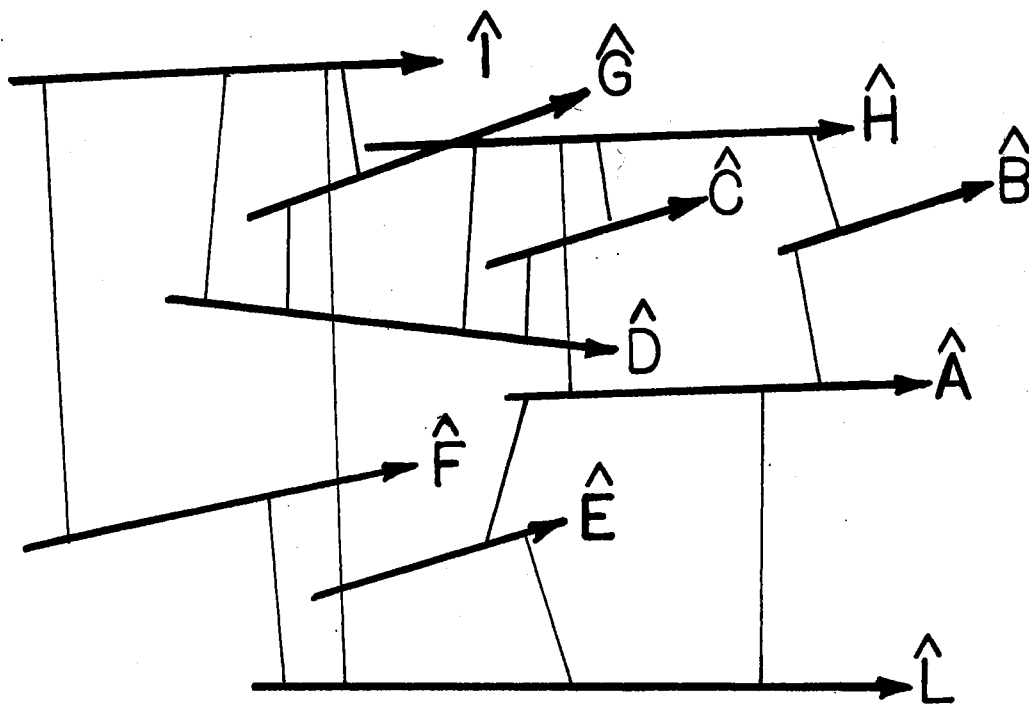


Figure 41. Screw Triangle Circuit for Stephenson-2 Fixed Type-2 Mechanism

## CHAPTER VI

### CONCLUSIONS

In this dissertation, a unified approach is developed for analysis and synthesis of spatial mechanisms and its use is demonstrated in analysis and synthesis of spatial, two-loop, six-link mechanisms. Throughout this work, rigid body spatial motion is expressed in terms of screws. This brings a uniformity and provides a visual insight into the mechanism motion.

The successive screw displacement method for analysis, developed here is believed to be more general, simple and useful than other methods of analysis. It seems it is directly extendable to mechanisms which contain slotted sphere, planar pairs in addition to revolute, cylinder, helical, spherical and prismatic pairs. The expressions obtained for velocity and acceleration analysis are, in general, linear and compact.

An attempt has been made to demonstrate the relationship between screw triangle geometry method of synthesis [26] and pair constraint method developed in the present study. The pair constraint method is much more general and reduces to screw triangle geometry in special cases.

It is, thus, possible now using the methods developed here to analyze single and multi-loop mechanisms which contain prismatic, revolute, helical, cylinder and spheric pairs. Since planar and spherical mechanisms are but special cases of space mechanisms, the method is equally applicable to synthesis of these mechanisms. In planar motion,

a screw reduces to a pole while, in spherical motion, to a pole axis.

Apart from development of general procedures for analysis and synthesis of spatial mechanisms, the present study contributes immensely to the state-of-the-art of kinematic synthesis and analysis of spatial six-link mechanisms. The following are the main contributions.

1. For the first time, procedures are available for synthesis of spatial, two-loop, six-link mechanisms involving revolute, cylinder, helical, prismatic, and spheric pairs. The design equations are obtained in simple vector form and are solved for two types of problems. The design equations for synthesis of spherical mechanisms may be selected from this larger set of equations. We have also provided the screw triangle geometry constraints of five types of six-link mechanisms. These are constraints placed by the mechanism on the screws at joints and screws of the coupler links. Note that these constraints do not depend upon pair combinations but only on mechanism configuration. Additional constraints due to pair geometry and job specifications are also described. Thus, a designer must be able to select synthesis equations for his combination of pairs and job specification, without in depth knowledge of theory of screws.

2. A unified treatment of analysis is presented for the mechanisms involving spherical pairs, in addition to prismatic, cylinder, revolute and helical pairs. The method is used to conduct displacement, velocity and acceleration analysis of five types of six-link mechanisms. A designer may obtain closed form displacement, velocity and accelerations relationships using the method described in this work. It is seen that the whole procedure is well suited for computer programming. The expressions for velocity and accelerations are in general linear and



compact and thus, displacement analysis of more complicated mechanisms may be conducted by integrating these velocity equations.

3. The existence criteria of overconstrained, spatial, six-link mechanisms may be obtained by inducing passive couplings at joints, using the displacement relations described in this work. The synthesis and analysis of such overconstrained mechanisms is performed in the same way as the parent mechanism and is expected to present no further difficulty.

The present work is a basic study of motion of open-loop kinematic chains, constraints on motion of kinematic chains due to pair geometry, and constraints on motion of various links due to mechanism geometry. The pair combinations considered are revolute, prismatic, helical, spherical and cylinder. The method is directly extendable to other pairs such as slotted sphere, planar, etc. Since a wrench is resultant loading of a rigid body and is similar in expression to screw for rigid body displacement, it seems logical to conclude that a similar method could be developed for dynamic analysis and synthesis of spatial mechanisms. The procedures for analysis and synthesis of open-loop chains are described in this work and may be used for design and analysis of manipulators. Further work on manipulators requires procedures for computing influences of obstacles on the terminal body of the open-loop screw chain. This is expected to be rewarding future study.

## BIBLIOGRAPHY

1. Soni, A. H., and Lee Harrisberger. "Wanted: A Mechanism Information Research Center." Mechanical Engineering, Vol. 91, No. 7 (July, 1969), 30-34.
2. de Groot, J. Bibliography in Kinematics. Vol. I, II. Delft, Netherlands: Eindhoven University of Technology, 1970.
3. Soni, A. H., J. Church, et.al. Bibliography on Kinematics. Stillwater: Oklahoma State University, 1968.
4. Novodvorskii, E. P. "A Method of Synthesis of Mechanisms." Transactions of the Seminar on the Theory of Machines and Mechanisms, Akad. Nauk SSSR 42 (1951).
5. Stepanoff, B. I. "Design of Spatial Transmission Mechanisms With Lower Pairs." Transaction of the Seminar on the Theory of Machines and Mechanisms, Akad. Nauk. SSSR 45 (1951).
6. Levitskii, N. I., and Sh. Shakvasian. "Synthesis of Spatial Four-Link Mechanisms With Lower Pairs." Akademiya Nauk. SSSR, Trudyi Seminara Teor. Mash. Mekh., Vol. 14, No. 54 (1954), 5-24. Translated into English by F. Freudenstein, International Journal of Mechanical Science, Pergamon Press, 1960, Vol. 2, 76-92.
7. Denavit, J., and R. S. Hartenberg. "Approximate Synthesis of Spatial Linkages." Journal of Applied Mechanics, Vol. 27, No. 1, Trans. of ASME, Series E, Vol. 82 (1960), 201-206.
8. Wilson, J. T., III. "Analytical Kinematic Synthesis by Finite Displacements." Journal of Engineering for Industry, Trans. ASME, Series B, Vol. 87, No. 2 (May, 1965), 161-169.
9. Harrisberger, L. "A Number Synthesis Survey of Three-Dimensional Mechanisms." Journal of Engineering for Industry, Trans. ASME, Series B, Vol. 87, No. 2 (May, 1965), 213-220.
10. Roth, B. "Finite Position Theory Applied to Mechanisms Synthesis." Journal of Applied Mechanics, Vol. 34, Trans. ASME, Series E, Vol. 89, No. 3 (September, 1967), 591-598.
11. Roth, B. "The Kinematics of Motion Through Finitely Separated Positions." Journal of Applied Mechanics, Vol. 34, No. 3, Trans. ASME, Series E, Vol. 89 (September, 1967), 591-598.

12. Roth, B. "On the Screw Axis and Other Special Lines Associated With Spatial Displacements of a Rigid Body." Journal of Engineering for Industry, Trans. ASME, Series B, Vol. 89, No. 1 (1967), 102-110.
13. Chen, P., and B. Roth. "Design Equations for the Finitely and Infinitesimally Separated Position Synthesis of Binary Links and Combined Link Chains." Journal of Engineering for Industry, Trans. ASME, Series B, Vol. 91 (1969), 209-219.
14. Chen, P. and B. Roth. "A Unified Theory for the Finitely and Infinitesimally Separated Position Problems of Kinematic Synthesis." Journal of Engineering for Industry, Trans. ASME, Vol. 91, Series B (1969), 209-219.
15. Soni, A. H., and Lee Harrisberger. "The Design of Spherical Drag-Link Mechanisms." Journal of Engineering for Industry, Trans. ASME, Series B, Vol. 89, No. 1 (February, 1967), 177-181.
16. Huang, M., P. R. Pamidi, and A. H. Soni. "Design of Spherical Crank-Rocker Mechanism." Journal of Mechanisms, Vol. 9, No. 1 (1970).
17. Soni, A. H., and M. Huang. "Synthesis of Four-Link Space Mechanisms via Extension of Point-Position-Reduction Technique." Journal of Engineering for Industry, Trans. ASME, Vol. 93, No. 1 (1971), 85-89.
18. Rao, A. V. M., G. N. Sandor, D. Kohli, and A. H. Soni. "Closed Form Synthesis of Spatial Function Generating Mechanisms for Maximum Number of Precision Points." Journal of Engineering for Industry, Trans. ASME, Series B, Vol. 95, No. 3 (August, 1973), 725-736.
19. Sandor, G. N. "Principles of a General Quaternion-Operation Method of Spatial Kinematic Synthesis." Journal of Applied Mechanics, Vol. 35, No. 1, Trans. ASME, Series E, Vol. 90 (March, 1968), 40-46.
20. Sandor, G. N., and K. E. Bisshop. "On a General Method of Spatial Kinematic Synthesis of Means of a Stretch-Rotation Tensor." Journal of Engineering for Industry, Trans. ASME, Series B, Vol. 91, No. 1 (1969), 115-121.
21. Suh, G. H. "Design of Space Mechanisms for Rigid Body Guidance." Journal of Engineering for Industry, Trans. ASME, Series B, Vol. 90, No. 3 (1968), 499-506.
22. Suh, G. H. "Design of Space Mechanisms for Function Generation." Journal of Engineering for Industry, Trans. ASME, Series B, Vol. 90, No. 3 (1968), 507-513.

23. Suh, C. H. "Synthesis and Analysis of Space Mechanisms With Use of the Displacement Matrix." (Ph.D. Dissertation, University of California, Berkeley, 1966.)
- \*24. Kohli, D., and A. H. Soni. "Synthesis of Spherical Mechanisms for Multiply-Separated Positions of a Rigid Body." Proceedings of IFToMM International Symposium on Linkages, Bucharest, Romania, June 6-13, 1973.
25. Tsai, L. W., and B. Roth. "Design of Dyads With Helical, Cylindrical, Spherical, Revolute, and Prismatic Joints." Mechanisms and Machine Theory, Vol. 7 (1972), 85-102.
- △ 26. Tsai, L. W., and B. Roth. "Design of Triads Using the Screw-Triangle Chain." Proceedings of the Third World Congress for the Theory of Machines and Mechanisms, Kupari, Yugoslavia, Vol. D, Paper D-19, September 13-20, 1971, 273-286.
- △ 27. Tsai, L. W. and B. Roth. "Incompletely Specified Displacements: Geometry and Spatial Linkage Synthesis." Presented at 12th ASME Mechanisms Conference, ASME Paper No. 72-MECH-13. Journal of Engineering for Industry, Trans. ASME, Series B, Vol. 95, No. 3 (August, 1973), 725-736.
28. Kohli, D., and A. H. Soni. "Synthesis of Spatial Two-Loop Mechanisms Involving R, C, and H Pairs." Proceedings of IFToMM International Symposium on Linkages, Bucharest, Romania, June 6-13, 1973.
29. Gupta, V. K. "Optimum Finite Displacement Synthesis of Spatial Linkages." (Ph.D. Dissertation, U. C. Berkeley, June 1970, 100 pg.)
30. Dimentberg, F. M. "A General Method for the Investigation of Finite Displacements of Spatial Mechanisms and Certain Cases of Passive Joints." Akad. Nauk. SSSR. Trudii Sem. Teorri Mash. Mekh. 5, No. 17, 1948, 5-39.
31. Dimentberg, F. M. "The Determination of the Positions of Spatial Mechanisms." (Russian) Akad. Nauk., Moscow, 1950.
32. Dimentberg, F. M. The Screw Calculus and Its Applications in Mechanics, Izdatel'stvo "Nauka," Glavnaya Redaktsiya, Fiziko, Matematicheskoy Literatury, Moscow, 1965.
33. Denavit, J. "Description and Displacement Analysis of Mechanisms Based on (2 x 2) Dual Matrices." (Ph.D. Dissertation, Northwestern University, 1956.)
34. Yang, A. T. "Application of Quaternion Algebra and Dual Numbers to the Analysis of Spatial Mechanisms." (Ph.D. Dissertation, Columbia University, New York, N.Y., 1963, University Microfilms, Library of Congress Card No. Mic. 64-2803, Ann Arbor, Michigan.)

35. Chace, M. A. "Vector Analysis of Linkages." Journal of Engineering for Industry, Trans. ASME, Series B, Vol. 84, No. 2 (May, 1963), 289-296.
36. Wallace, D. M., and F. Freudenstein. "The Displacement Analysis of the Generalized Tract Coupling." Journal of Applied Mechanics, Trans. ASME, Series E, Vol. 37, No. 3 (September, 1970), 713-719.
37. Yang, A. T. "Displacement Analysis of Spatial Five-Link Mechanisms Using (3 x 3) Matrices With Dual-Number Elements." Journal of Engineering for Industry, Trans. ASME, Series B, Vol. 91, No. 1 (February, 1969), 152-157.
38. Soni, A. H., and P. R. Pamidi. "Closed Form Displacement Relationships of a Five-Link R-R-G-C-R Spatial Mechanism." Journal of Engineering for Industry, Trans. ASME, Series B, Vol. 93, No. 1 (February, 1971), 221-226.
39. Yuan, M. S. C. "Displacement Analysis of the RRCCR Five-Link Spatial Mechanism." Journal of Applied Mechanics, Trans. ASME, Series E, Vol. 37 (September, 1970), 689-696.
40. Jenkins, E. M., F. R. E. Crossley, and K. H. Hunt. "Gross Motion Attributes of Certain Spatial Mechanisms." Journal of Engineering for Industry, Trans. ASME, Series B, Vol. 90, No. 1 (February, 1969), 83-90.
41. Torfason, L. E. , and A. K. Sharma. "Analysis of Spatial RRGR Mechanisms by the Method of Generated Surface." Journal of Engineering for Industry, Trans. ASME, Series B, Vol. 95, No. 3 (August, 1973), 704-708.
42. Dukkipati, R. V., and A. H. Soni. "Displacement Analysis of RPSPR, RPSRR Mechanisms." Proceedings of the 3rd World Congress of the Theory of Machines and Mechanisms, Kupari, Yugoslavia, Vol. D, Paper D-4 (1971), 49-61.
43. Hartenberg, R. S., and J. Denavit. Kinematic Synthesis of Linkages. New York: McGraw-Hill, 1964.
44. Uicker, J. J., J. Denavit, and R. Hartenberg. "An Iterative Method for the Displacement Analysis of Spatial Mechanisms." Journal of Applied Mechanics, Trans. ASME, Series E, Vol. 86 (1964), 309-314.
45. Uicker, J. J., J. Denavit, and R. S. Hartenberg. "An Iterative Method for the Displacement Analysis of Spatial Mechanisms." Journal of Applied Mechanics, Vol. 31, Trans. ASME, Series E, Vol. 86, No. 2 (June, 1964), 309-314.
46. Soni, A. H. and Lee Harrisberger. "Application of (3 x 3) Screw Matrix to Kinematic and Dynamic Analysis of Mechanisms." VDI-Brichte, 1968.

47. Kohli, D., and A. H. Soni. "Displacement Analysis of Spatial Two-Loop Mechanisms." Proceedings of IFTOMM International Symposium on Linkages, Bucharest, Romania, June 6-13, 1973.
- \* 48. Kohli, D., and A. H. Soni. "Displacement Analysis of Single-Loop Spatial Mechanisms." Proceedings of IFTOMM International Symposium on Linkages, Bucharest, Romania, June 6-13, 1973.
49. Huang, M., and A. H. Soni. "Application of Linear and Non-Linear Graphs in Structural Synthesis of Kinematic Chains." ASME Paper No. 72-MECH-48, Journal of Engineering for Industry, Trans. ASME, (May, 1973), 603-611.
50. Huang, M., and A. H. Soni. "Synthesis of Kinematic Chains via Method of Cut Set Matrix With Modulo-2 Operation." Presented at the 12th ASME Mechanisms Conference, October 9-11, 1972, ASME Paper 72-MECH-34, Journal of Engineering for Industry, Trans. ASME, Series B, Vol. 95, No. 2, (May, 1973), 681-684.
51. Bottema, O. "On a Set of Displacements in Space." Presented at the 12th ASME Mechanisms Conference, Paper No. 72-MECH-19. Journal of Engineering for Industry, Trans. ASME, (May, 1973), 451-454.
52. Dimentberg, F. M. and S. G. Kislitsin. "Application of Screw Calculus to the Analysis of Spatial Mechanisms." Akad. Nauk. SSSR, Izvestiia. Otdelenie Tekhnichesk. Nauk., Vol. 8 (1965), 55-65.
53. Woo, L. and F. Freudenstein. "Application of Line Geometry to Theoretical Kinematics and the Kinematic Analysis of Mechanical Systems." IBM New York Scientific Center Technical Report No. 320-2982, November 1969, 103.
54. Soni, A. H., R. V. Dukupati, and M. Huang. "Closed-Form Displacement Relationships of Single and Multi-Loop Six-Link Spatial Mechanisms." ASME 12th Mechanisms Conference, Paper No. 72-MECH-50. Trans. ASME, Journal of Engineering for Industry, (August, 1973), 709-716.
55. Dobrovolskii, V. V. "Synthesis of Spherical Mechanisms." Akad. Nauk. SSSR. Trudy Sem. Teorii Masin i Mehanizmov, Vol. 2, No. 14 (1943), 5-20.
56. Denavit, J., et. al. "Velocity, Acceleration, and Static-Force Analysis of Spatial Linkages." Journal of Applied Mechanics, Vol. 32, Trans. ASME, Series E, Vol. 87, No. 4 (December, 1965), 903-910.
57. Suh, C. H., and C. W. Radcliffe. "Synthesis of Spherical Linkages With Use of the Displacement Matrix." Journal of Engineering for Industry, Trans. ASME, Series B, Vol. 89, No. 2 (May, 1967), 215-222.

58. Beyer, R. A. "Space Mechanisms." Transactions, Fifth Conference on Mechanisms, Purdue University, Lafayette, Ind., 1953, 140-163.
59. Yuan, M. S. C. "Kinematic Analysis of Spatial Mechanisms by Means of Screw Coordinates." (Ph.D. Dissertation, Columbia University, 1970.)
60. Wallace, D. M. "Displacement Analysis of Spatial Mechanisms With More Than Four Links." (Ph.D. Dissertation, Columbia University, 1968.)
61. Bagci, Cemil. "Dynamic Force and Torque Analysis of Mechanisms Using Dual Vectors and 3 x 3 Screw Matrix." ASME paper presented at the 6th U. S. National Congress of Applied Mechanics, Harvard University, Cambridge, Mass., June 1970.
62. Denavit, J., and R. S. Hartenberg. "A Kinematic Notation for Lower-Pair Mechanisms Based on Matrices." Journal of Applied Mechanics, Vol. 21, Trans. ASME, Vol. 76 (June, 1955), 215-221.
63. Roth, B. "The Design of Binary Cranks With Revolute, Cylindric, and Prismatic Joints." Journal of Mechanisms, Vol. 3 (1968), 61-72.
64. Chace, M. A. "Solutions to the Vector Tetrahedron Equation." Journal of Engineering for Industry, Trans. ASME, Series B, Vol. 87, No. 2 (1965), 228-234.
65. Bisshop, K. E. "Rodrigues' Formula and the Screw Matrix." Journal of Engineering for Industry, Trans. ASME, Series B, Vol. 91, No. 1 (February, 1969), 178-184.
66. Yang, A. T., and F. Freudenstein. "Application of Dual Number Quaternion Algebra to the Analysis of Spatial Mechanisms." Journal of Applied Mechanics, Vol. 31, Trans. ASME, Series E, Vol. 86, No. 2 (June, 1964), 300-308.
67. Goldstein, H. Classical Mechanics. Reading, Mass.: Addison Wesley, 1957.
68. Bagci, C. "The RSRC Space Mechanism--Analysis by a 3 x 3 Screw Matrix, Synthesis for Screw Generation by Variational Methods." (Ph.D. Dissertation, Oklahoma State University, Stillwater, Oklahoma, 1969.)
69. Uicker, J. J., JR. "On the Dynamic Analysis of Spatial Linkages Using 4 x 4 Matrices." (Ph.D. Dissertation, Northwestern University, Evanston, Ill., August, 1965.)
70. Levitskii, N. I., and Y. Sarkisian. "On the Special Properties of LaGrange's Multipliers in the Least Square Synthesis of Mechanisms." Journal of Mechanisms, Vol. 3 (1968), 3-10.

71. Bagci, C. "Minimum EMR Synthesis of Space Mechanisms for the Generation of Constrained and Unconstrained Screws." Journal of Engineering for Industry, Trans. ASME, Series B, Vol. 93 (1971), 165-175.
72. Denavit, J. "Displacement Analysis of Mechanisms Based on (2 x 2) Matrices of Dual Numbers." VDI-Berichte, Vol. 29 (1953), 81-88.
73. Skreiner, M. "A Study of the Geometry and the Kinematic Instantaneous Spatial Motion." Journal of Mechanisms, Vol. 1, No. 2 (1966), 115-143.
74. Hall, A. S. "Notes and Lectures on Matrix Methods in Spatial Kinematics." NSF-M.I.T. Summer Conference on "Recent Developments in Kinematics," Cambridge, Mass., July 11-22, 1966.
75. Beggs, J. S. Advanced Mechanism. New York: Macmillan, 1966.
76. Artobolevskii, I. I. Teoria Mehanismow i Masin. Gosudarstv. Izdatl Tehn-Teori. Lit, Moscow, 1953.
77. Dobrovolski, W. Teoria Mehanismow. Maxchgis, Moskau, 1953.
78. Hain, K. Applied Kinematics. New York: McGraw-Hill, 1967.
79. Reuleaux, F. The Kinematics of Machinery. New York: Macmillan & Co., 1876. (Translated by Alex B. W. Kennedy.)
80. Kotelnikoff, A. P. "Screw Calculus and Some Applications of the Same to Geometry and Mechanics." Annals of the Imperial University of Kazan, 1895.
81. Ball, R. S. A Treatise on the Theory of Screws. Cambridge, Massachusetts: Cambridge University Press, 1900.



VITA <sup>2</sup>

Dilip Kohli

Candidate for the Degree of

Doctor of Philosophy

**Thesis:** SYNTHESIS AND ANALYSIS OF SPATIAL, TWO-LOOP, SIX-LINK MECHANISMS

**Major Field:** Mechanical Engineering

**Biographical:**

**Personal Data:** Born in Lucknow, India, July 22, 1947, the son of Raj Kishore and Sudesh Kohli.

**Education:** Graduated from Colvin Taluquader's College, Lucknow, India in 1964; received the Bachelor of Technology degree in Mechanical Engineering from Indian Institute of Technology, Kanpur, India, in 1969; received the Master of Technology degree in Mechanical Engineering from Indian Institute of Technology, Kanpur, India, in 1971; completed the requirements for the Doctor of Philosophy degree at Oklahoma State University in December, 1973.

**Professional Experience:** Sri Raun graduate fellow at Indian Institute of Technology, Kanpur, India, 1969-71; graduate research assistant in the Department of Mechanical Engineering, Oklahoma State University, 1971-73.